NASA CONTRACTOR REPORT

NASA CR-650

NASA CR-650

STUDY OF LUNAR, PLANETARY, AND SOLAR TOPOGRAPHY

PROJECT TECH TOP

by C. E. Campbell

Prepared by
CORNELL AERONAUTICAL LABORATORY, INC.
Buffalo, N. Y.
for Electronics Research Center

NATIONAL AERONAUTICS AND SPACE ADMINISTRATION • WASHINGTON, D. C. • NOVEMBER 1966

NASA CR-650

STUDY OF LUNAR, PLANETARY, AND SOLAR TOPOGRAPHY

PROJECT TECH TOP

By C. E. Campbell

Prepared under Contract No. NAS 12-19 by
CORNELL AERONAUTICAL LABORATORY, INC.
Buffalo, N.Y.

for Electronics Research Center

NATIONAL AERONAUTICS AND SPACE ADMINISTRATION

For sale by the Clearinghouse for Federal Scientific and Technical Information
Springfield, Virginia 22151 – Price $3.75

TABLE OF CONTENTS

TABLE OF CONTENTS (Cont'd)

TABLE OF CONTENTS (Cont'd)

TABLE OF CONTENTS (Cont'd)

SUMMARY

This report presents the results of the first phase of a program to assess the state of the art in topographic information collection systems for application to the space program. The methods of acquisition that may apply for lunar, planetary and solar surfaces are described. A detailed investigation of the stereo imagery method is reported including requirements, sensors and errors involved. The applicability of holographic methods is evaluated with the most promising application concluded to be in the area of image enhancement.

The transmission and display of three-dimensional information are examined in terms of requirements and methods.

Other subjects surveyed include the peculiar problems of changing solar topography, measurements to test the general theory of relativity and measurement of stellar parallax from a space vehicle.

Conclusions and recommendations for improving the state of the art, where possible, are given. Numerous references are included.

LIST OF FIGURES

LIST OF TABLES

1. INTRODUCTION

This First Phase Report describes the work performed under NASA Contract NAS 12-19 during the period from 1 July 1965 to 15 April 1966.

1.1 Objectives

The objectives of the program are: (1) to study, and to determine the state of the art of topographical data acquisition, transmissio and display techniques, (2) to identify technical areas where additional research is needed in order to satisfy the future requirements of space exploration, and (3) to recommend laboratory and simulation experiments which will lead to the advancement of the state of the art.

1.2 Work Requirements

Specific work requirements in the area of data acquisition covered under this contract include the determination of available basic methods and the development of concepts of new techniques for obtaining lunar, planetary and solar topographic data and stellar parallax measurements The relative merits, limitations and obtainable accuracies of the techniques, are to be defined and compared. Both real time and non-real time systems are to be considered for spaceflight and astronomical applications in orbital, fly-by, landing and space probe situations using manned and unmanned single or cooperating spacecraft. Consideration is to be given to techniques such as, but not limited to, multiple channel optical radar using lasers in combination with fiber optics, parallax methods using spaceborne single point radiation detectors and stereoscopic techniques using single and cooperating, paired, spaceborne TV systems.

In the areas of transmission and display, the work requirements call for a review of current real time and non-real time techniques for recording, transmitting and displaying topographical and three-dimensional information presentations, and the development of new

concepts. The relative merits, obtainable accuracies and limitations of the current and proposed techniques, are to be defined and compared. Methods are to be considered for extracting the desired topographical information from displays and recordings that are optically or electronically distorted, motion-blurred, smeared, or photometrically degraded. The study includes the investigation of the application of holographic techniques to the acquisition, transmission and display of three-dimensional data, including their potential utility for the extraction of data from degraded imagery.

In all areas of investigation, the associated problem areas are to be specified and the research needs defined. A bibliography covering the areas studied is to be compiled.

1.3 Work Performed to Date

During the first phase of the program nearly all of the subjects mentioned above under the work requirements were covered, although because of the broad spectrum of subjects included, it was not possible to treat all of them in depth. Thus, some sections of this report are limited primarily to a discussion of the state of the art and in these instances details relating to specific space missions are lacking. Studies in these areas will be extended during the second phase of the program.

In the area of topographic data acquisition, emphasis was given to stereoscopic (or parallax) methods, which require two images of the surface obtained from two different observation points. In this study consideration was given to: (1) the requirements for obtaining accurate topographical information from stereo imagery, (2) the various sensors which are presently available or future possibilities for obtaining this imagery, and (3) the errors involved in such a collection effort and ensuing data reduction.

The investigation of holographic techniques under Phase I included an assessment of the direct use of the three-dimensional properties of hologram images to acquire topographic data from space vehicles, an analysis of the problems of transmitting a hologram via a data link, and a preliminary study of how holographic techniques might be employed to improve the quality of degraded images. A detailed analysis was made of the influence of non-linearities in the hologram recording process on image reconstruction.

The application of holographic techniques to the acquisition of three-dimensional data from space vehicles was also investigated with respect to the laser power requirements and the dimensions of the holograms required to achieve adequate depth perception.

The work done to date in the area of data transmission consisted primarily of a review of the state of the art with consideration of the general requirements for space applications, bandwidth compression, and laser communication systems.

In the area of displays, both stereoscopic and non-stereoscopic methods of displaying three-dimensional information were reviewed to determine their applicability to space missions. The various methods were compared with respect to resolution, convenience, distortion and their adaptability to real time situations.

A study of stellar parallax measurements was conducted which included consideration of the implications of improving the accuracy of stellar parallax measurements from the astronomical point of view. The engineering problems associated with obtaining improved stellar parallax measurements from space vehicles operating at distances of 50 to 100 astronomical units from the earth were studied.

The problems of solar topography differ considerably from those of lunar and planetary topography where the surface features are well defined and do not vary in time. The effort in this area under Phase I was limited to a survey of the literature to determine the specific types of data that are of major importance. Only preliminary consideration has been given to methods for acquiring the desired data. During the study relating to solar topographic measurements, it became apparent that optical observations from space vehicles might be advantageously employed to verify various relativistic and cosmological theories. The significance of performing such measurements was assessed.

1.4 Report Organization

The details of the work performed under the first phase of the program are described in the following sections. Each of the major subjects discussed in the previous subsections are presented in a separate section. Because of the variety of subjects covered, each major section contains conclusions and recommendations relative to subject matter included in that section. Specific references and the entries in the bibliography are grouped according to the individual sections to which they relate.

1.5 Acknowledgements

Acknowledgement is made of the contributions of the following individuals to this report. Robert Kinzly for the work on holography, Robert Talley for the astronomical considerations of stellar parallax measurements, Gerhard Neumaier for the engineering considerations of stellar parallax measurements and the work on obtaining solar imagery and relativistic measurements, John Gallatin for the work on error analysis and displays, and Jerome Mantell for the work on conventional electro-optical systems and transmission.

2. ACQUISITION OF TOPOGRAPHIC INFORMATION

An important aspect of planetary exploration is the acquisition of topographical information. This information can be defined as those data which enable one to find the distance between any two points on a surface and the elevation of any point relative to some reference level.

There are basically four different methods that have been considered for obtaining three dimensional information from a planetary surface. They are: stereoscopic imaging, laser ranging, holographic techniques and photometric techniques.

Stereoscopic imaging utilizes two images of the same scene taken from different positions so that elevation of a point can be derived from the difference in its positions as presented in the two images. The requirements, sensors and errors involved in such a technique are described in the remainder of this section.

Laser ranging would be utilized in a scanning mode to give not only range but also directional information. The discrepancy between what ranges would be recorded for a level terrain and the actual ranges measured could be used to derive the elevation of the scanned scene. This method requires a more detailed examination.

The ability of holography to record three dimensional information has suggested its use in topographical information collection. An analysis of this possibility is presented in Section 3.

A photometric method has been proposed to determine topographic relief from a single photograph based on a knowledge of the surface photometry. If we know the illumination value and the source target sensor geometry, the slopes in the resulting image can be determined with a knowledge of the reflectance of the surface and how it varies with angle. The method was originally suggested in connection with the lunar surface because of its peculiar reflectivity (see Figure 2-1). Its applicability is highly limited when surface photometric properties are not known accurately or the surface is diffuse. A more detailed treatment of this technique is presented in Reference 1 and will not be discussed any further in this report.

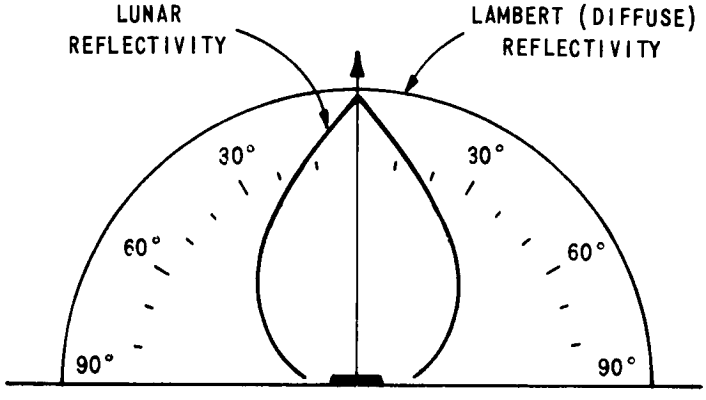

Figure 2-1 LUNAR SURFACE REFLECTIVITY

Other than the methods just described, there are three which might be mentioned for the sake of completeness. One is a radar technique using radar imagery in stereoscopic methods similar to photography. Another is the use of a radar interferometer for determining elevations by utilizing null points in the combined antenna pattern. Both these methods are described further in Reference 2. The development of these radar techniques is proceeding slowly; however, the requirements for large area topographic mapping of cloud-covered Venus indicate that they hold promise for the future.

A third method is that of shadowing. Imagery is taken when the sun's rays are at grazing incidence so that shadows are elongated. Measurements of the shadow lengths can be correlated with feature height. Many uncertainities in this method make its value very limited.

The remainder of this section is concerned with the method of stereoscopic imaging including its requirements, sensors and errors.

2.1 Stereo Requirements

As described above, stereoscopic imaging utilizes two images* of the same scene taken from different positions so that elevation of a point can be derived from the difference in its positions as presented in the two images. The apparent displacement of the position of a body, with respect to a reference point or system, caused by a shift in the point of observation is called parallax. Considering a pair of aerial photographs of equal scale, the absolute stereoscopic parallax of a point is the algebraic difference of the distances of the two images from their

*Although there are displacements due to elevation in a single photograph and some elevations can be determined from measurements of these displacements,

$$h = d_e \frac{H}{r}$$

(where h is elevation, d_e is elevation displacement, H is flight altitude and r is the radial distance from the center of the photo to the top of the object), they generally require some additional knowledge on the part of the user such as position of object base, verticality of object, etc. Such special cases are not of sufficient value for problems such as mapping and will not be considered any further.

respective photographic nadirs, measured in a horizontal plane and parallel to the line joining the observation stations. The difference in the absolute stereoscopic parallaxes of two points imaged on a pair of photographs, called parallax difference, is used in the determination of the difference in elevations of objects. The measurement of elevations by means of parallax difference derived from two images is the subject of stereophotogrammetry.

The difference in elevation of a point represented in a stereo pair from the nadir point of one of them is given as

$$\Delta h = \frac{H'}{b + \Delta p} \Delta p \qquad (2\text{-}1)$$

where Δh is the elevation difference, H' is the flight altitude above the nadir, b is the photographic base (the parallax of the nadir point as measured in the other photograph), and Δp is the parallax difference. For a derivation of this equation, the reader is referred to Reference 3.

From equation (2-1) we can see that the only measurement required that is not taken directly from the imagery is the flight altitude. This can be derived in one of three different manners: first, by direct measurement with an instrument such as the laser rangefinder or radar altimeter; second, by use of a known distance in the scene to derive the scale which in combination with the focal length can give the flight altitude; and third, by the direct measurement of the baseline (the distance between stations) which when combined with a measurement of the photographic base can give the scale and thus the flight altitude.

Equation (2-1) has been derived with the assumptions of vertical (untilted) photographs, equal flight altitudes and equal focal lengths. More rigorous analytical expressions are presented in Reference 3 for other than these conditions.

If the parallax difference is measured with the best stereoscopic plotting instruments, the result, in terms of elevation difference, is generated directly by the instrument without computation. In an accurate stereoscopic instrument, the tilt is taken into account automatically.

There are basically two distinct methods of obtaining a stereo pair: simultaneously or consecutively. Obtaining two images at the same instant with enough separation in stations in general requires two platforms. This involves the attendant complications of coordination. However, it does obviate the requirement of a stationary scene.

If this requirement is not present to begin with, then images obtained consecutively can be used to obtain stereo. By taking overlapping images (at least 50% and normally 60%) from a single station moving over the scene, the required separation of observation points is obtained by the velocity of the vehicle and the time between exposures. If the scene is not changing rapidly with respect to this time duration, the imagery will be satisfactory for stereo viewing and data reduction.

There are three other major factors which can degrade an elevation determination from parallax measurements on two images: resolution, geometric fidelity, and attitude.

Resolution may be defined as the minimum distance between two adjacent features, or the minimum size of a feature, which can be detected by an imaging system. It is discussed in Section 2.1.1

Geometric fidelity may be defined as that aspect of imagery which describes how well positional information is preserved in transferring detail from a scene to an image. It is discussed in Section 2.1.2.

Attitude is the angular orientation of an imaging system with respect to some external reference system. It is discussed further in Section 2.1.3.

2.1.1 Resolution

The minimum size or separation that is required to be observable in the image of a scene establishes the resolution requirements of a system to obtain that image. In the image plane it is generally measured in line pairs per millimeter. In terms of the size of objects in the scene, it is called ground resolution.

In a study to determine the most effective method of obtaining topographical information from a planetary surface, it is appropriate to first consider what purpose the results of the collection effort will serve, that is, what is the ground resolution requirement. We can (rather arbitrarily) distinguish four different types of space missions in this respect: reconnaissance, local, cartographic and surface.

A reconnaissance mission would have as its purpose a general survey of the planetary topography. An example of this would be a fly-by operation such as the MARINER. Only large general features would be discerned.

A local mission would have as its purpose an area survey of a particular region of the planet surface. Such information could be used to designate future landing sites or to examine a particularly interesting anomaly discovered by a reconnaissance mission or earthbound observations. An example of this type of mission would be the RANGER. Only the relative features of a local area would be obtained.

A cartographic mission would have as its purpose a complete survey of the entire surface. It could be limited to less than the total area but it would be distinguished from a local mission in that areas would be tied together with respect to some reference system (latitude, longitude and datum level). This could be accomplished from a vehicle such as the ORBITER. Features would be detailed to some specified (by desire or by equipment) limits for mapping.

A surface mission would have as its purpose a ground survey of some parts of the surface to establish accurate control for a cartographic mission. A landing vehicle such as the SURVEYOR could perform such a task. Specific features would be pin-pointed as to location with respect to the starting points of the reference system established.

Once this requirement has been established, system components to meet it can be chosen and evaluated.

2.1.2 Geometric Fidelity

A shift in the position of a point in the image of a scene which does not alter the perspective of the image is called a displacement. Displacements can be caused by tilt from the vertical, scale change in the image and relief of the objects.

A shift in the position of a point in the image of a scene which alters the perspective is called a distortion. Causes of image distortion include lens aberrations, differential shrinkage of film, and motion of the camera during exposure. Those displacements which are due to other causes than relief and are not removed or accounted for together with those distortions introduced by the system which are not removed by calibrations can produce non-uniform shifts in image points that will be interpreted as relief displacements. Therefore, for imagery collected to produce elevation information the preservation of the geometric fidelity is of great importance. If the geometrical errors, or the random distortions, are sufficiently low, then the system geometric fidelity will be determined by the resolution.

Degradation in fidelity is usually greatest in the readout and reconstruction processes. High quality optics are available to present an image of high geometric fidelity to the readout device. However, non-linearities and drift in the photo-electronic devices necessary for readout when photographic film is not returned from the mission, result in a lowering of this fidelity. The most common means of reducing the errors that could result from such degradation is the use of an optical grid or reseau mark pattern in the image plane of the sensor. These highly calibrated marks are superimposed on the imagery to provide a reference grid of accurately known distances and two dimensional geometry. This method was used successfully on the Ranger and Mariner missions.

2.1.3 Attitude

Attitude is the angular orientation of an imaging system with respect to some external reference system. Ideally, all mapping imagery would be taken from the vertical; however, a vehicle with three

angular degrees of freedom (roll, pitch and yaw) can rotate the orientation of an image with their photogrammetric counterparts (tilt, swing and azimuth). The effects these angles have on the accurate determination of elevation are discussed at length in Section 2.3.

2.1.4 Limits

The actual values of ground resolution required, tolerable geometrical errors or uncertainties in attitude are not specified here. They would be determined by the user requirements and decisions of the system designer based on component capabilities and costs. For example, although it might be desirable in some sense to have a total mapping of the moon to an accuracy of an inch (since this would probably satisfy the vast majority of users the practicality in terms of cost, time and effort make such a requirement too stringent. What it is relaxed to will be the result of a compromise between user requirements and practical system constraints.

In Table 2-1 a summary of selected space missions[4, 5] is listed along with individual requirements and characteristics.

2.2 Sensors for Stereo

2.2.1 Photographic Cameras

Several different types of cameras and camera configurations can be employed for obtaining stereoscopic information from which a quantitative determination of the three-dimensional features of the surface can be made. The sensing element may be either film or some type of electro-optical element. The discussion in this section is confined primarily to the camera types and configurations. The details of image sensing elements, including film, are discussed in subsequent sections.

Table 2-I
SUMMARY OF SPACE IMAGERY REQUIREMENTS

APPLICATION	PRIMARY REQUIREMENTS	SECONDARY REQUIREMENTS	LIKELY METHOD OF TRANSMISSION
REAL-TIME (MANNED AND UNMANNED SPACECRAFT)	HIGH S/N "CLEAN" PICTURE FREE FROM SPURIOUS PATTERNS "WATCHABLE" OVER LONG TIME PERIOD HIGH FRAME RATE	MEDIUM RESOLUTION GOOD GRAY SCALE LITTLE EQUIPMENT MODIFICATION	ANALOG FOR NEAR EARTH
PLANETARY FLY-BY	POWER SEVERELY LIMITED GREAT DISTANCE LARGE TOTAL NUMBER OF PICTURES WIDE DYNAMIC RANGE	HIGH RESOLUTION GOOD GRAY SCALE INDEPENDENCE IN ERRORS	DIGITAL FOR LOW BIT RATES
MAPPING (MOON, EARTH)	HIGH RESOLUTION (STEREO) VERY HIGH RESOLUTION (PHOTOMETRIC) WIDE DYNAMIC RANGE GOOD GRAY SCALE (STEREO) EXCELLENT GRAY SCALE (PHOTOMETRIC)	PICTURE STORAGE IN VEHICLE LOW ERROR PROBABILITY	DIGITAL FOR ACCURACY (7 BITS QUANTIZATION)
ASTRONOMICAL	VERY LOW AVERAGE DATA RATE WIDE DYNAMIC RANGE GOOD GRAY SCALE	ACCURATE POSITION INFORMATION LOW ERROR PROBABILITY PICTURE STORAGE (LONG-TIME)	DIGITAL TIME BUFFERING FOR STARFIELDS ANALOG, POSSIBLY, FOR PLANETS
DEEP SPACE (RELAYED SIGNALS)	SIGNALS RELAYED VIA INTERMEDIATE VEHICLES ERRORS MUST NOT ACCUMULATE UNNECESSARILY IN RELAYING POWER LIMITED TRANSMISSION IN OUTER VEHICLES	WIDE DYNAMIC RANGE GOOD GRAY SCALE	DIGITAL FOR REGENERATION AND LOW BIT RATES

a) Vertical Frame Camera - One of the most common methods for obtaining topographic information is the use of a frame camera pointing vertically downward. Pictures are taken at regular intervals so the overlap is 60-70%. When the next pass is made over the adjacent area, an overlap of 10-20% is usually desired. This may be accomplished in photographing the moon or planet by following a polar orbit and using the rotation of the planet or moon to cover an adjacent strip on the next series of photographs. The frame camera with a between the lens shutter has the unique advantage of exposing all points in the format simultaneously so that distortion is not caused by the motion of the vehicle while different portions of the format are being exposed.

An interesting potential application of the frame camera is that of obtaining near real time stereoscopic views of a surface from a moving spacecraft. A camera employing either film and a rapid development capability or an electronic image storage system would obtain a single picture at one location of the spacecraft. At some time later, when the image had been processed and the spacecraft had moved sufficiently far to provide an adequate baseline for stereoscopic viewing, the observer would view (through a suitable optical arrangement) the stored image with one eye and the ground with the other. Depending on the speed and altitude of the spacecraft, fusing the two images might become difficult. It would probably be necessary to devise a tracking technique in order to have the real time image remain stationary.

b) Two Oblique Frame Cameras - In mapping photography the ratio of the baseline (distance between points where the frames are exposed) to the altitude is usually slightly less than unity. This ratio enables the vertical distances associated with the surface to be obtained accurately. However, if a long focal length is used in order to obtain the desired surface resolution, the ratio of the base line to the altitude for a vertical frame camera is reduced in order to provide the required overlap, resulting in a decreased accuracy in the measurement of the vertical distances. In order to avoid this difficulty, two frame cameras mounted

obliquely can be used. One points downward and to the front of the vehicle while the other points downward and to the rear. Both cameras photograph the entire strip, with each camera having a suitable overlap.

c) Split Field Oblique Frame Camera - Instead of two cameras for oblique photography as described above, a single camera may be employed having two lenses pointed at oblique angles and a split field. Where oblique views are required, this method has the advantages of simplicity and lighter weight, but because there is only one film, image motion compensation, if used, must be the same for both halves of the field. This requires precise control of the spacecraft attitude.

d) Nodding Frame Camera - In order to save the weight of a second oblique camera, a nodding frame camera could obtain pictures in oblique directions at the ends of its nods. However, this method is complex and has the disadvantage that motion might have an adverse effect on the stability of the vehicle.

e) Two Strip Cameras at Oblique Angles - The strip camera derives its name from the fact that only a single "strip" of the image is recorded at any instant. The strip is perpendicular to the direction of motion of the vehicle and a complete image is obtained as a result of the forward motion. The conventional strip camera employing film has no shutter and a slit is provided in the image plane which defines the extent of the image being recorded at any instant. The film is driven in synchronism with the image so that no relative motion exists between the film and the image. Alternative arrangements might employ a row of fiber optics in place of the slit with the opposite ends of the fibers coupled to a photo-electronic sensor such as a vidicon tube, or a mechanical-optical scanning system in place of the slit. The scanning forms of this method are excellent for real time transmission because no storage is required. However, because vehicular motions cause random distortions in the reconstructed images, the stability of the vehicle must be carefully controlled in order to limit the distortions to acceptably low values.

For stereoscopic data acquisition, two strip cameras must be employed, one pointing downward and to the front and the other pointing downward and to the rear.

f) Stereo Pairs Obtained from Two Vehicles - Two vertical or oblique frame cameras in different vehicles have the capability of obtaining simultaneously the two stereo pictures required for stereo-triangulation. Thus, this technique has application in cases where transient phenomena are occurring on the surface (e.g., in the case of the sun). Of course, some means must be provided for synchronizing the cameras. The measured distance required for stereotriangulation control can be the distance between the two points at which the stereo pair of pictures is obtained. In the case of two separate vehicles, this measurement can be made by means of a transponder in one vehicle and a transmitter, receiver and timer in the other vehicle.

For real time stereoscopic viewing of a surface, possibly in connection with a landing mission, two TV cameras in separate vehicles might be used. The TV image from one vehicle could be transmitted to the other to provide a stereo pair. Of course, means would have to be provided to insure that the two cameras were viewing the same area.

g) Panoramic Cameras - The essential feature of panoramic cameras is scanning, transverse to the direction of motion, of many resolution elements at the same time. This is done in some cameras by rotating the lens about a nodal point, and in others by drawing film past a slit in the image plane in synchronism with the rotation of the image produced by a rotating mirror or prism. The advantages of the panoramic camera are primarily its high resolution over a greater precentage of the format than a frame camera, and its greater width of coverage per frame. However, because of the 60% overlap requirements for stereo at the center of two adjacent frames, the overlap at the edge of format becomes excessive wasteful of film. Also, since all parts of the image are not exposed at the same time, geometric distortion is introduced due to the motion of the vehicles. The scale of panoramic imagery varies greatly from center to edge of format. This makes the problem of data reduction more complex.

From these considerations, it is concluded that panoramic cameras are not well suited for acquiring imagery for space applications.

2.2.2 Film

Film may either be used as a permanent storage medium, (e.g., if the film is brought back to earth) or it may be used as a temporary storage medium to record and store the imagery so that it can be scanned and transmitted, as in the case of the Lunar Orbiter. The advantage of retrieving the film is that its capabilities with respect to dimensional stability (which affects the geometrical fidelity of the imagery) and resolution can be fully utilized. If the data must be transmitted, both geometrical fidelity and resolution are degraded by the scanning system and the image reconstruction process.

The minimum area of film in square meters required to photograph a planet or the moon is given by

$$A = 4\pi \left(\frac{r}{R_g R_c}\right)^2 \frac{1}{(1-F)(1-S)} \qquad (2\text{-}2)$$

where r is the radius of the planet or moon, in kilometers, R_g is the ground resolution, i.e., the distance across a resolution element, in meters, R_c is the resolution of the camera system in lines per millimeter, F is the fractional forward overlap and S is the fractional sidelap. This equation does not take into account the fact that the desired sidelap cannot be obtained exactly for an orbiting vehicle in a polar orbit. The sidelap must be greater which may increase the required amount of film by as much as 50%.

As an example of the storage capability of photographic film, consider the extreme case of 649F film which has a resolution of over 1000 lines/mm. In theory, the entire surface of the moon could be photographed with 10 meter resolution on one square meter of film, neglecting sidelap. For SO-243 film and a system resolution of 100 lines/mm, 100 square meters of film is required. A more practical example is the case of Plus-X film used in a KC-6A mapping camera with a Geocon-IV lens. For this combination, a resolution in excess of 30 lines/mm can be attained and

the film requirement is 1000 square meters. Since the KC-6A camera uses a 9" x 9" format, this would require approximately 4500 meters of 9 inch film.

The weight of film according to Kodak's Handbook varies from 0.11 to 0.20 kilograms per square meter for an estar base film, depending upon how thick the base is. For Plus-X film, it is 0.2 kilograms per square meter. Thus, for the case of the KC-6A camera cited above, approximately 275 kilograms of film would be required, assuming 40% extra for sidelap and wastage.

Estar base film is better than cellulose acetate because of its better dimensional stability for the same thickness and thus is superior on a weight basis. The thicker bases have superior stability because they resist the stress imposed by the emulsion better. The humidity coefficient of linear expansion is 0.0015 - 0.0035% per one percent relative humidity for estar base films. The thermal coefficient of linear expansion is 0.0015% per degree F. For a detailed discussion of the physical properties of film, see Reference 6.

One disadvantage of film is that it is very sensitive to gamma radiation. For example, 1 roentgen will expose TRI-X to the point where it cannot be used. Thus, in missions requiring film, adequate shielding must be provided to protect the film against the anticipated radiation field.

2.2.3 Photo-Electronic Imaging

This section presents the results of an investigation of photo-electronic imaging devices and related systems as they apply to imagery acquisition for space missions. A review of the image tube state of the art, which includes discussions of the slow scan mode of operation and future developments, is followed by an analysis of camera tube sensitivity. Transmission requirements are examined in Section 4.

Television techniques have come to play an integral part in the rapidly expanding space program. In designing such systems for selected missions in space, a number of factors must be considered and many variables must be taken into account. A few of the many possible variables include pictorial data required, camera tube, transmission characteristics, system weight, modulation techniques, bandwidth, and resolution.[7]

The selected equipment must withstand such hazards as launch (shock, vibration, acceleration), solar heat and radiation and must have unattended operation capability as well as long life reliability.

The general requirements for stereo imaging also apply to photo-electronic imaging when three-dimensional information is desired.

2.2.3.1 Image Tube State of the Art

The transmission of pictorial information to some remote place so that it can be reconstructed in usuable form admits of no unique solution. However, when considering the communication of image information in space applications (e.g., probe to earth) it becomes mandatory to convert the image of the object (or scene) under observation into an electrical signal which can be much more readily processed for transmission to a remote point. We shall call this process photo-electronic image conversion. (N.B., we must distinguish between photo-electronic conversion and photo-electronic image conversion. The former converts photons to electrons via the photo-electric effect, photoconductive effect or photovoltaic effect. The latter converts an area flux of photons into a video signal.) Devices which can effect photo-electronic image conversion are commonly called image tubes, camera tubes or television pickup tubes.

2.2.3.1.1 Operation in General

A light image corresponding to some remote scene and produced by an optical system is essentially continuous in the microscopic order over a two dimensional surface and in time. The brightness of any point in this image is a function of the three coordinates: x, y and t. To transmit such a picture over a single communication channel in real time,

it is generally necessary to adopt some sort of scanning system which can read the two dimensional brightness field quickly with respect to motions in the scene.

First, the incoming light image is converted to some storable form. Then an exploring element or spot is moved over the stored image in a periodically repeated path covering the entire image area to be transmitted. The exploring element is so constructed that it generates a signal which indicates the brightness (either instantaneous or averaged over a short time) of its instantaneous position. The scanning process may or may not return the storage target to its previous unexposed state. If it does not, a separate erasing mechanism is required so that cyclic operation is possible. It is also highly desirable to have some essentially noiseless amplification within the pickup tube so that it can produce a conveniently high signal level to overcome the inherent noise of the following electronic stages.

From this we see that there are basically five distinct subprocesses in the overall process of photo-electronic image conversion. They are photoconversion, storage, readout, erasure and amplification. It is the various combinations of the particular possibilities in each of these functions which produce the variety of imaging devices available to the space program at this time.

There are many excellent references which describe the operations of particular image tubes. It is felt, that repeating such an exposition is not warranted here and the reader is referred to Reference 3 for an excellent treatment of such details. It is our purpose here to describe individual types only for comparison to obtain an overall view of the image tube state of the art.

2.2.3.2 Types of Image Tubes

A great variety of camera types is available to the application engineer. Each has its own peculiar advantages and disadvantages. This section will discuss these characteristics for three major types of image tubes, namely, the image orthicon, the vidicon and the image dissector, with some comments on other types following these.

2.2.3.2.1 The Image Orthicon

Some of the major characteristics of the image orthicon include: very high sensitivity, high resolution storage capability, good signal-to-noise behavior, high degree of complexity, and heavy and bulky packaging.

The normal image orthicon is two inches to three inches in diameter. Development of larger types (for more TV lines) has been primarily limited by electron beam aberrations at the larger deflection angles.[11]

In space applications, the image orthicon is usually considered in a slow scan mode (for a saving in bandwidth). A special type of slow scan technique known as Isocon[12, 13] scanning has greatly improved standard orthicon performance. In the following brief description, the Isocon procedure and its advantages will be given. In a later section, a detailed comparison with the slow scan vidicon will be noted.

The Isocon scanning beam electrons are of higher energy than ordinarily used in image orthicon operation. Instead of depositing electrons on the target to obtain an equipotential, these high energy electrons are scattered from the target. The output video signal is then obtained from the electron beam sensing rather than measuring the potential distribution at the target.[12, 14] In using this technique, experimental operation has indicated a S/N improvement of 2-3 with a dynamic range extension of at least an order of magnitude. This is combined with the increased detectability of an output signal with as high as 90% modulation. Another problem which Isocon scanning alleviates is the presence of image defects arising from the electron beam velocity distribution in the reading beam.[14] This distribution is of Maxwellian form and for low beam energies (in normal orthicon operation) may have voltage variations greater than the variations it is supposed to read. The high beam energy of the Isocon method shows considerably less relative variation. Of course, use of an electron monochromator would eliminate all variation but would cause a loss of sensitivity.

Advanced research with the 3" image orthicon has shown[15, 16] resolutions of 900 TV lines for normal incident intensities at 50% square wave response (1500 TV lines at 10% response) with as much as 3000 lines* (10% response) for higher incident illuminations. Tube electrical parameters must be varied to produce the latter resolution figure, although the image intensifier orthicon might be employed.** The characteristics and operating suggestions include:

a) Cooled target - resolution drops by a factor of 4 as the target temperature increases from 0°C to 35°C.

b) Significantly higher than standard photocathode voltage.***

c) Slow scan with attendant bandwidth reduction.

d) 50% duty cycle - field mesh (42.5 microns).

e) High secondary emission coefficient.

f) High lateral resistance so that large patterns may be stored.

g) If the conduction mechanism were electronic rather than ionic, the problem of charge carrier loss with life as exists in glass targets would be eliminated.

h) Strong focusing by use of an axial magnetic field[17] to improve resolution capability.

The image orthicon camera tube shows to best advantage when used in astronomical[18] observation (Stratoscope II

---

* The size of the image is necessary to convert TV lines to line pairs per mm. For example, if 3000 lines scan a one inch image, the resolution equivalent is 60 line pairs per millimeter.

** Higher sensitivity image orthicon.

*** This is used to decrease the image smear of photoelectrons whose release velocities vary in magnitude and direction. It can be shown that the smear radius is inversely proportional to the square root of of the photocathode potential--hence providing higher resolution at increased photocathode voltage.

Program). The properties of very high sensitivity, output signal linearity (with brightness) and long time signal integration (with detailed charge pattern storage) render the image orthicon superior to photographic film for astronomical observation. For a given exposure time type 103aO astronomical film can detect 20th order star magnitudes compared to 25th magnitude for the image orthicon (5 stellar magnitudes equal $(2.5)^5$ brightness ratio) with isocon scan at standard scan rates. Integration (exposure) times without image degradation for an MgO membrane target can be as long as 3 hours if cooled to -25°C (or 3 minutes at +20°C). Within this temperature range tube sensitivity is approximately constant.

The choice of target mesh dimensions represents a compromise between resolution, beam modulation, S/N ratio, and linear dynamic range as shown below.

TABLE 2-2

IMAGE ORTHICON TARGET MESH SPACING

	1 Mil	20 Mils
Signal Modulation	Up to 40% better	-
Linear Dynamic Range	-	Broader
Resolution	Better (20-30%)	-
S/N Ratio[19]	Better (2 : 1)	-

As for scan technique, the Isocon method is preferable (as noted). As much as 97% of the stored signal amplitude can be read from the initial scan in a one sec sweep time compared to 63% of the amplitude from a 1/20 sec sweep time. Rapid scan thus requires many more scans to return the target to its desired fixed starting condition -- eliminating effects of previous exposures.

In spite of the obvious advantages of the image orthicon in astronomical application, many serious problems remain. Incomplete collection of secondary electrons produce distortions in the areas surrounding highlights. Also, the lack of ruggedness of image orthicons contributes to a general lack of reliability.

2.2.3.2.2 The Vidicon

The many advantages of the vidicon have made it very appropriate to space[20] applications. Some of these desirable features include:[21, 22, 23]

a) a lightweight and compact system,
b) adaptability to unattended operation,
c) no requirement for very critical adjustment,
d) long lifetime,
e) less complexity, smaller cost, higher reliability (compared with the orthicon)
f) good sensitivity
g) high resolution and
h) storage capability.

Some undesirable vidicon characteristics which are the objects of further research (discussed later) includes:

a) dark current, especially in slow scan application,
b) target temperature sensitivity (less than orthicon),
c) loss of resolution due to lateral target resistivity in slow scan operation,
d) beam landing error -- non-perpendicular scanning beam incidence, causing sensitivity variation across the target face,
e) resolution limited by relatively large spot size of low energy electron scanning beam, and
f) small available sensitive areas (maximum $\approx$ 1 inch square).

The basis for vidicon dark current is the normal bulk conductivity of the target. At commercial scan rates, dark current is a relatively unimportant factor even though it is non-uniform over the target. With reduced signal

levels in the slow scan mode, dark current becomes a factor. At temperatures above 30°C, the dark current doubles for every additional 10°C rise (satisfactory vidicon performance is obtained up to 45°C target temperature). The dark current may be reduced by decreasing the signal electrode voltage (cubic dependency). Such action would, in addition, lower the output sensitivity. Vidicon tube sensitivity is proportional to the square of the signal electrode voltage. Similarly, beam landing distortion is less severe at high signal electrode voltages. The effect may be eliminated entirely by a complex and costly modification[23] of the alignment fields in addition to shaping (physically) the focusing and deflection fields to insure a beam landing angle normal to the target surface. The most significant advance in high resolution vidicons stems from Shade, et al.[24] An experimental 4-1/2" vidicon with a 2" square target area was constructed. The assistance of computer designed field configuration (magnetic focusing) and a field mesh (100 mesh/inch) to eliminate electrostatic diverging target effects have made the following results possible.

TABLE 2-3

FUTURE VIDICON CAPABILITY

Tube Resolution (Lines)	Signal-to-Noise Ratio
2000 lines [at 50% MTF]	42 db
5000 lines [at 10% MTF]	42 db

Two other proposed vidicon sensors designed to approach image orthicon sensitivity are the image intensifier vidicon and the secondary electron conduction (SEC) vidicon tubes. The image intensifier is a small unit used in conjunction with the vidicon. A phosphor layer re-emits the amplified image pattern to the vidicon as received from the intensifier cathode. The increased sensitivity may be of the order of 3×10^{-4} ft-candle-sec. The SEC tube produces similar increased sensitivity by causing high gain secondary emission from a sandwich type porous target.

2.2.3.2.3 The Image Dissector

The image dissector, a very early TV pickup type, has come back into a certain amount of use because of its lack of an electron gun, which aids reliability, and its nonstorage characteristic which allows scan rate changes without affecting signal current amplitude. One of these tubes was used as a navigational sensor on the Mars Mariner spacecraft. Its low sensitivity might also make it a candidate for a solar probe where an abundance of signal is available.

Some of the more desirable characteristics of the image dissector are:

a) Excellent signal linearity for all inputs levels below saturation of the final stages of the electron multiplier.

b) Pictorial resolution which is determined only by the aperture size of the collector (and the magnification of the image from the photocathode to the plane on which the image is focused). A square wave amplitude response of about 60% is achieved for a resolution of 1/a line pairs/mm (a = aperture width [length]). A 10% response is achievable at R=1.75 (1/a) line/pairs/mm. Apertures as small as 0.01 mm would resolve $\approx$ 100 lines pairs/mm or $\approx$ 5000 lines over present tube areas.

c) A large photosensitive area of 5.6 cm x 4.2 cm is presently available and does not represent the state of the art limit.

Along with the lack of storage capability, the major disadvantage of the image dissector is its lack of sensitivity (for normal operations). The image dissector tube has about 1/100 the sensitivity of a comparably operated standard vidicon tube (about 4 orders of magnitude below the image orthicon).

Experimental studies[25, 26] for use of an image dissector in a star tracker system concluded that aperture geometry was of primary importance for extending the linearity of the output signal. A saw-tooth shaped aperture and a straight line scan afforded the best operating compromise. An interesting application of the image dissector

tube would have been in high resolution photographic facsimile scanning[27] such as was contemplated for the lunar orbiter mission. The latter output resolution figure of 30 line pairs/mm, which is limited by the diameter of fiber optics and the vidicon system, might have been significantly improved by use of a very high brightness CRT scanner* and smaller diameter fiber in conjunction with a very small aperture image dissector.

2.2.3.2.4 Others

There are several other camera tubes and methods of photo-electronic image conversion not included in the previous three sections. The iconoscope (and image iconoscope) represents the earliest example of a camera tube with storage. Although the iconoscope does not make full use of storage and is somewhat handicapped by a characteristic nonuniform shading pattern, it made possible the transmission of high quality real-time pictures. In fact, one of the very elements in its operation that is responsible for its inefficiency also leads to a reproduction of tonal values that has been difficult for other more sensitive tubes to match. The reason for this is the incomplete collection of photoemitted electrons from scene highlights.

By recording the image on film and then reading out with a flying spot scanner consisting of a kinescope, optics and a photomultiplier, we realize a very excellent means of photo-electronic conversion. It is, however, bulky and costly. The film must be processed and is not erasable. No real time transmission can be realized.

There are many special purpose pickup tubes which are sensitive to different regions of the spectrum than the visible. The iricon and uvicon are examples of these.

2.2.3.3 Comparison

The following table is presented to give some comparison of image tube capabilities and operating characteristics.

*Flying spot scanners are available with faceplate brightnesses of 10,000 ft. lamberts (luminous emittance $\sim 10^5 \frac{\text{lumens}}{\text{m}^2}$).

TABLE 2-4

TYPICAL NOISE EQUIVALENT POWER (NEP) PER RESOLUTION ELEMENT AND SENSITIVITY FOR REPRESENTATIVE IMAGE TUBES

Image Tube	NEP at Spectral Peak watts	Sensitivity in ft-candle-sec
Intensifier image orthicon	1.4×10^{-17}	10^{-5}
Image orthicon	1.4×10^{-16}	10^{-4}
Image dissector	3×10^{-11}	1
SEC vidicon	1.3×10^{-15}	5×10^{-4}
Vidicon	1.6×10^{-13}	10^{-2}

2.2.3.4 Slow Scan

As we shall see in Section 4, weight and power restrictions on space missions often lead to bandwidth reduction techniques in pick-up tubes. One scheme to reduce bandwidth, yet conserve high resolution, is to employ slow-scanning rates. Slow-scanning introduces a new dimension to the properties of the two tube types to be discussed.

The effect of slow-scan operation can best be noted by considering the operation of the target in both the image orthicon and vidicon tubes. The target section is the only portion of the device markedly affected by a non-standard scanning rate. Following this, the consequences of dynamic range linearity, S/N ratio, sensitivity, dark current, and resolution will be noted.

In the orthicon (Figure 2-2(a)) the scan beam brings the backside of the target section to zero potential during the scan period. The front side is at a low potential (approx. zero) due to the divider action of C_M and C_T distributing the +2 potential of the mesh, (i.e., $C_T >> C_M$). At scanning rates of interest there is no effect due to R_T . Between scans high velocity electrons striking from the photocathode cause secondary electrons to be emitted from the target. The secondaries are collected by the mesh which then leaves a positive charge distribution on the front side

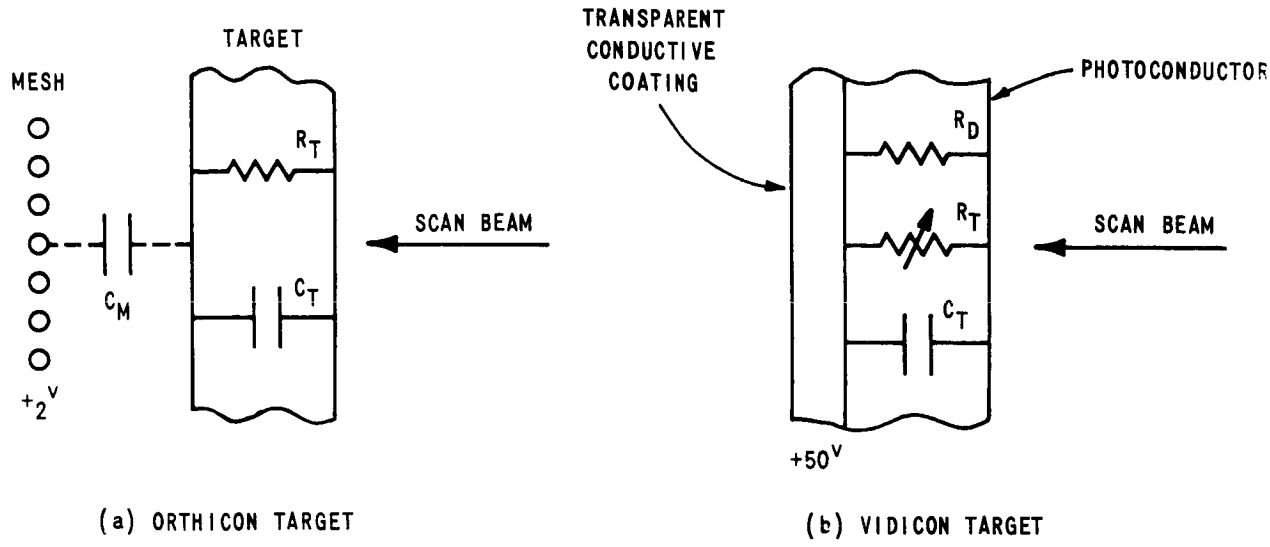

Figure 2-2 EQUIVALENT CIRCUIT OF A SMALL TARGET ELEMENT

of the target. The charge distribution across C_T then discharges through to the rear by R_T* with a time constant $R_T C_T$ sec. The output signal is obtained from the varying current of the returning scan beam indicating how many electrons/element were required to return the target to zero potential.

In comparison, the vidicon (Figure 2-2(b)) receives the incident light directly and causes a spatial redistribution of the photo resistive element R_T with light level. As with the orthicon, the scan beam returns the target to zero potential with the current required to charge to zero volts constituting the useful output signal. The discharge across the target has a time constant $C_T(R_T + R_D)$ sec where R_D represents a fixed

*If R_T is too small, there is a possibility of conduction between adjacent elements causing resolution loss; if R_T is too large, loss of signal strength will occur at higher frame times due to incomplete discharging across the target.

resistive element which will enable signal flow even without incident light. This, as previously mentioned, is known as dark current; and is an innate problem for slow scan operation.

Parametric effects due to slow scan operation

a) S/N and sensitivity

Orthicon - For a constant number of raster lines the bandwidth will vary inversely as frame time, and for a constant target charge so will the signal current. The primary noise source is thermal, with a flat frequency (power) spectrum. Thus the noise will vary as the square root of the bandwidth. Similarly, increasing beam current brings increasing noise, so that noise also varies as the square root of the signal, and, as summarized below, S/N ratio is independent of frame time.

$$\begin{aligned} B &\propto \frac{1}{T} \\ S &\propto \frac{1}{T} \\ N &\propto \sqrt{B} \\ N &\propto \sqrt{S} \\ \frac{S}{N} &\propto \frac{1/T}{\sqrt{1/T}\,\sqrt{1/T}} = \text{Constant} \end{aligned} \qquad (2\text{-}3)$$

Thus with orthicon operation, low scan rates constitute no S/N loss and experimentally show improved sensitivity as well (low light intensity x longer frame time).

Vidicon - In the vidicon, the significant noise voltage source is in the video amplifier which exhibit a linear rise with frequency, hence the S/N ratio is found to vary directly as the square root of T

$$\frac{S}{N} \propto \frac{1/T}{\sqrt{1/T}\;1/T} = \sqrt{T} \qquad (2\text{-}4)$$

Slow scan vidicon operation can therefore radically improve sensitivity at constant S/N ratio.*

*At commercial scanning rates, the vidicon enjoys about a 5db[28] advantage over the orthicon for equivalent image quality due to its frequency proportional noise spectrum.

b) Dark Current

Vidicon dark current, unfortunately does not just add a higher D-C component to the signal output at low scan-rates, the effect is nonuniform and causes shading and spot patterns to the image (among other deleterious effects). It can be controlled, within reason, by reduction of the signal electrode voltage which would represent a compromise with sensitivity. In actual operation, dark current can constitute about 3/4 of the total signal at low light levels.

c) Linearity of Sensitivity

In both the orthicon and vidicon, the linear range of response was reduced from over two orders of magnitude in light intensity to less than one when scan rates were reduced from 10 frames/sec to 1/30 frame/sec. Vidicon behavior is preferable, as better tonal reproduction is retained with higher light levels. Slow scan operation with the orthicon results in dips in the sensitivity plotted as a function of intensity.

d) Resolution

Orthicon resolution does not depend on frame rate per se except for the appearance of target mesh shadow at very low frame rates (due to reduced beam current). Target temperature, however, strongly limits orthicon resolution as typically noted below in Table 2-5.

TABLE 2-5

ORTHICON RESOLUTION AS A FUNCTION OF TEMPERATURE[29]

Target Temperature	Rel. Response(MTF)	No. Lines (Resolution)
35°C	50%	70 lines
0	50%	290 lines

Vidicon tubes do not exhibit this pronounced temperature sensitivity of the image orthicon and, in addition, show slightly improved resolutions at lower scan rates. This is probably due to smaller spot size resulting from a beam current reduction.

e) Vidicon Lag

Vidicon lag is only a problem at standard frame rates and becomes inconsequential at low scan rates.

2.2.3.5 Future Developments

The most promising new device for higher resolution is the grating storage target. This target consists of a set of closely spaced dielectric strips evaporatively coated onto the grooves of a grating ruled in metal tape. A charge pattern on the dielectric strips acts as a control grid, modulating the landing of beam electrons on the metal electrode. Operating voltages are chosen to prevent the beam from landing on the dielectric, both to provide multi-copy readout and to permit the use of a large reading beam current to provide a large signal output current, independent of the rate of scanning. Picture resolutions as high as 3800 TV lines per inch (75 line pairs per mm) at the tape have been reproduced. Although development of this device is not yet complete, Hall[30] predicts that the future of high resolution electron cameras will involve a choice of three approaches -- the grating storage tape system, the film record-flying spot scanner readout system, or the image dissector.

2.2.3.6 Television Camera Tube Sensitivity

We now turn to an investigation of the camera tube sensitivity levels necessary to provide minimal contrast detection between given picture elements. Considerations of system optics, statistical nature of photon emission, resolution and object luminance will determine the minimum tube sensitivity necessary to provide maximum contrast detection.

2.2.3.6.1 Statistical Nature of Photon Emission[31]

In television operation an image of a given scene is focused on a camera tube target. An ideal imaging device would be one which counted the photons arriving at each element during the integration period, (i.e., exposure time). It would then compare the results to determine whether a given element is brighter or darker than its neighbors. The arrival of photons, however, is a random process[32] and by experiment[33] has been shown to be gaussian in nature with a standard deviation equal to $\sqrt{n}$, where n represents the average number of photons striking the target from a given object element. Thus, the probability of the number of photons arriving from the given elemental area lying between is 0.69 (level of confidence). Consider the number of photons collected from two distinct elements, namely

$$n_1 \pm \sqrt{n_1} \tag{2-5}$$

$$n_2 \pm \sqrt{n_2} \tag{2-6}$$

For individual contrast detection we are interested in the obtained difference signal which, employing random process statistics, becomes

$$\text{Difference Signal} \propto n_2 - n_1 \pm \sqrt{n_2 + n_1} \tag{2-7}$$

The quantity $n_2 - n_1$ can be likened to the desired signal while the uncertainty $\sqrt{n_2 + n_1}$ provides noise, hence

$$S/N \propto \frac{n_2 - n_1}{\sqrt{n_2 + n_1}} \tag{2-8}$$

2.2.3.6.2 Minimum Contrast Detection

If the difference between n_2 and n_1 is large, it is seen that the S/N improves as $\sqrt{n_2}$. Suppose, however, we wish to determine the relationship between n_1 and n_2 under the imposed criterion of detection with a selected minimum contrast difference between them. As, for example, an often used contrast detection figure in digital TV transmission is 64 gray shades, indicating that 64 equal density steps

provide categories for each elemental area. Consider a desired number of gray levels to be k (requiring $\log_2 k$ digits for transmission).* We must, therefore, be able to detect a density change between elements of

$$\Delta D = \frac{|D_{MAX} - D_{MIN}|}{k} \tag{2-9}$$

where D_{MAX} and D_{MIN} represent the variation in dynamic range over a typical scene. A typical example might be $D_{MAX} = 2.1$, $D_{MIN} = 0.1$.

The densities are determined from the luminous flux gathered from the respective picture elements and may be denoted by

$$D \propto \log n \tag{2-10}$$

For the extreme case of minimum contrast difference detection, the difference of the average number of detected photons for the two elements may be approximated as

$$n_2 - n_1 = \left[\frac{2.3\,|D_{MAX} - D_{MIN}|}{k}\right] n_1 = \delta n_1 \tag{2-11}$$

The quantity, δ, is small and can be neglected in the denominator as (2-11) is substituted into (2-8)

$$\left(\frac{S}{N}\right)_{\substack{MINIMUM \\ CONTRAST}} = \frac{\delta n_1}{\sqrt{(2+\delta) n_1}} \simeq \delta \left(\frac{n_1}{2}\right)^{1/2} \tag{2-12}$$

or

$$(n_1)_{MINIMUM} \geq \frac{2\,(S/N)^2}{\delta^2} \ PHOTONS \tag{2-13}$$

2.2.3.6.3 Television Target Characteristics

Consider a TV raster of L lines with L resolvable bits/line** in a square array " a " millimeters on a side.

---

* or an analog sensitivity of ΔD .

** neglecting Kell factor and transfer function characteristics.

The L^2 picture elements have an integration time (exposure time) of τ seconds.*

The flux density required at the target is then given by

$$\frac{(n_1)_{MIN}}{\tau}\left(\frac{L}{a}\right)^2 = \frac{2\times 10^6 (S/N)^2}{\delta^2 \tau}\left(\frac{L}{a}\right)^2 \frac{PHOTONS}{METERS^2-SEC} \qquad (2\text{-}14)$$

giving a required target illuminance (for white light) of**

$$E \geq \frac{1.25\times 10^{-11}}{\tau}\left[\frac{(S/N)(L/a)}{\Delta D}\right]^2 \frac{LUMENS}{METER^2} \qquad (2\text{-}15)$$

Tube Characteristics - The sensitivity A of image tubes is usually expressed in terms of the minimum luminous energy (ft-candle-sec), necessary for satisfactory tube operation, hence, overcoming internal restrictions and equipment noise. The required target illuminance during exposure time τ is given by

$$E' = \frac{10A}{\tau} \frac{LUMENS}{METER^2} \qquad (2\text{-}16)$$

It is clear that

$$E \geq E'$$

or

$$A \leq 1.25\times 10^{-12}\left[\frac{(S/N)(L/a)}{\Delta D}\right]^2 \qquad (2\text{-}17)$$

---

* Note: Assuming that the scan time can be no shorter than the exposure time τ, the maximum bandwidth (for digital operation) is given by

$$B \leq \frac{L^2}{2\tau} \log_2 k$$

If the frame time T is greater than τ, the video bandwidth becomes

$$B \leq \left(\frac{\tau}{T}\right)\frac{L^2}{2\tau} \log_2 k$$

** The conversion of photons/sec to lumens depends on the spectral sensitivity of the detector. For this analysis a value of 3×10^{16} photons/sec/lumen was assumed.

2.2.3.6.4 Optics Considerations

The target illuminance is obtained from the luminous flux of the object regions as focused by a lens system. It can be easily shown that target illuminance is related to object luminance by

$$E = \frac{\pi B}{4f^2} \frac{LUMENS}{METER^2} \qquad (2\text{-}18)$$

where

B luminance (candles/m^2)

f f/no. of optical system

πB luminous emittance

neglecting absorption by the atmosphere and the optical elements.

2.2.3.6.5 Example

From the above considerations it can be shown that a sensitivity of 5.5×10^{-5} ft-candle-sec is necessary to distinguish 64 gray levels in a scene having a luminance of 1.7 candles/m^2. Other parameters used to obtain this result were: S/N = 10, L = 500, a = 25mm, f# = 2 and τ = 1/60 sec.

Thus it is seen how the various scene and system parameters define the sensitivity requirement.

2.2.4 Unconventional TV Systems

2.2.4.1 Electrophotography - A method which has considerable potential as a temporary storage medium for transmitting topographic imagery is electrophotography. Its potential advantages are high geometrical fidelity, high resolution, a large number of resolution elements on the format, operation in a vacuum and at a low temperature and an extremely high resistance to gamma radiation. It is reusable, light, and, in principle, simple. However, the performance is determined by the present methods of readout, during which some of the above advantages are lost so that further development is necessary. The present methods of readout and their limitations are discussed and possible techniques for minimizing them are described. It is not known which is the best method. It is believed that despite present limitations the potential advantages are sufficient to justify consideration of electrophotography as a temporary storage medium.

Among the many variations of electrophotography described in recent books by Dessauer & Clark[34] and by Schaffert[35] is the frost process which permits optical readout. The maximum resolution which has been achieved is 400 photographic lines/mm. A permanent layer of plastic is deposited over the selenium. The surface is charged and exposed. The original charge is neutralized by a second corona discharge of opposite sign, but a double layer of charges remains on the plastic, resulting in a voltage gradient across the plastic. Heat or solvent vapor weakens the plastic and the electrostatic forces wrinkle it. Readout is made optically by picking up the light scattered from the wrinkles and arranging the optical elements so the specular reflection from the unexposed areas is not intercepted, or by intercepting the specularly reflected light only. After readout, and after the double layer has been dissipated by leakage, the plastic can be resoftened, whereupon surface tension restores the specular surface, and the plastic

is reused. (The name frost comes from the frosty appearance of the image). To date, however, this process has not been sufficiently developed to assess its utility. Other processes with which we are concerned use a plate which consists of a metal conductor upon which a layer of selenium about 25 to 100 microns thick is deposited. The plate is charged by spraying the selenium surface with ions from a corona discharge while the proper potential difference is maintained between the discharge device and the conducting substrate. The selenium plate is then placed in the image plane of a camera system, if it is not already there. The incident light causes the selenium to conduct and the surface charge to decrease. When properly exposed, the image appears as a surface charge distribution. The surface potential or charge can then be detected or measured by a suitable readout technique and the information transmitted.

A method of coating the selenium photoconductor on a belt without degradation of the image upon flexure has been developed. Thus, frames could be exposed on a continuous belt and the belt could be moved so that several pictures could be scanned for transmission at a convenient time.

Resolution - A resolving capability of 1000 line pairs per millimeter has been claimed[36] for the electrostatic image. However, in practice, one achieves less depending upon the method of readout. For example, 200 lines/mm is the limit for particle development on the selenium surface and 50 lines/mm after the particles are removed to a paper. The resolution achievable with vidicon (electron beam) scanning is 100 lines per mm. The frost process with its 400 lines/mm has more resolution than most of the other techniques.

Charging and Maintaining the Charge - The usual procedure of charging with a corona discharge is not applicable in

a vacuum, but there exist several possible alternatives. If an electron gun is used for readout, the same gun which scans the image could be used. Another method is the reverse of the image forming process. A voltage gradient would be applied and the surface flooded with light, the upper electrode being a thin transparent layer of conducting material deposited on glass and separated a small distance from the selenium. The glass would be removed if necessary when the surface is scanned. Still another possible method would be to use the image forming light to charge the surface.

The usual half life for the decay of the surface charge is about five minutes for commercial selenium plates. However, plates have been made by a Xerox proprietary process which have a vastly extended half life. (A well-known method of increasing the dark resistance of an insulator is to use a purer material). This half life would be long enough to permit transmission of the information in most cases. If air were present, it would be necessary to control the humidity in order to prevent loss of charge through the air.

Applications and Associated Readout Methods - Different applications require different readout techniques. The applications described are: (1) transmitting topographical imagery with sufficient resolution and geometrical fidelity to make a map and (2) transmitting star imagery, especially with the extreme precision required for stellar parallax measurement. Methods applicable to topographic information only are discussed first below.

A fast readout can be obtained with a vidicon gun. In fact, a vidicon consists of an electron gun, a photoconductor and a third electrode. The limitations of the vidicon are the limit of a total of 1,000 resolution elements in a row, the resolution limited to 100 lines/mm on the photoconductor and the expected geometrical error of $\pm$ 1/2% of the distance across the format. The problem of the limited number of resolution elements can be elininated by mosaicing, i.e., by moving

the gun with a mechanical "coarse scan" while the motion of the beam performs the fine scan. This kind of mosaicing causes less loss of information than the mosaicing of images obtained from different locations in space where there are discontinuities of the solar and reflection angles. The geometrical error is $\pm$ 1/2% of the distance across one of the mosaicing elements and the absolute error in measuring the distance across the format is no worse than the case of measuring a distance from one mosaicing element to the next.

If the geometrical error is too large using the above method, mechanical scanning could eliminate this error. The location of the resolution elements would be fixed mechanically in the system. The error in distance measurements would be determined by the error of the mechanical positioning of the elements which would be small, or by the effect of the resolution limit of the system. Mechanical scanning is admittedly slow but this would be the price necessary to pay for precision. Moreover, for some types of missions, particularly to the more distant planets, the available bandwidth may limit the transmission rate. Also, it may be possible to use multiple probes to speed up the readout.

One method of mechanical scanning is to scan with an electrometer probe. The main difficulty with this method is that the maximum resolution which can be obtained at the present time is about one line per millimeter. The ultimate limit of this method is not known but it should be possible to increase this resolution.

Another possible mechanical method of scanning would be to scan by moving a microscope objective which focuses a glow tube on an extremely small area of the selenium surface. The glow tube would be pulsed and each pulse would correspond to a TV resolution element. The light pulse would discharge the selenium plate over the resolution element. Some charge would disappear from the

substrate of the selenium as well as from the surface of the selenium and there would be an excess of charge on the development electrode. A voltage transient would appear across the high resistance connecting the development electrode with the conducting substrate of the selenium plate. This voltage, when amplified, would be the signal voltage. The pulse would eliminate the need for DC amplification. The duration of the light pulse and its magnitude should be small enough to minimize lateral diffusion of charges.

The nondestructive techniques of scanning an electrostatic image may have value as a point detector for stellar imagery because repeated measurements can be used to reduce certain errors. Nondestructive methods may also be applied to topographical imagery if desired.

In the following, a scanning technique will be described in which the potential distribution on a camera tube target is read by a scanning beam without destroying the charge pattern on the target.[37] Although the experimental work was accomplished for image orthicon application, it may well be feasible for similar type behavior to be utilized for proposed electrophotographic high resolution systems.

The underlying principle is similar to the image isocon, the major differences being that electrons from the scanning electron beam are not scattered but reflected from the target, and thus do not discharge the target. In operation, a field mesh alters the potential uniformly such that the reflected scan electrons have return trajectories which are distorted by the stored charge gradients on the target. The output signal is essentially the first spatial derivative of the charge density.

Notes:

1) Resolution of the system is a function of beam spread, of the order of several microns diameter,

2) Use of a velocity selector on the scanning beam will increase signal modulation and avoid image defects.

Another possible method of nondestructive readout which should be investigated is scanning with a field effect transistor. Such a transistor can be made very small, a few microns across. It would be moved across the plate as close as possible. The current passing through the transistor would be controlled by the field near the plate. Such a technique, hopefully, would eliminate the problems associated with the grid leak of a vacuum tube and have the required high input impedance.

Another possible method to be investigated does not destroy the charge on the surface. A small electrical probe protrudes through a hole in the conducting electrode. The oscillation of a piezoelectric crystal causes the probe to oscillate between a location close to the selenium surface and a location shielded by a hollow electrode. The potential of the probe oscillates with an amplitude proportional to the difference in potential of the selenium surface and the electrode. In order to obtain high resolution, the probe must be close to the surface and all the clearances must be small.

It should also be recalled that the optical readout of the frost process is nondestructive. It is not known whether the frost process has adequate geometrical fidelity for stellar imagery. The optical readout also permits considerably greater mechanical scanning rates than other mechanical systems because the optical lever may be used.

Response Characteristics - The photographic speed of the selenium plate varies according to the processes, but it corresponds to an ASA speed of 1 to 3 (image orthicon ASA rating $\approx$ 1000). This compares with SO-243 which has a Kodak speed for aerial films of 1.6 or about 3.2 ASA.

The spectral response of pure amorphous selenium has a peak at 4400 angstroms and cuts off at 5800. However, by the addition of impurities and varying the technique of depositing the selenium, sensitivity in the red can be obtained.

A quantum efficiency of 50 to 100% has been calculated in the spectral region of high sensitivity, neglecting the reflected light which is about 25%.

The response is linear with exposure, provided over-exposure does not occur.

Comparison with Other Methods - Because the electrostatic storage is temporary, it is not possible to bring the imagery back to earth unless it is converted to some permanent form. Admittedly, such a process may be complicated in a space vehicle without gravity or air.

One advantage over film is the radiation resistance. One roentgen is sufficient to fully expose TRI-X film. Film must be developed before the X-ray exposure is excessive. A heavy exposure of X-rays causes no deterioration of the simple selenium layer; however, X-rays can discharge a stored electrostatic image. For transmission purposes, the radiation limit would be determined by the radiation limit of the associated electronics. Thus, where a planet has a strong magnetic field, electrophotographic methods must be preferred to film either for temporary or permanent storage.

The high quantum efficiency, 50% versus 1% at best for film, shows that electrophotography is potentially superior. The quantum efficiency sets an upper limit for the resolution and is important in determining the speed, but the present lack of amplification methods and readout techniques has limited the performance. The speed is

almost equal to SO-243, the Kodak High-Definition aerial film which is slower than optimum, but is usable in high altitude aerial camera systems.

The maximum number of lines on the format would be determined by the lens rather than the sensing surface as is the case of fine grain film. This greatly exceeds the 1000 TV lines which is the state of the art for standard TV tubes.

The maximum temperature to which the selenium can be subjected is about 105 degrees Fahrenheit at which temperature crystallization begins to occur. Other materials exist which can withstand higher temperatures, but their properties are not so favorable. Film and TV can withstand somewhat higher temperatures, but they have shorter lives at higher temperatures.

In comparison with film, no development is necessary, except for frost. Operation could probably be maintained at a very cold temperature as would be the case when photographing the outer planets and the selenium plate is reusable.

Conclusions Regarding Electrophotography - If a mechanical scan type of readout is necessary to obtain geometrical fidelity, film is objectionable because of its susceptibility to radiation and the excessive weight required because it is not reusable and because of the requirement for development. Thus, electrophotography has not been developed sufficiently to prove experimentally that it is feasible. Moreover it is not known which of several methods of readout is the best. More theoretical and experimental work is necessary in order to evaluate it properly.

2.2.4.2 Rotating Mirror Scanners - A sensor similar to the strip camera has a rotating mirror which keeps sweeping

the image past an electro-optical transducer or detector. The most common form is the infrared strip mapper which is too well known to be described further. Its steady output minimizes the band requirement of the following system whether it be a transmission system or a recording system.

One objection to this scanner is the short residence time of a detector on a resolution element. This time is sometimes as short as one microsecond for an IR scanner. This short period of time is necessary in order to obtain a large number of resolution elements. However, this short exposure or integrating time means that the signal-to-noise ratio is relatively small. This problem would be aggravated by the high speeds of satellites. The use of multiple detectors would improve the situation. Another objection is the rapidly rotating parts which may be a cause of failure. The mechanical scanner is a state of the art device in subsonic aircraft, but obtaining a sufficient number of resolution elements to form useful imagery from a satellite is doubtful because the vehicle will have moved too great a distance between scan lines.

2.2.4.3 Fiber Optics Scan Technique - A most interesting scan technique is described in the literature[38] with possible applications to the lunar orbiter mission. The scan system employs a unique fiber optic geometrical arrangement which transforms a CRT circularly scanned spot into a line (as in Figure 2-3)which scans the transported processed film orthogonal to its motion. The weight of a conventional camera system performing the same tasks is more than double that of the fiber-vidicon unit. The scanning resolution of 50 lines/mm is primarily limited by fiber diameter (20μ)* and not electron beam width. If smaller fibers were manufactured, perhaps

*Practical figures based on the state of the art.

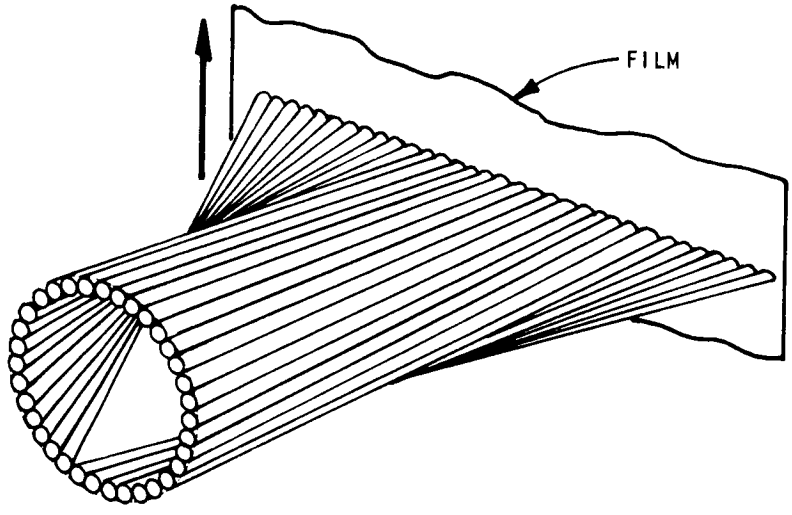

Figure 2-3 FIBER OPTICS SCANNER

1μ, this would probably represent an upper resolution limit consistent with state of the art electrom beam widths of $\sim 1\mu$.

Although there are certainly more resolution elements/line due to larger usable area, the major advantage of photographic film, i.e., very high resolution, is not retained. The film is used primarily as a storage medium. Real time TV transmission is impossible from the moon's dark side due to communication problems and is not feasible from the bright side due to high TV bandwidth requirements (necessitated by short orbit period of the vehicle). The use of photography is engendered by the urgent program schedule, requiring the use of proven processes.

The strip film technique is necessary to provide a good base/height ratio with high resolution. For example, a typical photographic coverage of the moon according to Lunar Orbiter Mission goals requires an 8 meter resolution at a 46 km vehicle altitude with $\sim$ 35 km base coverage; a 500 line TV system would only be able to cover a base width of 4 km with the same resolution. An improved TV system (larger area) of say 4000 lines would be necessary for comparable base width coverage.

2.2.4.4 Sequential Switching Scanner - A strip camera using a row of detectors is called a sequential switching scanner. It has the advantages of no moving parts, no limitations on the number of lines resolved across the format except as limited by the lens or the number of detectors which it is convenient to fabricate, lightness in weight, simplicity, and resumably high reliability. A block diagram of a system to be investigated is shown in Figure 2-4. No device as described has actually been built but the components are believed to be within the state of the art.

The photodetectors can be made by thin film techniques. It is believed that detectors as small as 10 microns across

can be made although this may be smaller than the optimum size. It is believed that the other electrical components can be made by similar techniques.

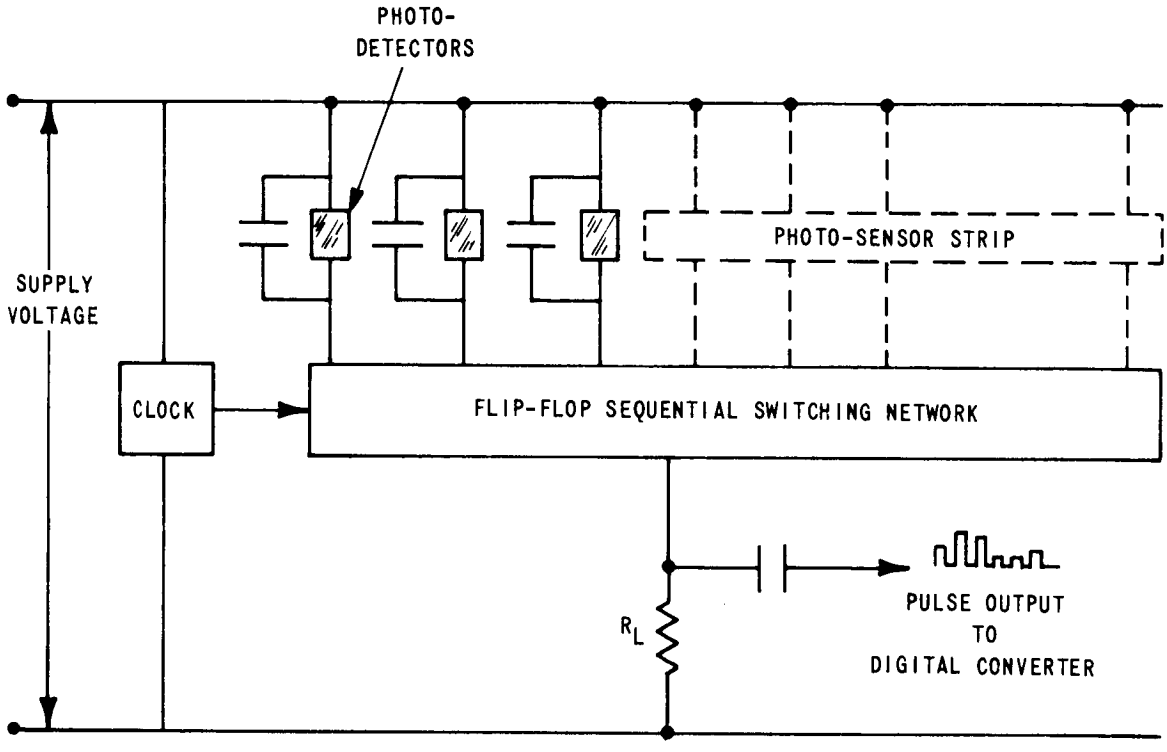

Figure 2-4 SEQUENTIAL SWITCHING SCANNER

A voltage is to be applied to each semiconductor. A charge proportional to the incident illumination plus a quantity dependent upon the dark current would build up on each ferroelectric condenser. A flip-flop sequential switching network causes each condenser sequentially to discharge through the load resistor. An electronic timer provides the proper timing for each discharge. The maximum voltage across the load resistor is measured and expressed in digital form.

At some stage it would be necessary to subtract an amplitude corresponding to the dark current. Also, it would be difficult to make each detector with exactly the same sensitivity. Therefore, it would be necessary to calibrate each detector by using, as the object of the lens, a surface with uniform illumination. The variation in sensitivity would be corrected for each detector by a computer as part of the data processing before display. If the sensitivity of the detectors should vary during flight, corrections could be made on a statistical basis, i.e., the average output of each detector should be the same.

This arrangement would preserve the photometric information better than other systems. A row of detectors has been suggested as a means of obtaining photometric information.[39] This method would work for the near infrared and probably the thermal infrared. By using several rows of detectors with different filters and/or detectors in each row, spectral information could be obtained. This system is similar to the strip camera in that stereo is most conveniently obtained by the use of two sensors. It should also be pointed out that image motion compensation will be difficult to obtain in this system.

2.2.5 Conclusions and Recommendations

From the previous subsections, we can conclude the following:

The requirements for stereo include two images of the same scene taken from separated observation points, a distance measurement to provide scale and some attitude control or measurement. Resolution requirements are determined from the mission objective.

A review of the cameras available indicates that a frame camera with a between-the-lens shutter is necessary in order to prevent vehicle motion from causing distortion. Photographic film

provides an excellent high resolution storage medium for topographical information but suffers from lack of real time capability. Processing requirements and non-reusability are additional disadvantages which contribute to extra weight.

Photo-electronic imaging systems are rapidly advancing to rival film as a high resolution medium. The variety of tubes available and their numerous applications, as well as the real time capability they provide, indicate an over-all ability which makes them desirable for most space applications.

Methods of imaging such as electrography, as yet untried in space applications, offer hope of further improvement.

The present review has considered the capabilities and limitations of imaging devices for stereo acquisition, primarily as separate subsystems. Therefore, it is recommended that before a choice of acquisition method or sensor is made, an analysis of a total system model should be carried out in order to pinpoint whether a subsystem requires more research (e.g., electrography) or more development (e.g., line resolution in image tubes) to accomplish the mission established by user requirements. If state-of-the-art subsystems do not meet these requirements, each subsystem should be evaluated to determine which one most severely limits the total system to establish priorities of limitation elimination by further research and development effort.

2.3 Errors in Stereophotogrammetry

Errors in cartography are conveniently divided into: (1) errors in identification of detail because of limited sensor resolution, (2) errors in the relative location of two features in the same stereo pair, and (3) residual errors after triangulation for the planet or satellite as a whole. The next subsection presents motivation for acquiring high resolution

reconnaissance data separate from the coarse cartographic data, discusses the types of cameras suited for this task, and includes equations and tables, giving the resolution to be expected under various conditions. In subsequent subsections a specific cartographic system is considered and the local and long distance errors of this system are analyzed.

2.3.1 Resolution Limits in Planetary and Satellite Cartography

In this subsection the resolution possible using separate reconnaissance imagery of a planet or satellite is discussed. The imagery is to be obtained by using an artificial satellite and used to supply the finer detail for the map. The discussion is limited to planets and satellites assumed without atmospheres.

The description of the surface is, on earth, usually divided into a coarse and fine scale. The coarse relief is shown by the use of contour lines, and the fine detail is shown by means of notes and legends. The fine detail referred to above includes whether the area is swampy, well drained, or desert; whether it is rough or smooth on a scale finer than that of the contour interval; and if there are any types of cultural features. The use of coarse and fine scales results in maps which are considerably easier to draw and read than, for example, the hypothetical process of showing swamps by the use of a 5 cm contour interval. Similarly it may reasonably be expected that there will exist in planetary topography detail considerably smaller than the contour interval which should be included in maps. On earth this fine detail is obtained, in part, by field inspection from previous maps made to a poorer standard of geometric fidelity, but with fine specification of detail, and by questioning inhabitants of the area. Other sources of detailed information are reconnaissance efforts and the source of information used for the coarse topography. Because the first mentioned sources of detail information will not, in most cases, be available, and because the requirements of topographical imagery are somewhat incompatible with those of detail or reconnaissance imagery, it may be necessary to obtain separate reconnaissance imagery for cartographic use.

The relationship between the visibility of detail in imagery and resolution as measured by bar charts or spatial square waves is not exact. However, the resolution is a good indicator if it is measured at about the same contrast as the detail desired. The complete study of image quality versus detail detectibility is beyond the scope of this section.

To obtain three dimensional information in a readily extractible form by using a film or television camera, one takes pictures from two stations. Reasonable values for the angle between these stations might be from 25° to 75°, depending on the desired relationship of detail in the three dimensions. Because aberrations decrease the resolution of lenses off axis, when the highest resolution is sought , the lens is designed for and used only near axis. These requirements imply oblique photography. Because, as shown below, in many cases the resolution will be limited by the available illumination rather than by diffraction, improved resolution can be obtained by using image motion compensation. Because of considerable difficulties in obtaining proper compensation over the format in other types of cameras, a strip camera is preferred. Since there are no requirements for geometric fidelity, this camera could use either film or a television pickup tube. If the latter is used, the tube must be either an orthicon or some other tube without noticeable lag under the conditions used, and a suitable image compensation method must be developed.

Derivation of Resolution Equation - Assuming that focal length and exposure time are chosen so as to maximize resolution, a formula is derived in the following paragraphs which gives the resolution as a function of surface and sensor characteristics, lens aperture, vehicle stability, and IMC accuracy. The plan of attack is to find the relationship between exposure time and the degradation caused by uncompensated image motion, and that between exposure time and sensor degradation. Then the total degradation may be minimized with respect to exposure time, and the resolution computed.

The apparent speed of motion of a fixed point viewed from a rotating (but otherwise assumed stationary) vehicle is

$$v_r = \left[(QZ - RY)^2 + (RX - PZ)^2 + (PY - QX)^2\right]^{1/2} \qquad (2\text{-}19)$$

where P, Q, R = roll, pitch, yaw rates in radians per second
and X, Y, Z = perpendicular components of distance to the fixed point, X along P, etc.

Because we are dealing here with oblique strip cameras and considering only points in object space which are near the optic axis Y will be small compared to X and Z. Also, letting $X = \pm Z \tan \alpha$, where α is the look angle of the camera measured from the vertical, the above expression may be simplified to

$$v_r = Z\left[P^2 \mp 2PR\tan\alpha + R^2\tan^2\alpha + Q^2\sec^2\alpha\right]^{1/2} \qquad (2\text{-}20)$$

The above equation applies to instantaneous values. To obtain expected values, it is assumed that the expected value of PR is zero, so that the equation for expected values is

$$\hat{v}_r = Z\left[P^2 + R^2\tan^2\alpha + Q^2\sec^2\alpha\right]^{1/2} \qquad (2\text{-}21)$$

As noted before, IMC is necessary when the highest resolution is being sought. The compensation requires the measurement of the angular velocity of the area being photographed due to linear vehicle motion. This is given by

$$\vec{I} = \frac{\vec{V} \times \vec{S}}{|\vec{S}|^2} \qquad (2\text{-}22)$$

where $\vec{V}$ = velocity of vehicle with respect to a coordinate system whose origin is fixed with respect to the ground but whose axes are parallel to the vehicle axes, and
$\vec{S}$ = vector from vehicle to area being photographed.

This expression reduced to the more familiar v/h for vertical photography from a vehicle which is not crabbed. The apparent velocity normal to the line of sight is then

$$\vec{v}_N = \vec{S} \times \vec{I} \tag{2-23}$$

If there are errors in measurement or implementation of the compensation, then there will be an error velocity

$$\vec{v}_\epsilon = \vec{S} \times \Delta\vec{I} \tag{2-24}$$

where $\Delta\vec{I}$ = IMC error.

Because $\vec{I}$ is be definition normal to $\vec{S}$, and the measured value of $\vec{I}$ may be resolved normal to $\vec{S}$ without error, the IMC error will be normal to $\vec{S}$ and the magnitude of its effect may be found by the simple product,

$$|\vec{v}_\epsilon| = |\vec{S}||\Delta\vec{I}| \tag{2-25}$$

If it is assumed that the IMC error is not correlated with the instability, the total expected uncompensated velocity is

$$|\vec{v}_\Sigma| = \mathcal{Z}\left[P^2 + R^2\tan^2\alpha + Q^2\sec^2\alpha + |\Delta\vec{I}|^2\sec^2\alpha\right]^{1/2} \tag{2-26}$$

The expected image smear, scaled to object space, is thus the product of the expected apparent object speed and the exposure time t, or

$$s_1 = v_\Sigma \cdot t \tag{2-27}$$

The exposure on axis of a camera is given by

$$X' = \frac{E_i \rho t}{4(T\#)^2} \tag{2-28}$$

where E_i is the incident illumination, $(T\#)$ is the lens focal ratio (or f-number) divided by the square root of lens transmittance, and ρ is the reflectance. The above formula is an approximation which assumes that the focal ratio squared is considerably larger than 1/4. The reflectance ρ must be defined as the ratio of luminous flux reflected in the direction of interest to that which would be so reflected by the ideal diffuse reflector. This definition of reflectance yields an applicable, measurable (on laboratory

samples) concept, but it may result in reflectances greater than one. The above formula was then found by combining Lambert's Law, the law of conservation of brightness, and the above definitions of $T^{\#}$ and reflectance.

The sun is the only significant source of illumination in the solar system for planets and most satellites. Some of the inner satellites of Jupiter and Saturn are sufficiently close to their primaries in comparison to the size of their primaries to receive significant light by reflection. However, the maximum total illumination on these satellites is not significantly greater than that due to the sun alone, except possibly at their extreme northern and southern regions. This condition exists because it is obviously impossible for any area to be in full sunlight and full primary light at the same time. Accordingly, only sunlight is considered

The illumination by the sun on a normal plane at a distance equal to the mean earth to sun distance, or one astronomical unit (AU), is given by Reference 40 as 1.367×10^5 lumens/meter^2. The solar illumination on any surface not protected by an atmosphere is then given by

$$E_i = \frac{1.367 \times 10^5 \ (\text{LUMENS/METER}^2) \sin L}{a^2} \qquad (2\text{-}29)$$

where a = semi-major axis of orbit, taken as a typical distance measured in astronomical units

L = sun elevation.

The luminous energy per television type resolution element required for an adequate exposure may be found by multiplying the exposure by the resolution element size, or half the reciprocal of the optical (line and space) resolution in lines per unit distance. This is done because the luminous energy is a more useful parameter than the exposure. This quantity will depend on the choice of the point on the transfer function and the signal-to-noise ratio.

Letting δ_2 be the above mentioned resolution element size and q be the luminous energy required, one has

$$q = X' \delta_2^2 \tag{2-30}$$

This may be related to resolution in object space normal to the line of sight by the scale, or

$$q = \frac{X' \delta_3^2 F^2}{Z^2 \sec^2 \alpha} \tag{2-31}$$

where δ_3 is the resolution element size in object space, and F is the focal length.

The above equations may be combined to yield,

$$\delta_3^2 = \frac{q Z^2 \sec^2 \alpha (4a^2)(T\#)^2}{F^2 \rho t \sin L \ (1.367 \times 10^5)} \tag{2-32}$$

If D is taken as the diameter of the entrance pupil, reduced to compensate for observation and absorption, or $D = F/T\#$, then

$$\delta_3^2 = \frac{4a^2 q Z^2 \sec^2 \alpha}{D^2 \rho t \sin L \ (1.367 \times 10^5)} \tag{2-33}$$

This is to be compared to the square of the motion degradation, also from above, which is

$$\delta_1^2 = Z^2 \left[P^2 + R^2 \tan^2 \alpha + Q^2 \sec^2 \alpha + |\Delta \bar{I}|^2 \sec^2 \alpha \right] t^2 \tag{2-34}$$

Assuming that the resolution may be estimated by combining these degradations in a root-sum-square manner, the overall resolution in object space normal to the line of sight is

$$r_0 = \frac{1}{2\sqrt{\delta_1^2 + \delta_2^2}} \text{ line pairs/unit distance} \tag{2-35}$$

where the factor of 2 arises from the conversion from lines to line pairs. Substitution of the previous values into equation (2-35) and choice of optimum exposure time obtained by differentiation gives

$$r_o = \frac{2^{-\frac{1}{3}}\, 3^{-\frac{1}{2}}}{\bar{z}\sec\alpha} \sqrt[3]{\frac{\rho(\sin L)\, D^2 (1.367\times 10^5)\ \frac{\text{LUMENS (AU)}^2}{\text{METER}^2}}{q\, a^2 [P^2\cos^2\alpha + R^2\sin^2\alpha + Q^2 + |\Delta\bar{I}|^2]^{1/2}}} \qquad (2\text{-}36)$$

The combination $\rho \sin L$ is, in astronomy, replaced by $A\phi$, where A is called the normal abedo, and ϕ the photometric function. A is the reflectance for normal incidence and viewing, and the directional properties of reflectance are combined with the sun elevation into the photometric function ϕ. By incorporating this change, one has

$$r_o = \frac{0.229}{\bar{z}\sec\alpha} \sqrt[3]{\frac{D^2 A\phi\, (1.367\times 10^5)\ \frac{\text{LUMENS (AU)}^2}{\text{METER}^2}}{q\, a^2 [P^2\cos^2\alpha + R^2\sin^2\alpha + Q^2 + |\Delta\bar{I}|^2]^{1/2}}} \qquad (2\text{-}37)$$

In some cases, however, the resolution may be limited by diffraction. It is therefore necessary to compute the resolution assuming diffraction limits and take the lesser of the two resolutions. Taking the diameter of the airy disc as the width of a resolution element gives, by using standard diffraction theory,

$$r_o' = \frac{1}{\bar{z}\sec\alpha}\left[\frac{D}{4.88\lambda}\right] \qquad (2\text{-}38)$$

where λ is the effective wavelength. Taking $\lambda = 0.55 \times 10^{-6}$ meter, one has

$$r_o' = \frac{1}{\bar{z}\sec\alpha}\left[\frac{D}{2.68\times 10^{-5}\ \text{METER}}\right] \qquad (2\text{-}39)$$

Determination of "q"

In order to substitute values into equation (2-37) and determine the available resolution, one must determine q, which as noted before, depends on the resolution criterion. This was done for three films using manufacturers' data. It was assumed that the films were sufficiently

exposed to give a density of 1 with maximum recommended development, and the resolution corresponding to a test object contrast of 1.6:1 was used. The image quality parameters of television pickup tubes are usually stated in a different manner. For such tubes it was assumed that the resolution is given by the 40% point on the square wave transfer function, and that 6 : 1 is an acceptable (voltage) signal-to-noise ratio. It is believed that this corresponds to the film case. The q value for the RCA-4401VI image orthicon was computed from the manufacturer's data by the following steps. First, the number of resolution elements corresponding to the 40% point was noted. The bandwidth corresponding to this normal broadcast conditions was computed. Using the rule that the noise is proportional to the square root of the bandwidth and the specification signal-to-noise ratio, the signal-to-noise ratio was computed for the new bandwidth. Then, a new operating point was found such that the signal-to-noise ratio would be 6 : 1. Next, the number of resolution elements was divided into the horizontally scanned dimension of the tube to find the horizontal dimension of the elements. The vertical dimension was found by using the standard 500 lines per frame and a Kell factor of 0.7, together with the vertical scanned area dimension. Finally, the luminous energy per resolution element may be found by multiplying the area by the exposure. The calculation is summarized below.

The values are also listed for the films considered. No vidicons were considered because their noise depends on amplifier characteristics.

40% resolution	425 elements
Implied bandwidth	4.08 megahz
Signal-to-noise ratio for 4.5 megahz and 7.5×10^{-2} $\frac{\text{lumen}}{\text{m}^2}$ input	40 to 1
Signal-to-noise for 7.5×10^{-2} $\frac{\text{lumen}}{\text{m}^2}$ and 4.08 megahz	42 to 1

Input for signal-to-noise ratio of 6 : 1	$1.08 \times 10^{-2} \frac{\text{lumen}}{\text{m}^2}$
Exposure (Time = 1/30 sec)	$3.58 \times 10^{-4} \frac{\text{lumen-sec}}{\text{m}^2}$
Width of scanned area	3.66 cm
Element width	$\frac{3.66}{425} = 8.6 \times 10^{-3}$ cm
Height of scanned area	2.83 cm
Element height (Kell factor = 0.7)	$\frac{2.83}{500 \times 0.7} = 8.1 \times 10^{-3}$ cm
Luminous energy per resolution element	2.42×10^{-12} lumen-sec

TABLE 2-6

ENERGIES PER RESOLUTION ELEMENT

(Computed from Manufacturer's Data)

RCA	4401VI	Image Orthicon	2.34×10^{-12} lumen·sec
E K	SO-243	Film	1.67×10^{-12} lumen·sec
E K	SO-136	Film	1.66×10^{-12} lumen·sec
E K	8401	Film	0.99×10^{-12} lumen·sec

Calculation of Resolution Values

Using the above formulas, resolutions were computed for two planets and two satellites, all assumed to have negligible atmospheres. Those chosen were Mercury, Moon, Ganeymede, and Pluto. Not much is known about the atmosphere of Pluto, but it was decided to include it as an extreme case. The data listed in Table 2-7 were used.

TABLE 2-7

ASTRONOMICAL DATA

Object	Normal Albedo "A"	Orbit Semi-Major Axis, in A. U. "a"	Satellite Velocity km/sec
Mercury	0.06	0.387	2.94
Moon	0.07	1.0	1.68
Ganymede	0.20	5.20	1.56
Pluto	0.16	39.52	4.94

Two values were chosen for

$$\left[P^2\cos^2\alpha + R^2\sin^2\alpha + Q^2\right]^{1/2}$$

The first was 0.05 radian per second and is considered to be an example of a very unstable vehicle. The other was 0.0005 radian per second* and is a reasonable performance target for stabilization. Two values were chosen for $|\Delta\vec{I}|$, one corresponding to no compensation (i.e., $|\Delta\vec{I}| = |\vec{I}|$) the other to compensation with 1% error. As in the case of the moon, it was assumed that imagery can be obtained when $\phi > 0.1$. Other parameters chosen were

D = 0.06, 0.2 and 0.6 meters

z = 100, 30 and 10 kilometers and

α = 45°.

The luminous energy value for SO-243 film was used. Computation shows that the resolution values for the 4401VI would be only about 11% less, assuming (where IMC is shown) that a suitable IMC mechanism could be devised for use with a television camera tube. The results are shown in Table 2-8. In those cases, in which the resolution was limited by diffraction rather than illumination, the resolution values are underlined.

*For the Apollo spacecraft the stabilization requirement is 0.00035 radian/sec (see Reference 1).

TABLE 2-8

COMPUTED RECONNAISSANCE RESOLUTIONS

(In line pairs per meter)

Altitude Km	Aperture Cm	Mercury	Moon	Ganymede	Pluto
		NO COMPENSATION, 0.05 Radian/Sec			
100	6	0.117	0.0554	0.0262	0.00571
	20	0.261	0.1164	0.0583	0.01276
	60	0.542	0.256	0.1215	0.0266
30	6	0.311	0.1655	0.0785	0.01414
	20	0.692	0.378	0.1748	0.0315
	60	1.440	0.766	0.366	0.0646
10	6	0.668	0.358	0.1793	0.0298
	20	1.488	0.829	0.399	0.0665
	30	3.08	1.73	0.835	0.1383
		NO COMPENSATION, 0.0005 Radian/Sec			
100	6	0.1447	0.0812	0.0392	0.00642
	20	0.337	0.1806	0.0874	0.0143
	60	0.669	0.376	0.182	0.0298
30	6	0.323	0.1843	0.0875	0.01434
	20	0.720	0.396	0.1952	0.0320
	60	1.493	0.854	0.406	0.0656
10	6	0.672	0.376	0.175	0.0298
	20	1.496	0.837	0.406	0.0665
	60	3.11	1.742	0.846	0.1383
		1% COMPENSATION, 0.05 Radian/Sec			
100	6	1.209	0.0564	0.0266	0.00639
	20	0.270	0.1254	0.0593	0.01426
	60	0.560	0.261	0.1164	0.0297
30	6	0.404	0.1881	0.0887	0.0213
	20	0.899	0.419	0.1977	0.051
	60	1.867	0.871	0.417	0.0974

TABLE 2-8 (CONTINUED)

Altitude Km	Aperture Cm	Mercury	Moon	Ganymede	Pluto
10	6	1.209	0.564	0.266	0.0639
	20	0.269	1.254	0.593	0.1424
	60	5.59	2.61	1.164	0.296
		1% COMPENSATION, 0.0005 Radian/Sec			
100	6	0.158	0.158	0.1216	0.0265
	20	0.527	0.527	0.272	0.0594
	60	1.58	1.189	0.564	0.1230
30	6	0.527	0.527	0.363	0.656
	20	1.58	1.58	0.813	0.1462
	60	5.27	3.56	0.171	0.300
10	6	1.58	1.58	0.833	0.1383
	20	6.93	3.83	1.85	0.308
	60	14.4*	7.99	3.86	0.642

The relationship between resolution and the size of detectable objects is complicated by psychological effects. As a rough approximation one may take the requirement that the object size be about the distance covered by three line pairs; this may vary by a factor two depending on the training and fatigue of the observer and shape of the object.

Assuming that three line pairs are required for detection, inspection of Table 2-8 reveals that, except on Mercury (see asterisk), direct stereo detection of 0.3 meter objects (10 line pairs/meter resolution) is not possible within the assumed parameter values. However, sufficient resolution (20.6 line pair/meter) is available from direct stereo to determine slopes over regions on the order of the size of landing vehicles. The 0.3 meter objects may be detected by their shadows because (1) the shadows will be of high contrast, increasing system resolution, and (2) magnification is possible by using low sun angles. Thus, it appears that insufficient resolution is available to investigate prospective landing sites throughout the solar system.

Inspection of equation (2-37), which is repeated here for convenience of the reader,

$$r_o = \frac{0.229}{Z \sec \alpha} \sqrt[3]{\frac{D^2 A \phi (1.367 \times 10^5) \frac{\text{LUMENS (AU)}^2}{\text{METERS}^2}}{q a^2 \left[P^2 \cos^2\alpha + R^2 \sin^2\alpha + Q^2 + |\Delta \vec{I}|^2\right]^{1/2}}} \qquad (2\text{-}37)$$

reveals that little improvement in resolution is to be expected by improving vehicle stability, image motion compensation, or the characteristics of the sensitive surface, since these factors enter as the cube root. It appears that a more profitable approach for improving resolution is to improve the vehicle capabilities so that larger diameter lenses can be carried at lower altitudes, since the altitude and lens diameter have a more direct influence on the resolution.

2.3.2 Choice of Cartographic System to be Analyzed for Positional Errors

Any analysis of positional errors in topographical information must be based on the equipment and method used in obtaining this information. Therefore, a short study was performed to synthesize a likely system so that the error analysis would be applicable. The characteristics of several systems are discussed below and on the basis of this discussion, one of these was chosen for the error analysis.

The simplest system would use only a camera. Scale would be obtained by fitting together a sufficient number of photographs to include a recognizable feature which could be measured by some other means. It may be noted that if the other means is to measure from Earth, then a larger number of pictures must be fitted together to obtain scale information on the far side of the moon. For the planets, measurements made from Earth would not be possible. Because of the large errors anticipated with this system, it was not considered further.

The next more complicated system would consist of a camera and an altimeter. The purpose of the altimeter is to provide scale. This method could provide cartographic data over a small area, assuming a local datum surface and choice of directions. Problems would arise in attempting to tie together many stereo pairs taken this way because a small angular error in aligning two models would be multiplied by a long lever arm.

In order to permit the independent determinations of the directions of the upper base lines, or lines between camera stations, it has been proposed to use a star camera rigidly attached to the topographical camera. This would prevent the accumulation of errors discussed above. There are two problems associated with star cameras. The first is that the camera must have a large aperture, or sufficient shielding, so that fast film can be used, in order to secure sufficient exposure. The other is that the star camera will only determine the orientation of the topographical camera with respect to sidereal space. In order to determine

its orientation with respect to the body being photographed, it is necessary that the orientation of the object being photographed be known with respect to sidereal space. The orientation of the moon may be observed from Earth. It may be the object of another study to determine how accurately this may be done. The surface features of the planets, and hence the rates of change of orientations in sidereal space, are not visible to any degree of accuracy from Earth.

Finally, one may consider a system in which the camera location is to be determined by independent measurements from Earth. These measurements can be divided into two groups, those in which the camera location is to be determined instantaneously, and those in which it is to be determined by means of the orbit. Instantaneous determinations are inapplicable to the remote side of the moon. The determination of camera stations for planets and satellites other than earth and moon is limited because of the difficulty of observation. Determinations by interpolation in the orbit can be influenced by gravitational anomalies which are unknown.

On the basis of the above considerations, it was decided to analyze errors for the system using camera, altimeter, clock, and star camera, as this appears to be the most universal type of system.

Cameras are generally divided into the three classes of frame, strip, and panoramic (as discussed in Section 2.2.1). Because of difficulties in determining the orientation of strip and panoramic cameras, it is concluded that only frame cameras would be useful for securing the required coarse cartographic information.

Star cameras must be frame cameras in order to cover a sufficiently large part of the celestial sphere to insure that some stars will actually be photographed on any attempt, assuming reasonable exposure time, film speed, and camera dimensions.

2.3.3 Local Errors

As noted before, it is assumed that the cartographic system consists of a cartographic camera, an altimeter, a stellar camera rigidly fastened to the cartographic camera, and a clock. It is further assumed that a major portion of the surface is covered without gaps by one or many similar systems, so that the location of any image chosen for analysis may be determined from the triangulation which is discussed in Sub-section 2.3.4. The errors discussed in this sub-section are the most local errors imaginable, namely, errors in the relative location of two points both of which are imaged in each of two adjacent frames, chosen as a stereo pair for plotting. It is further assumed that the spot altitudes are to be given for these two points of interest to avoid the difficulties of including errors caused by interpolation between contour lines to find spot altitudes in the final maps. It is also assumed that the area covered by the stereo pair is sufficiently small that, for analysis, the datum surface may be taken as a plane.

Sub-section 2.3.3.1 contains a short description of the stereoplotting problem; portions of this sub-section may be omitted by readers familiar with the problem. Sub-section 2.3.3.2 lists sources of stereoplotting errors, and discusses those which are significant for planetary and satellite topography. Sub-section 2.3.3.3 contains an analysis of the effects of these most significant errors on the errors in relative location of the two points.

2.3.3.1 Discussion of Stereoplotting

The photogrammetrist has the following information available for analysis: (1) Two images of a portion of the surface to be mapped. Each of these images is (ideally) the projection of

surface features through a point onto a plane of (at this stage) unknown orientation. (2) A measured distance in object space from which scale can be determined. It has been assumed here that it is the distance from one of the projection points (or camera stations) to one of the object points. In other situations, the known distance could be that between two image points or between the two camera stations. (3) The location of the projection point* with respect to the image as given by location of the principal point**, the calibrated focal length***, and the distortion plot. If the camera has distortion, the location of the projection point may be considered to be a function of format position, as given by the distortion plots. (4) The orientation of at least one of the images with respect to sidereal space, as given by the star camera, and (5) The orientation of a co-ordinate system, including a datum surface, with respect to sidereal space.

Using the above information, the photogrammetrist is required to: (1) locate the feet of perpendiculars from the object points to the datum surface, and plot them, and (2) determine the lengths of these perpendiculars, which are called spot altitudes. As noted before, only spot altitudes are considered in this analysis.

The principal methods of stereoplotting are: The use of optical projection stereoplotters, the use of mechanical projection stereoplotters, or the use of analytic photogrammetry. Various

---

* The projection point corresponds to the second nodal point of the lens in an ideal system

** The principal point may be defined as the intersection of the lens axis with the film, as the foot of a perpendicular from the nodal point to the film, or as the point about which the simplest equation for image location gives the most symmetric errors.

*** In an ideal system, calibrated focal length is the distance from the second nodal point to the film measured along the lens axis.

combinations of these methods are possible, such as using analytic corrections with a direct viewing projection instrument.

In an optical projection instrument, the geometry of the exposure is duplicated on a smaller scale. Two or more projectors, similar to slide projectors, are set up to represent the cameras. The projected images form a stereo model. This stereo model is like an actual model of the surface to be investigated in that the line of intersection of an actual model surface and any arbitrary surface shows in the stereo model in the following way. If the arbitrary surface is introduced into the stereo model as a diffusing surface, then the intersection referred to above shows as the line along which there is no displacement between the optical projections of small parts of the two images. Stereo viewing techniques are used to accentuate displacements so that three-dimensional locations of these no displacement points, also called no parallax points, may be measured accurately. Various optical and mechanical arrangements may be used to compensate for known distortions. After the datum surface has been introduced into the stereo model (it may be the top surface of a large piece of slate, etc.), spot altitudes and locations of important features may be determined by measurements on the stereo model.

Mechanical projection plotters are much like stereoscopes. They contain in addition to regular stereoscope equipment, however, adjustments for properly orientating the images, compensation for various distortions, and a floating mark. The floating mark is a three-dimensional illusion of a spot of light which may be moved about so that measurements may be made. Analytic photogrammetry is performed by measuring the co-ordinates of the important features in both images by the use of a comparator, and using these co-ordinates and a digital computer to solve the photogrammetric problem.

Any of these methods (suitably modified) may be used to solve the photogrammetric problem in satellite photography. The

projection plotters require the addition of suitable reference points and surfaces so that the novel type of control may be introduced. Similarly analytic solutions require a modified program for the same reason. It appears that the projection plotters are least afflicted with errors caused by mechanical slack or play. The advantage of analytic plotting; namely the exact compensation of atmospheric refraction for off-vertical photography, is of no value when planets and satellites without atmospheres are considered. The error analysis in this section is based on the use of projection plotters as an aid in visualizing the situation; it should be realized that the analysis also applies for other methods.

When a stereo model is first set up on a projection plotter, it will be found that there are displacements normal to the plane continuing the two projectors and the vertical, between optical projections of the images of the same object. The projectors are moved until these displacements, called y parallaxes, are eliminated over the entire model. This elimination of y parallax establishes, except for the scale, the location and orientation of each projector in terms of the other, which is said to establish the relative orientation. If the absolute orientation of only one of the projectors is known, the relative orientation permits the absolute orientation of the stereo model to be determined from reduction of stellar and other data. Similarly, if the absolute orientation at each projector is known, a compromise may be effected which is likely to have less error than if the absolute orientation of only one is known.

2.3.3.2 Error Sources

Any error or deficiency in any of the data supplied to the photogrammetrist can cause errors in the results. Also, errors can arise in the photogrammetric process through the use of devices and techniques of limited accuracy. Finally, errors can arise in the presentation and publication process. Because of the large cost of obtaining the data supplied to the photogrammetrist, and because vehicle altitude will not be limited (downward) by vehicle performance, it may be safely assumed

that the data reduction and publication processes would be performed wherever possible with sufficient care and at a large enough scale to make errors introduced in these processes negligible. Hence, the errors to be considered are those in the data supplied to the photogrammetrist, with two exceptions which are noted later.

A critical examination of the data supplied to the photogrammetrist indicates the following possible sources of error:

1) Film distortion and unsharpness in the cartographic camera. (a) The film may be buckled or warped and not have the assumed plane surface at the time of exposure. (b) The film may shrink or stretch in an undeterminable manner during processing. (c) Images on the film may not be sufficiently sharp to permit their accurate location. *

2) Errors in the altimeter or other distance-measuring device.

3) Errors in the location of the projection point. (a) The shock of launch may cause the camera to distort mechanically, causing a change in the location of the lens with respect to the film. (b) It may also change the spacings of the lens elements, causing a change in the location of the (on axis) projection point. It may also change the distortion plot. These mechanical distortions can, in summary, change the calibrated focal length, distortion plot, and location of the principal point.

4) The orientation of the cartographic camera with respect to sidereal space will contain errors because: (a) all of the film and camera problems discussed above for the cartographic camera apply to the stellar camera also, (b) The orientation between the star camera and the cartographic camera may be changed as a result of mechanical shock.

---

* These factors have their counterparts in the case of recording media other than film; e. g., vidicon or orthicon image surfaces.

5) The orientation of the local co-ordinate system with respect to sidereal space depends upon the location of the local area and the orientation of the planet or satellite as a whole with respect to sidereal space. Hence, it will be subject to errors in (a) the location of the area covered by the stereo pair with respect to the planet or satellite, (b) errors in measuring the times at which the exposures were made, and (c) errors in the orientation of the planet or satellite given as a function of time.

Not all of these errors are included in the analysis. It is assumed that both cameras will be recalibrated, and their relative orientations redetermined by taking simultaneous stellar imagery enroute to the planet or satellite to be mapped. This implies that there are a large number of fiducial markers in both cameras so that orientation may be transferred from one to the other with negligible error. It is noted that the markers in both cameras will require illumination for the calibration where a star field is being recorded. The errors in the local co-ordinate system are eliminated from the analysis as follows: (a) The analysis of long-distance errors, presented in sub-section 2.3.4, shows that errors in location will be small in effect compared to other errors retained in the analysis. (b) It is assumed that the planet or satellite has sufficiently slow motion that clock errors will be negligible, and (c) Errors in determining the orientation of the planet or satellite are not included in this analysis. It is thought that further investigation will be required to determine likely values of these errors.

Therefore, the only errors retained for the analysis are film warpage, distortion and unsharpness in the cartographic camera, altimeter error, and similar film limitations in the stellar camera.

2.3.3.3 Local Error Analysis

Of the three types of errors retained, it is obvious that stellar camera errors cause errors in the orientation of the

stereo model, the altimeter errors cause errors in the scale of the stereo model, and the cartographic camera errors cause errors in the location of points with respect to the stereo model. In this sub-section, the effects of these errors are found and combined with previous errors.

It is in the determination of orientation that data processing errors are inherent. First, due to the great distances to the stars, analytical data reduction methods appear most suitable for determining absolute orientation. These analytic methods imply the use of a comparator. Because comparators do not use magnification (except possibly for viewing and setting cross hairs), any errors in the comparator will apply at film scale. Thus, it may be necessary to include comparator error in the stellar camera imagery error.

As noted before, the relative orientation permits the reduction of absolute orientation error. Because each image is part of at least two stereo pairs, it is possible to use a plotter with more than two projectors to permit absolute orientation of a stereo model to be based on absolute orientation data at more than two camera stations. A disadvantage of this system is that more projectors are required. Also, a practical limit to the number of projectors which can be used to advantage is reached when the error in the absolute orientation, as reduced by redundancy, is equal to the error in the relative orientation. The analysis in this sub-section is based on the use of a plotter using only two projectors; smaller orientation errors would result from the use of multiple projector plotters.

The orientation relationship between the model and the situation is represented by the Euler angles which are ψ, θ, ϕ. A complete description includes the order in which rotations of real space must be performed to arrive at model space. A local coordinate system is defined with x north, y east, z down. Then the rotations are ψ about z (yaw), θ about the new y axis (pitch) and ϕ about the new x axis (roll). All of these rotations are taken positive in the direction in which a righthanded screw must be turned to advance upon the named axis. This choice of angles was made in preference to others because it is well

defined and complete. Evaluation of the errors caused by model orientation consists of two parts; first, evaluation of probabilistic values of the Euler angles, and second, determining the effects of them.

The latitude and longitude considered as angles are expected to be considerably more accurate than the angles derived from the star camera. Thus, assuming triangulation has been performed, as discussed in a later sub-section, the latitude and longitude may be used together with the orientation of the planet or satellite to compute the location of the zenith on the celestial sphere, and the direction of north. Then the Euler angles are the rotations which must be performed to match the celestial sphere to the stellar imagery (see Figure 2-5). If the angles are small, they are approximately

$\psi \approx$ Angle between N-S line on imagery and computed N-S line (N-S means north-south)

$\theta \approx$ Component, along N-S line, of distance from center of format to zenith, divided by focal length of stellar camera

$\phi \approx$ Component, normal to N-S line of distance from center of format to zenith, divided by focal length of stellar camera

The rms errors in θ and ϕ, then, are the rms errors in zenith location divided by the focal length of the stellar camera. Assuming an rms error of μ_s in the location, * in one coordinate of a stellar image, and that M stars appear in the imagery, one has

$$\sigma\theta = \sigma\phi = \frac{\mu_s}{F_s\sqrt{M}} \qquad (2\text{-}40)$$

where

$\sigma\theta$ = rms error in θ

$\sigma\phi$ = rms error in ϕ

F_s = focal length of the star camera

* μ_s is the composite error due to film warpage and distortion and image unsharpness in the star camera and comparator error.

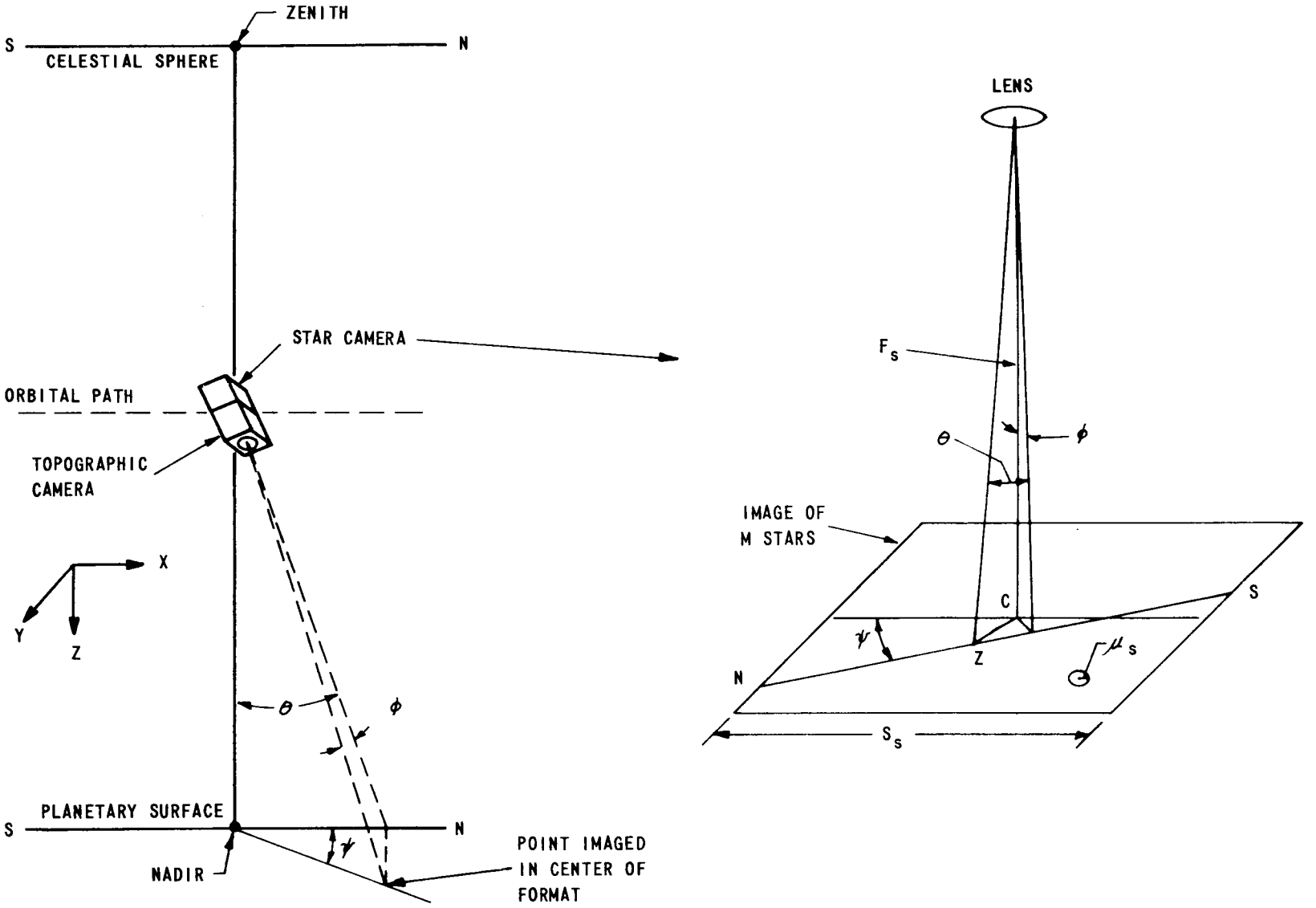

Figure 2-5 GEOMETRY OF ORIENTATION

The divisor for $\delta\psi$ differs from frame to frame, depending on the location of the stellar images. On the basis of an analysis not presented here, the expected value for the divisor was found to be $0.3826\, S_s$ where S_s is the side of the (assumed) square format of the stellar camera; thus

$$\delta\psi = \frac{\mu_s}{0.3826\, S_s \sqrt{M}} \tag{2-41}$$

It may be seen that larger errors are to be anticipated in yaw than in pitch and roll.

The error vector to be associated with the vector between two points on the surface is the difference between the actual vector and the indicated one. The indicated vector may be determined by multiplication of the actual vector by the transformation matrix from the local coordinate system to the erroneously oriented, distended one. Because the scale factor for the whole model is the altitude, as measured by the altimeter, the transformation, T, from the erroneously oriented system, to the distended, erroneously oriented one may be affected by multiplying by the scalar $\frac{h+\Delta h}{h}$, where

h = altitude

Δh = altitude error

Thus,

$$\delta\vec{V} = \left[\frac{h+\Delta h}{h}\, T - I\right]\vec{V} \tag{2-42}$$

where I = unit matrix. The transformation matrix can be derived to be using small angle approximations.

$$T = \begin{bmatrix} 1 & \delta\psi & -\delta\theta \\ -\delta\psi & 1 & \delta\phi \\ \delta\theta & -\delta\theta & 1 \end{bmatrix} \tag{2-43}$$

The error matrix may be found as indicated above. When this is done, and small terms are neglected, one has

$$\begin{bmatrix} \delta x \\ \delta y \\ \delta z \end{bmatrix} = \begin{bmatrix} \delta h/h & \delta\psi & -\delta\theta \\ -\delta\psi & \delta h/h & \delta\phi \\ \delta\theta & -\delta\phi & \delta h/h \end{bmatrix} \begin{bmatrix} x \\ y \\ z \end{bmatrix} \tag{2-44}$$

If it is assumed that the two points are about the same height above the datum plane, or $z \ll x$, and $z \ll y$, then a considerable simplification results. Then the horizontal error is given by

$$\delta r = \sqrt{(\delta x)^2 + (\delta y)^2} \tag{2-45}$$

where r = horizontal distance between the two points. Also, if it is assumed that one is interested in averages over many different directions, so that the $(-\delta\theta\delta\phi)$ terms may be discarded, then the vertical error is

$$\delta z = \sqrt{(\delta\theta)^2 x^2 + (\delta\phi)^2 y^2} \tag{2-46}$$

Since, however, these have the same value, in an average sense, the vertical error may be expressed as

$$\delta z = \frac{\mu_s r}{F_s \sqrt{M}} \tag{2-47}$$

Similarly, substitution gives

$$\delta r = \left[\left(\frac{\mu_s}{0.3826\, S_s \sqrt{M}} \right)^2 + \left(\frac{\delta h}{h} \right)^2 \right]^{1/2} r \tag{2-48}$$

The above equations are based on measurement of the angles and altitude at only one of the stations. If they are measured at both stations, the resulting horizontal and vertical errors must be divided by $\sqrt{2}$.

There will also be errors in locating the points with respect to the model. These errors arise from random distortion of film, etc., as discussed previously.

To evaluate the effects of these errors, it is assumed that vertical imagery is obtained with sufficient overlap to insure that objects appear in both frames of the stereo-pair. Then, assuming an error (rms) of μ_T in measurement in the image space, * the corresponding error in measurement in object space is

$$\mu_T' = \mu_T Z_T / F_T \tag{2-49}$$

obtained by dividing by the scale ratio of focal length to altitude. Letting be the linear error (as opposed to radial error) and recalling that and are to be measured in two frames, the horizontal errors are

$$\delta' x = \delta' y = \frac{\mu_T Z}{\sqrt{2}\, F_T} \tag{2-50}$$

To evaluate the vertical error, it is assumed that the line between stations is parallel to the x axis. The size of the error will not differ greatly if it is not. By similar triangles, the vertical displacement may be found from

$$\frac{z}{x_2 - x_1} = \frac{Z + z}{X_2 - X_1} \tag{2-51}$$

where x_1, x_2 = co-ordinate of point projected on datum plane from camera stations (available from imagery)

X_1, X_2 = camera station co-ordinates

as shown in Figure 2 - 5. Because $Z \gg |z|$ this is well approximated by

$$z = \frac{Z}{B}(x_2 - x_1) \tag{2-52}$$

where B is the distance between camera stations.

---

* μ_T is the composite error due to film warpage and distortion and image unsharpness in the topographic camera, and comparator error.

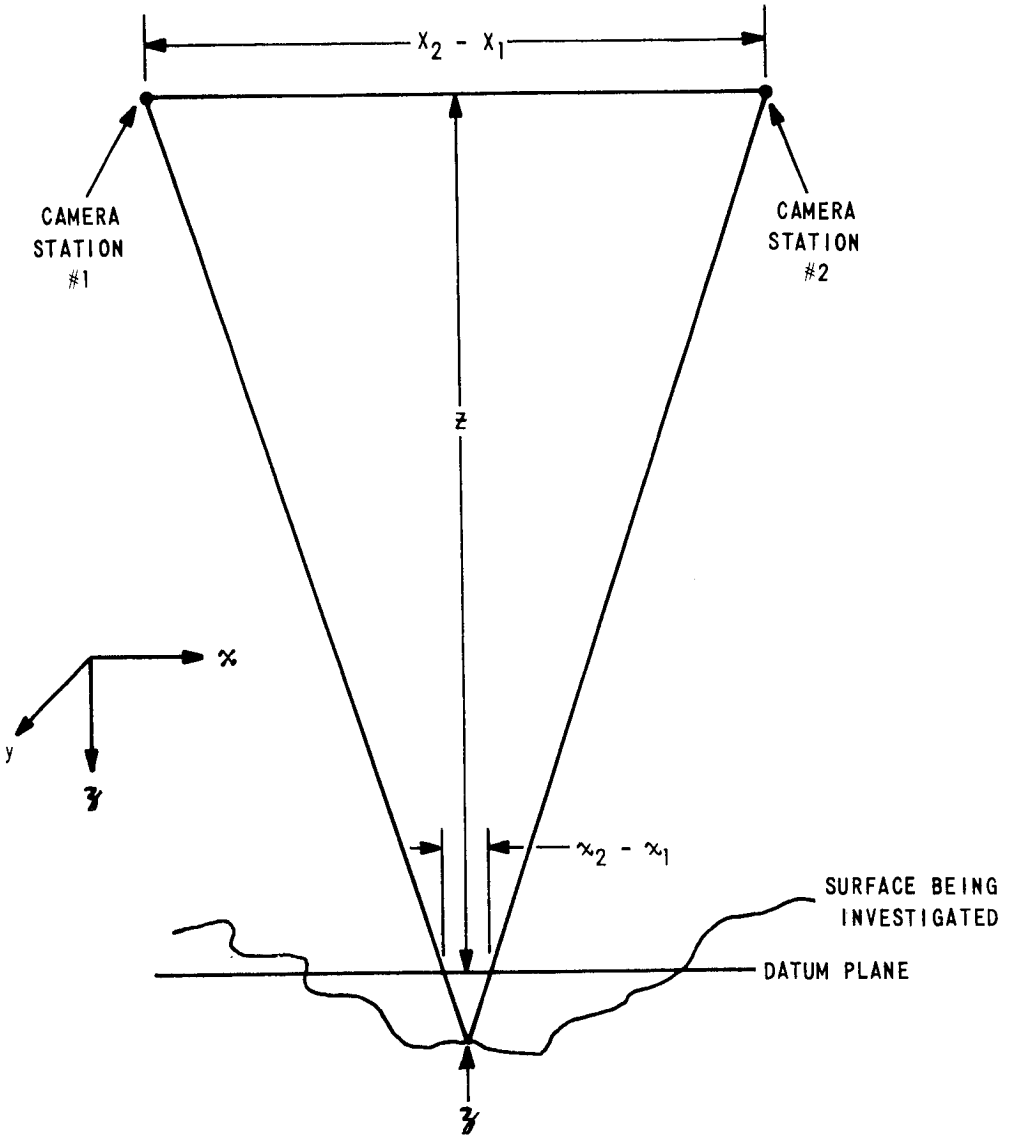

Figure 2-6 GEOMETRY OF STEREO PROJECTION

The distance between camera stations is equal to the advance (in object space) from one frame to the next, or the object format length multiplied by the fraction not overlapped by any one frame. This distance may be related to image format dimensions by the scale. The combination of these statements is that

$$B = (1-\mathcal{L})\, S_T \frac{Z}{F} \tag{2-53}$$

where $100\mathcal{L}$ = overlap percentage

and S_T = length of image format.

The two previous equations may be solved to yield

$$Z = \frac{F(x_2 - x_1)}{S_T(1-\mathcal{L})} \tag{2-54}$$

The rms errors in x_1 and x_2 are each μ'_T, as discussed above, hence the error in $(x_2 - x_1)$ is $\sqrt{2}\,\mu'_T$. This gives the rms verticle error from the topographical camera as

$$\delta'_Z = \frac{Z\,\mu_T\sqrt{2}}{S_T(1-\mathcal{L})} \tag{2-55}$$

for a single point. The vertical error in the comparison of two points will be $\sqrt{2}$ times as large, so that the total vertical error, including that from the model errors, is

$$\Delta Z = \left\{\left[\frac{2Z\mu_T}{S_T(1-\mathcal{L})}\right]^2 + \left[\frac{\mu_S r}{F_S\sqrt{M}}\right]^2\right\}^{1/2} \tag{2-56}$$

assuming orientation and scale at both stations. Similarly, the total horizontal error is

$$\Delta r = \left\{\left[\frac{\sqrt{2}\,Z\mu_T}{F_T}\right]^2 + \left[\left(\frac{\mu_S}{0.3826\,S_S\sqrt{M}}\right)^2 + \left(\frac{\delta h}{h}\right)^2\right] r^2\right\}^{1/2} \tag{2-57}$$

where the first term in brackets has been multiplied by the proper factors to account for two points with two dimensions each.

The above equations may be used both for computation of errors to be expected from a given system, and also to study the effects of system parameters on errors.

In some cases, vertical errors are considered to be much more serious than horizontal errors. In these cases, inspection of equation (2-56) indicates several important conclusions relating to design considerations. The first conclusion is that altimeter error does not have a major effect on vertical error. The second conclusion is that the component of vertical error due to the star camera (the second bracketed term) is expected to be small compared to that due to the topographic camera (the first bracketed term). This second conclusion may be supported in the following way: 1) $\bar{r}$, the maximum value of r , is not likely to be much greater than z because $\bar{r}/z$ is fixed by field angle and overlap considerations. 2) μ_s and μ_T are expected to be of comparable magnitude because it is expected that similar techniques would be used to collect both types of imagery. 3) S_T is not expected to be greater than 9" because of space limitations, and F_s is not expected to be less than 9", because of exposure problems in the star camera. By comparing the remaining factors in equation (2-56), and recalling that $\mathcal{L}$ must be at least 0.5 to obtain stereo and that M must be at least 2 to obtain information on yaw orientation, it is seen that the major source of vertical error is due to the topographic camera.

Two additional conclusions can be reached upon further inspection of the first term of equation (2-56), namely $\left[\frac{2z\mu_T}{S_T(1-\mathcal{L})}\right]^2$ It is seen that the ratio of the measurement error in image space (due to film warpage, etc.) to the format size is the important dimensionless parameter. Also, it is seen that the overlap should be made as small as possible, i.e., greather than, but as near 50% as possible, to minimize vertical errors.

2.3.4 Triangulation Errors over Large Distances

The process of fitting together stereo models so as to be able to locate points found in different stereo models is called adjustment, bridging, or triangulation, depending on the method used. None of the above methods are directly applicable to satellite or planetary topography because they are based on a type of control which will not, in general, be possible for satellite or planetary topography. However, the methods considered below are most analogous to triangulation and for convenience are referred to as such.

An interesting possibility is that, in many cases, it will be possible to extend the triangulation around the entire planet or satellite, because of the lack of oceans. Also, because there will be no surface control, there will be no way to determine latitude, longitude and hence the direction of the local datum surface except by triangulation. Thus, the problem of triangulation around the entire planet or satellite is considered.

Sub-section 2.3.4.1 contains a description of problems encountered in triangulation, particularly those unique to satellite or planetary topography. A possible mechanical scheme for triangulation is included in Sub-section 2.3.4.2 as an aid in visualizing error sources, which are also discussed in this sub-section. The error analysis is given in Sub-section 2.3.4.3, and some implications of the result of this analysis are discussed in Sub-section 2.3.4.4.

2.3.4.1 Difficulties in Triangulation

The universal difficulty in triangulation and similar processes is that a small error can cause a large error in the results. As an example of this, assume a polar orbit with forward overlap and the piecing together of stereo models along a meridian. The location of each camera station relative to the one adjacent to it may be found by the use of a stereoplotter, as discussed previously. One might think that fitting together in this manner would be satisfactory. However, consider a small error of 10^{-4}

radians, or about 21 seconds of arc, in relative orientation near the equator. This would result in an error, near the pole, of the order of 10^{-4} multiplied by half of the diameter of the satellite or planet depending upon the direction of the error; for the moon, about one-tenth of a mile. The cumulative effect of many such errors would be considerably larger. Such large errors, caused by the multiplication of a small error by a long lever arm, are avoided by using additional, or control, data applied in such a manner that significant portions of the errors cannot be propagated far along the chain. In the system described previously, the star camera can provide the additional data.

Because of errors the inclusion of additional, and hence redundant, data in triangulation implies that some compromise must be sought that does least violence to all of the input data. It is generally agreed that a good compromise is to minimize a weighted sum of the squares of the discrepancies between the data values supplied and those used in the final, consistent, result. Weighting factors are assigned on the basis of confidence in the measurements and the desire to make all discrepancies have the same dimensionality.

The above minimization may be obtained analytically by the use of a digital computer or in an analog manner by the use of a mechanical model. Mathematical procedures, usually iterative, exist to perform the analytic triangulation. In building a mechanical model, the members may be chosen such that their stiffnesses are proportional to the weighting factors. If this is done, and if the members are not strained beyond their elastic limits, the above minimization is secured as a result of Castigliano's theorem. Mechanical models are sometimes constructed without attention to the stiffnesses; this is equivalent to a different choice of weighting factors.

Either of these methods, suitably modified, may be used in satellite or planetary topography, but each has special difficulties which result from the unique characteristics of planetary topography. The analytical difficulties are the large amount of storage and number of

computations required as a result of the desire to perform the triangulation for the planet/satellite as a whole. Present mechanical methods use two-dimensional models. It appears that a three-dimensional model is required for topography without ground control. Such a model would be subject to errors caused by deflection under its own weight. Also, the large size of the model, again caused by the desire to perform triangulation for the planet or satellite as a whole, may result in errors from thermal expansion. Hopefully, these difficulties may be avoided by air conditioning and a system of counterweights, cables, and pulleys.

2.3.4.2 Mechanical System and Error Sources

Although it is not certain whether analytical or mechanical triangulation would be best, it is instructive to consider a mechanical system as an aid in visualizing the problem. This visualization is helpful in discovering error sources. The following paragraph describes the three-dimensional analog of a spider, or mechanical model of a camera station; the reader may imagine an approximately spherical framework formed by fitting these together from which the relative location of the camera stations may be measured.

As shown in Figure 2-7, the three-dimensional spider looks more like a jack. At the top, the absolute orientation from stellar imagery is supplied to the jack. As the stars may be considered at an infinite distance, the same relationship between discrepancy and torque must be maintained regardless of the location of the jack. This may be done by using flexible cables. Three are shown to represent the three angles required to fix the orientation of the jack. Below this are several freely telescoping arms, (only one is shown) which have their orientation with respect to the main stem fixed to represent rays to points found in more than one frame. The length of the main stem from the intersection of the radial arms to the ball at the bottom is adjustable to represent measured altitude. All of the bottom junctions of arms with each other and with main stems are made by suitable ball joints. There are deflections in the arms so that they may be arranged to pass one

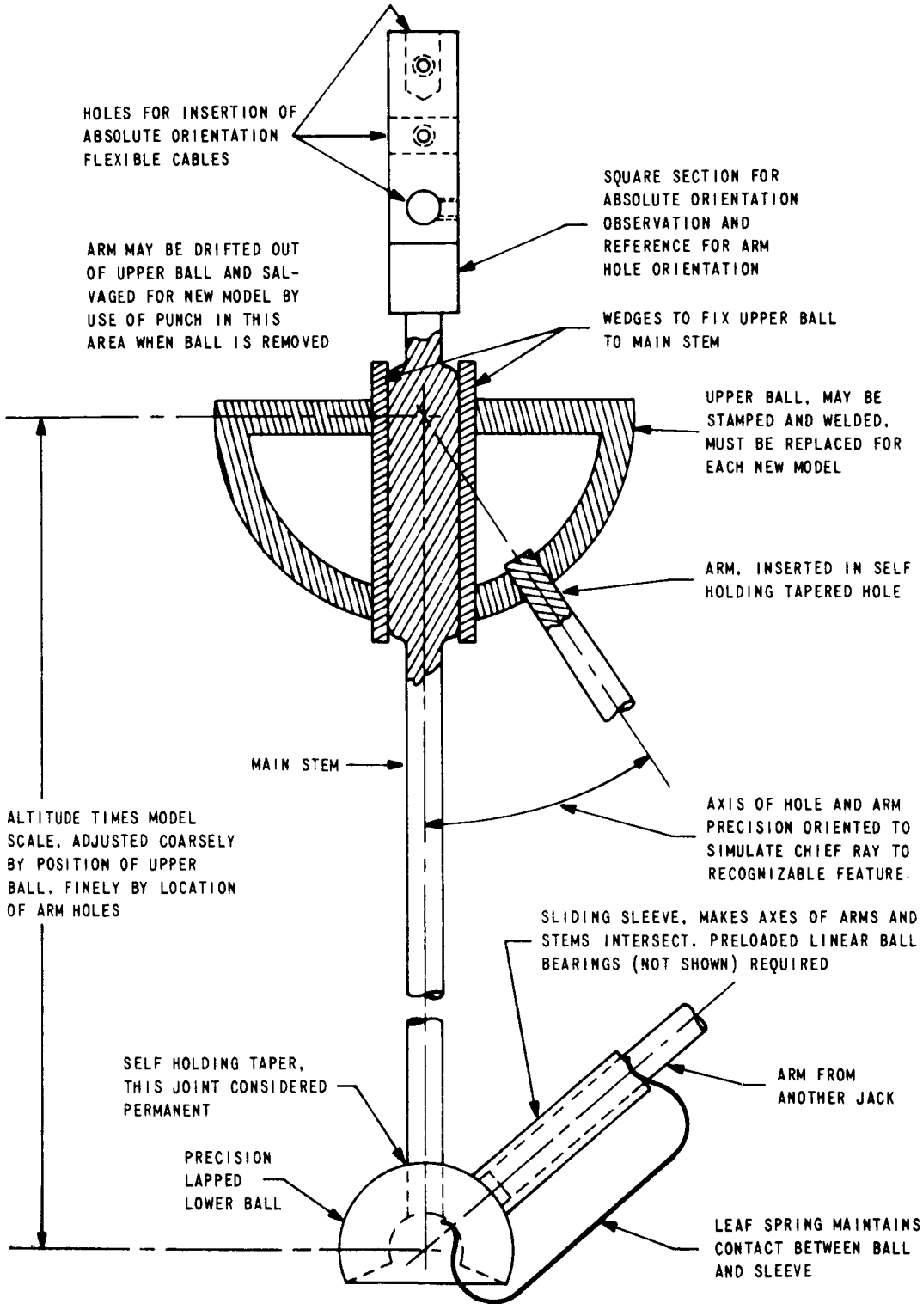

Figure 2-7 THREE DIMENSIONAL SPIDER

another without interference. Figure 2-8 shows a section of the model framework formed by connecting several jacks together.

Several conclusions may be drawn from an inspection of this model.

(1) No assumptions have been made (i.e., speed of satellite, shape of planet) and no useful data have been left out.

(2) The arms provide the strong relative orientation locally, while the many weaker cables prevent errors in relative orientation from being propagated.

(3) The length of the main stems provide the only scale available.

(4) It is not necessary to know the location of an image in order to determine the proper absolute orientation to be applied. It is sufficient to know the time of exposure and the orientation of the planet or satellite as a function of time. The latitudes and longitudes may be derived by measurements on the model. A critical examination of the information required to fabricate and install a jack tells us that the sources of error for triangulation are the same as those for local error, namely, film distortion, warpage, and unsharpness in the cartographic camera, altimeter error, similar film problems and measurement error in the stellar camera, and limitations imposed by data reduction methods. The film problems in the cartographic camera are not negligible because they result in errors in the relative orientation. These errors may not be taken as negligible because of propagation. Error mechanisms for the altimeter and star camera are obvious.

2.3.4.3 Error Analysis

To make an analysis of the errors to be expected in triangulation without solving the whole problem, it is necessary to make several assumptions and to inspect only a small part of the problem. This is because to analyze the errors in an analytical process, one should have the analytical program, and a complete mathematical simulation of the

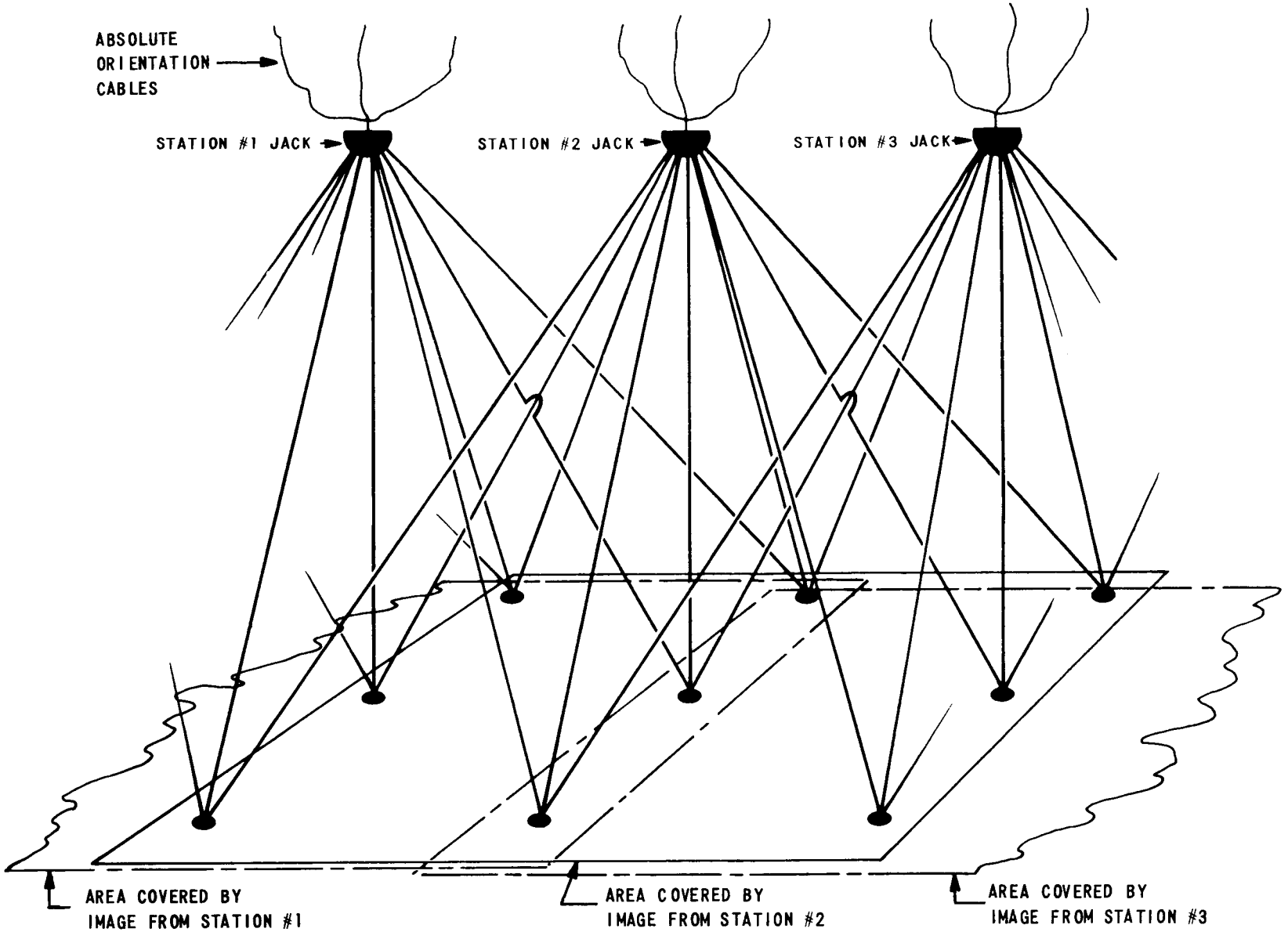

Figure 2-8 SECTION OF FRAME WORK FORMED BY ASSEMBLY OF JACKS

mechanical model is a valid analytical process in its own right. Consideration will be given to the situation in which a planet or satellite is photographed by a space vehicle in a polar orbit with sufficient forward overlap to secure stereo. Near $\pm$ 60° latitude there will be sufficient sidelap to secure stereo also. Mechanical triangulation is assumed, and it is supposed that the model is started by fitting an east-west belt of jacks at 60° latitude. The estimated distance (sealed to object space) which the last jack must be forced in order to fit the first jack will be taken as an indication of long distance error.

If two features are not in the same stereo model, their relative location may be found by finding the location of each with respect to a camera station from which it was implied, and finding the location of one of the stations with respect to the other. This last vector is subject to errors which increase with increasing separation between stations, and for sufficiently remote pairs, contains essentially all of the errors. The estimated distance discussed above is an indication of error in the relative location of camera stations, and hence, of widely separated features.

Although they do not appear in the model, it is convenient to use the vectors between adjacent camera stations in the analysis. Suppose that $\vec{V}_i$ is the vector from the ith to $(i+1)th$ camera station, in order of assembly. Then there are three ways to determine the direction of $\vec{V}_i$,

(1) by the absolute orientation at station i and the relative orientation of the $i, (i+1)$ stereo model (foresight),

(2) by the absolute orientation at station $i+1$ and the relative orientation of the $i, (i+1)$ stereo model (backsight),

(3) by the orientation of $\vec{V}_{i-1}$ and the relative orientation of the $(i-1)th$, ith , and $(i+1)th$ stereo models (extrapolation).

All three of these methods are used simultaneously in mechanical triangulation. However, for the analysis estimate, the extrapolation method is not counted. It should be noted that this will cause the estimated distance to be greater than

a more detailed analysis would indicate. As in the local error section, because the relative orientation is much stronger than the absolute orientation, the important errors are those due to absolute orientation and scale errors.

For the error estimate, suppose that a sphere has been taken as the reference surface for the planet. Then denote by Λ , Ω the latitude and longitude, respectively. The total error is to be found by adding vectorially the errors in each of the station to station vectors. Taking X , Y , Z as a rectangular coordinate system with

X = normal at Λ = 0, Ω = 0

Y = normal at Λ = 0, Ω = 90°

Z = normal at Λ = 90°

the errors ΔX , ΔY , and ΔZ contributed by the ith interstation vector are

$$\begin{bmatrix} \Delta X_i \\ \Delta Y_i \\ \Delta Z_i \end{bmatrix} = B_i \begin{bmatrix} \sin\Omega_i & -\cos\Omega_i \cos\Lambda & \cos\Omega_i \sin\Lambda \\ \cos\Omega_i & \sin\Omega_i \cos\Lambda & \sin\Omega_i \sin\Lambda \\ 0 & \sin\Lambda & -\cos\Lambda \end{bmatrix} \begin{bmatrix} \frac{\Delta B_i}{B_i} \\ \Delta E_i \\ \Delta A_i \end{bmatrix} \qquad (2\text{-}58)$$

where B = length of interstation vector,

E = elevation of interstation vector,

A = azimuth of interstation vector, and

Δ = denotes the error in these quantities.

These errors must be evaluated in terms of the star camera and altimeter errors. The errors in length, elevation, and azimuth correspond to errors in altitude, roll, and yaw, respectively, but they are the average of the two errors at the ends of the vector because both backsight and foresight are considered. Thus

$$\frac{\Delta B_i}{B_i} = \frac{1}{2}\left(\frac{\delta h_i}{h_i} + \frac{\delta h_{i+1}}{h_{i+1}}\right)$$
$$\Delta E_i = \frac{1}{2}\left(\delta\phi_i + \delta\phi_{i+1}\right) \qquad (2\text{-}59)$$
$$\Delta A_i = \frac{1}{2}\left(\delta\psi_i + \delta\psi_{i+1}\right)$$

It is apparent that the error $\delta h/h$ contributes to the error in $\vec{V}_i$ and to the error in $\vec{V}_{i-1}$. Because it is assumed that there are many pictures, so that each covers small ranges of Λ and Ω, and if it is assured that all of the B_i are approximately equal, it is valid to interchange the order of summation, arriving at

$$\begin{bmatrix}\Delta X_j\\ \Delta Y_j\\ \Delta Z_j\end{bmatrix} = B\begin{bmatrix}\sin\Omega_j & -\cos\Omega_j\cos\Lambda & \cos\Omega_j\sin\Lambda\\ \cos\Omega_j & \sin\Omega_j\cos\Lambda & \sin\Omega_j\sin\Lambda\\ 0 & \sin\Lambda & -\cos\Lambda\end{bmatrix}\begin{bmatrix}\frac{\delta h_j}{h_j}\\ \delta\phi_j\\ \delta\psi_j\end{bmatrix} \qquad (2\text{-}60)$$

where the closure errors are referred to errors made in measurements at the jth station. The next step is to take the errors as being independent from each other and uncorrelated with station location, and take the sum of the squares. To do this a method of finding the sum of the squares of the sines and cosines is required. This sum may be replaced by an integral, on account of the large number of stations. Using the integral evaluation, one finds that

$$\sum_{i=1}^{N}\sin^2\Omega = \sum_{i=1}^{N}\cos^2\Omega = \frac{N}{2} \qquad (2\text{-}61)$$

This gives the total closure errors as

$$\Delta X = \frac{B\sqrt{N}}{\sqrt{2}}\left[\left(\frac{\delta h}{h}\right)^2 + \cos^2\Lambda\,(\delta\phi)^2 + \sin^2\Lambda\,(\delta\psi)^2\right]^{1/2}$$
$$\Delta Y = \frac{B\sqrt{N}}{\sqrt{2}}\left[\left(\frac{\delta h}{h}\right)^2 + \cos^2\Lambda\,(\delta\phi)^2 + \sin^2\Lambda\,(\delta\psi)^2\right]^{1/2} \qquad (2\text{-}62)$$
$$\Delta Z = B\sqrt{N}\left[\sin^2\Lambda\,(\delta\phi)^2 + \cos^2\Lambda\,(\delta\psi)^2\right]^{1/2}$$

from which may be computed the total distance

$$d = \left[(\Delta X)^2 + (\Delta Y)^2 + (\Delta Z)^2\right]^{1/2} = B\sqrt{N}\left[\left(\frac{\delta h}{h}\right)^2 + (\delta\phi)^2 + (\delta\psi)^2\right]^{1/2} \tag{2-63}$$

By using the fact that BN is the circumference of the 60° small circle, the equation may be written in the form

$$d = \frac{C}{2\sqrt{N}}\left[\left(\frac{\delta h}{h}\right)^2 + (\delta\phi)^2 + (\delta\psi)^2\right]^{1/2} \tag{2-64}$$

where C is the planet circumference.

2.3.4.4 Implication

As noted previously, the errors referred to above must be considered as the sum of the errors in measuring the photos and in fabricating the jacks and assembling them. It is expected that 25 cm would be a reasonable value for the scaled altitude. Since it appears difficult to adjust this length to extreme precision, a tolerance of 25 microns may be expected, giving

$$\frac{\delta h}{h} = 10^{-4} \tag{2-65}$$

Similarly, the orientation of the jack must be measured prior to insertion in the assembly. This might be done by observing reflections from a flat reference surface on the jack in a transit telescope. This orientation also will be limited to about 10^{-4} radians. It should be noted that the angles corresponding to the relative orientation may be constructed into the jack an order of magnitude better. Assuming the 10^{-4} errors above, this gives the expected closure distance,

$$d = \frac{10^{-4} C}{2}\sqrt{\frac{3}{N}} \tag{2-66}$$

The level of this accuracy may be evaluated by assuming no interference from atmosphere, clouds, or oceans and substituting values for earth. By assuming an altitude of 100 km, 6" focal length lens and 60% overlap relative to a 9" format, one may conclude that 333 pictures

would be required. By substituting this value into the previous equation, one finds

$$d_e \approx 200 \text{ meters} \tag{2-67}$$

This apparently indicates long distance errors of the same order of magnitude as presently occurs on earth, when it is recalled that (1) the two ends would be forced to fit, resulting in less error than this for points opposite one another on the small circle, (2) additional data provided by extrapolation was not included in the estimate, and (3) additional strength is provided by adjacent jacks, also not considered in the estimate.

The accuracy standard for the altimeter such that it contributes negligible error is of course that its error be less than one part in 10^4 or 10 meters for a 100-km altitude. The standards required of the star camera are difficult to relate to the configuration of the camera, because the number of stars in the imagery depends on the focal length and format size. It appears that a format size approximately half of the focal length might be a good choice; this has not been carefully checked. With care, it should be possible to select an orbit such that there are at least 9 stars of the fourth magnitude or brighter, in each stellar image, given the field angle specified by the focal length and format above. The required accuracy in measurement of stellar images may be found by solving a previous equation. It is

$$\mu_s \ll \delta\psi \cdot 0.3826 S_s \sqrt{M} \tag{2-68}$$

For a 9" format, 9 stars, and 10^{-4} radians of yaw error, it is seen that

$$\mu_s \ll 30 \text{ microns} \tag{2-69}$$

This is much larger than the combination of errors in present films and comparators.

2.3.5 Conclusions

From the preceding analysis of errors involved in imagery collection from a space platform for mapping purposes, we can generally conclude that:

(1) Three cameras and an altimeter would be necessary. A reconnaissance camera is necessary for obtaining the high resolution required to discern detail. A cartographic camera is necessary to preserve the geometric fidelity necessary for mapping and contour plotting. A star camera is necessary to determine the attitude of the platform (and cameras) for triangulation purposes. The altimeter provides a means of obtaining scale.

(2) For reconnaissance, the stereo strip camera gives the highest resolution, which is usually limited by the illumination rather than the diffraction limit of the camera when used in this model. If compensation can be applied, image orthicons approach the sensitivity of film for reconnaissance application. Sufficient resolution may be obtained from orbiting vehicles to determine landing sites.

(3) Strip, panoramic, and focal plane shutter cameras are not as well suited for cartographic imagery collection as a frame camera with a between-the-lens shutter.

(4) The triangulation of a planet as a whole is necessary to determine the location of the camera stations. This is possible if no major cloud formations or oceans exist.

(5) For star cameras, only frame cameras with between-the-lens or equivalent shutters are suited. They may have a serious exposure problem (since only a few stars are sufficiently intense to give adequate exposure) and image motion compensation may be required.

(6) It may be desirable to take simultaneous star imagery enroute to the planet to be observed with both cameras to determine relative orientation and recheck the calibration of both cameras. The use of multiple exposures in a star camera to conserve film may also prove desirable.

(7) Largest errors for a star camera are yaw errors. Consideration should be given to the seriousness of various types of errors to determine if antipodal mounting is optimum. Many fiducial markers are required in both cameras if absolute orientation errors are to be limited by star measurement errors rather than those in transfer of orientation. (Markers in a star camera require illumination.)

(8) The problem of determining, as a function of time, the orientation of a planet being imaged for cartography requires serious consideration.

(9) For mechanical triangulation, errors over long distances are set at a low level by the mechanical model if the altimeter error is less than 100 parts per million and a star camera with film is used.

3. HOLOGRAPHIC TECHNIQUES

This section presents an analysis of the applicability of holographic techniques to the acquisition, transmission and enhancement of three-dimensional topographic information. The analysis is confined to the following topics:

(1) the direct use of the three-dimensional properties of hologram images to acquire topographic data from space,

(2) the transmission of a hologram by means of a data link and

(3) the enhancement of degraded photographic images containing topographic data. Some of the significant problems are defined and discussed for each of the topics.

Since many of the properties of the holographic process may be important in potential applications other than those considered here they are discussed first without reference to a particular application. Some of the conditions that must be fulfilled in the construction process are discussed in Sections 3.1 and 3.2. This is followed by a consideration of some properties of the reconstructed image resulting from the nonlinearity of the recording medium used in constructing a hologram and the geometry of the construction process. These properties which influence the applicability of holographic techniques in the acquisition and transmission of three-dimensional topographic data, are described in Section 3.3 and discussed in more detail in Appendix A. By relating these results to the specific topics previously enumerated conclusions and recommendations are made concerning the feasibility of these applications.

3.1 Conditions for Construction

A hologram is the recorded interference pattern formed by interfering a wavefront originating at the object and a controlled reference wavefront as shown in part (a) of Figure 3.1.

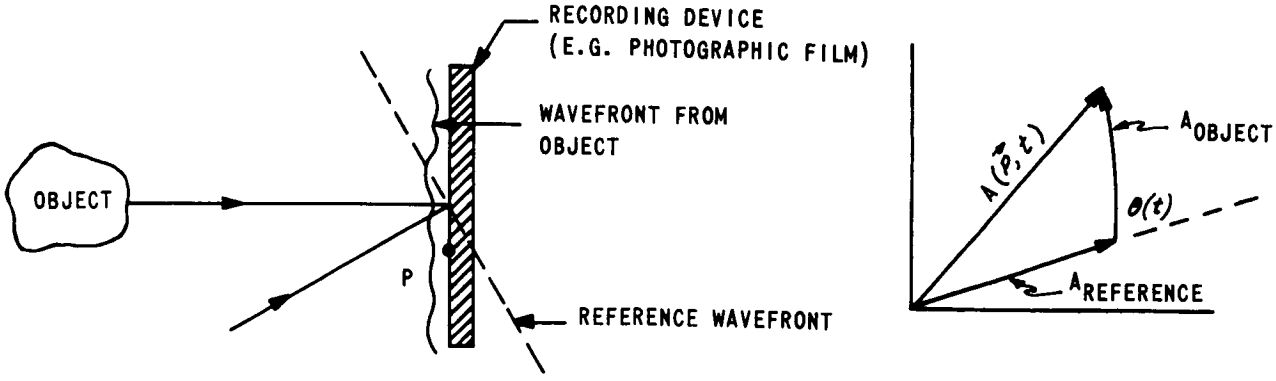

(a) CONSTRUCTION GEOMETRY

(b) VECTOR DIAGRAM OF WAVE AMPLITUDES AT POINT P.

Figure 3-1 HOLOGRAM CONSTRUCTION

Consider the intensity $I(\vec{P})$, recorded at a point $\vec{P}$ in the hologram, viz.

$$I(\vec{P}) = \langle |A(\vec{P}, t)|^2 \rangle \qquad (3\text{-}1)$$

where< > indicates a time average over the exposure time. As shown in part (b) of Figure (3-1), the complex amplitude $A(\vec{P}, t)$ is the vector sum of the complex amplitudes in the object wavefront and the reference wavefront. $A(\vec{P}, t)$, and consequently the instantaneous intensity at $\vec{P}$, depend upon the phase difference between reference amplitude and object amplitude, i.e., $\theta(t)$. If the object is stationary with respect to the hologram plane during the exposure time, $\theta(t)$ is constant and the time average, < >, in equation 3-1 may be omitted. If the object is moving during the exposure time the intensity at $\vec{P}$

will change with time. For random or uniform motion of the object, it is reasonable to assume that all values of $\theta(t)$ from 0 to 2π are equally likely and the hologram is destroyed or "washed out". An exception occurs for harmonic motion of the object where there are "preferred" values of $\theta(t)$ and the hologram retains information about the object. Several articles[1, 2] describe the use of holograms for the analysis of harmonic motion of an object. In general, however, the magnitude of the motion of the object during the exposure time must be small compared to the wavelength of the exposing radiation so that the variation of $\theta(t)$ is small during the exposure time. An approximate condition for obtaining good holograms is to restrict the magnitude of the object motion to less than one-eighth wavelength.[3] This requirement for stability is important when considering the use of holographic techniques from moving spacecraft.

Sources of random phase variations, other than object motion, must also be avoided when constructing a hologram. Such variations could be introduced by an atmosphere if it exists. All of the phase variations described above can be expressed in terms of decreasing the temporal coherence between the object wavefront and reference wavefront. If the coherence length becomes short enough no interference pattern or hologram is formed.

3.2 Requirements for Obtaining Three-Dimensional Information From a Hologram Image

This section discusses the use of a hologram for obtaining three-dimensional information. The hologram records the information in a form which is currently not retrievable except by reconstructing an image (real or virtual) of the original scene by illuminating the hologram with coherent light and observing the reconstructed wavefront with the eye or recording the image on film. Thus, in practice the hologram is used to "recreate" the wavefront that existed at the time the hologram was exposed and conventional methods for extracting three-dimensional information can be employed.

In the following discussion it is assumed that the hologram process is capable of reconstructing a wavefront exactly. In practice the recording medium, because of its finite resolution, limits the information reconstructed, and in addition contributes noise to the reconstructed wavefront. (See Appendix A).

Three-dimensional information is commonly obtained by viewing the surface from two separated vantage points. Therefore, depth resolution (three-dimensional information) in the reconstructed image of the hologram is achieved only when the hologram reconstructs the wavefront over a sufficient area to provide views from two separated vantage points. For a given separation the radius of stereoscopic vision, the distance beyond which depth resolution is lost (no relief is discernible), depends upon the resolution of the sensors and is given by [4]

$$\delta = \frac{b}{\alpha} \qquad (3\text{-}2)$$

where b is the separation of the sensors and α is the angular resolution of the sensors. In the case of the human observer the angular resolution of the sensor, namely the eye, is 0.00029 radian. Take as an example a spacecraft orbiting at an altitude of 80 km above a surface. It is seen from equation (3-2) that a hologram of the surface made from the spacecraft would have to have a width of 23.4 meters in order to permit an observer to perceive any depth information. In addition, only the wavefront originating at the extremities of the hologram would be of value in obtaining stereoscopic information. To acquire normal stereoscopic information δ must be much greater than the altitude of the spacecraft and therefore the wavefront must be reconstructed at two points separated by much more than 23.4 meters. It is conceivable that two separate holograms might be obtained but it would be more practical to take a pair of photographs using two cameras separated by the required distance.

The requirement on hologram size can be improved by introducing magnification into the viewing system or into the hologram process. This permits the value of b in equation (3-2) to be reduced by the magnification factor. For holograms of reasonable size say $b < 1$ meter one finds that a magnification on the order of 60,000 is required to insure that accurate three-dimensional information can be extracted from the reconstructed image of a hologram obtained at an altitude of 80 kilometers.* Such magnifications are beyond the "state-of-the-art".

From the preceding discussion it can be seen that three-dimensional information can be obtained only for objects within a range determined by the size of the hologram. A reasonable estimate of the maximum range obtainable is about 0.8 km depending upon the resolution of the recording medium and the stability condition discussed in section 3.1.

3.3 Properties of the Reconstructed Image Produced by a Non-linear Recording Medium

In order to evaluate the usefulness of the hologram in a particular application, the influence of the photographic process or another possible non-linear recording process upon the image reconstruction must be understood. In analyzing holograms, a linear amplitude transmittance-exposure characteristic is usually assumed.[3, 5, 6, 7] The analysis presented in Appendix A was performed independently at CAL. Some identical conclusions concerning the effects of the non-linearity of the exposure-amplitude transmittance characteristic upon the reconstructed image are obtained from both analyses. The results of the analysis presented in Appendix A are discussed below.

*In normal stereoscopic photography values of b/h of 2/3 are commonly employed to obtain accurate depth information. For an altitude, R, of 80 km, the effective base line, b, must be 50.3 kilometers.

As a consequence of the non-linear characteristic of the recording medium, a hologram reconstructs wavefronts modulated by higher powers of the complex amplitude of the object wavefront. These wavefronts or "harmonics" do not reconstruct an image of the object and may be a source of noise in the reconstructed images. To eliminate interference between the harmonics and the desired image, an appropriate carrier frequency must be employed when constructing the hologram. In addition, the analysis indicates that the non-linear characteristic introduces a multiplicative noise which degrades the reconstructed image. This noise depends upon the magnitude and frequency of variations in the amplitude of the object wavefront and requires additional investigation to determine what limitation, if any, it places upon the attainable resolution in the reconstructed image. The effect upon the reconstructed image is analogous to placing a mask with varying transmittance in front of a lens forming an image of the object. The amount of noise or degradation may be minimized, if necessary, by employing small modulations of the reference wavefront in forming the hologram. This in turn, however, produces the disadvantage that the fraction of the reconstructed energy obtained in the reconstructed image is small.

The analysis also indicates that severe non-linearities do not necessarily destroy the ability of the hologram to reconstruct the image and that it may be possible to minimize the gray scale used in the construction process by photographic clipping.

The non-linear relationship between the angle of diffraction and spatial frequency at large spatial frequencies introduces an additional distortion in the image when larger carrier frequencies are employed. Such degradation could be a disadvantage if the holograms were used as a multiplexing device where several images would be recorded using different carrier frequencies.

The degrading effects of non-linear response of the recording medium should be considered in applications where resolution in the reconstructed image is important.

3.4 Direct Use of the Three-Dimensional Properties of a Hologram Image to Acquire Topographic Data from Space

This section considers a particular application of the hologram process, namely one in which the three-dimensional properties of the hologram image are used to obtain stereoscopic information about a surface or object. The hologram is assumed to be acquired from a spacecraft above the surface.

From the analysis presented in Section 3.2, it may be concluded that a conventional Fresnel hologram of practical dimensions made from a spacecraft would not, in itself, contain any useful stereoscopic information. It is possible to simulate the required stereoscopic window or baseline by forming smaller holograms at two separated points. This is identical to the procedure used in conventional stereo photography. However, as the computations indicated, each hologram by itself would have no stereoscopic information and therefore no advantage over conventional photographs would be obtained. Due to the increased difficulty in obtaining holograms as opposed to photographs from space platforms, the conventional photographic technique for obtaining stereoscopic information is more desirable.

However, a technique has been suggested which employs contour generation by use of holograms.[12] Instead of recording the three-dimensional information in the usual way using the parallax property, this holographic technique provides contour lines of constant depth. One way to achieve this effect is to have the illuminating source consist of two distinct frequencies. Each frequency will produce a separate hologram. The developed hologram is illuminated with light of a single frequency. One image is magnified by an amount slightly different from the other. The light from the images interferes constructively or destructively depending upon the distance between them. At a fixed depth, a contour becomes visible. The increment in range corresponding to adjacent fringes is[12]

$$\Delta R = \frac{\bar{\lambda}^2}{\Delta\lambda}, \qquad \begin{aligned} \bar{\lambda} &= \text{average wavelength and} \\ \Delta\lambda &= \text{wavelength difference.} \end{aligned} \qquad (3\text{-}3)$$

Although this technique potentially eliminates the baseline requirement discussed in section 3.2, the stability requirements previously discussed in Section 3.1 must be satisfied. It will be recalled that the hologram exposure must be made in a time sufficiently short so that the magnitude of the relative motion of the object and hologram plane is less than a wavelength ($\sim 1/8\ \lambda$). In order to meet this requirement for a platform with a speed of 1.65 km/sec (comparable to the velocity of a moon satellite) with respect to the surface being examined, less than 0.1 nanosecond exposure would have to be employed. A short pulse coherent source with a large energy output (i.e., a high peak power) is required. In order to estimate the approximate energy output required from the coherent source to expose a hologram, the following parameters are defined:

1) R, range or distance between the hologram plane and the target surface.
2) α, the half-angle of the illuminating cone from the source.
3) ρ_o, the normal albedo of the target surface.
4) S, the specified sensitivity (area/energy) of the film used to record the hologram, and
5) $(\bar{\rho})^2$, the ratio of the intensity of the signal to the reference wavefront.

An approximate expression for the required energy output of the source is*

$$E = \frac{(\bar{\rho})^2 \pi R^2 \tan^2\alpha}{\rho_o S(2/3)(1-\cos^3\alpha)} \sim \frac{\pi R^2 (\bar{\rho})^2}{\rho_o S \cos^2\alpha} \quad \text{for small } \alpha \qquad (3\text{-}4)$$

Reasonable values for the parameters are:

R = 80 kilometers

α = 5 degrees, corresponding to a ground diameter coverage of 14 kilometers

*This calculation assumes a diffusely reflecting surface. If the surface is not diffusely reflecting (e.g., as in the case of the moon), appropriate account must be taken of the angular dependence of the reflectivity. However, for small values of the angle α, Equation 3-4 is a reasonable approximation.

ρ_o = 0.16 (for the lunar surface using red light)
S = 0.4 cm^2/erg, and
$\bar{\rho}$ = 0.005

This value of the sensitivity selected is that of Kodak SO-243 film at 700 $m\mu$ wavelength. If higher resolution films such as Kodak 649-F are considered the values of S will be much smaller requiring a correspondingly larger energy output from the source. Using these values the required output is $\sim 10^6$ joules during the exposure time. Considering exposure times of 0.1 nanosecond, which are required to circumvent motion problems, the average power output of the source over the pulse interval would have to be 10^{16} watts. It is doubtful that stable coherent sources could be developed with such enormous power outputs even for intermittent operation.

It appears rather unfeasible to employ Fresnel holographic techniques to acquire topographic data from spacecraft due to the high peak power and large baselines required. In other applications, such as a survey mission using ground based instruments, where the range to the target is much less than that of a spacecraft, holographic techniques are more feasible.

3.5 Transmission of Holograms by Means of a Data Link

The purpose of this section is to discuss the problems associated with the transmission of holographic information. Several important factors must be given consideration in establishing the feasibility of transmitting holograms. These include:

a) the possibility of gray scale compression
b) minimum format size required to transmit information versus resolution in the image
c) decreased size of a resolution element in a hologram
d) required geometrical fidelity and
e) possible multiplexing techniques.

The partial analysis of these factors is given below.

A hologram can be developed to a high contrast or film γ to produce a black-and-white structure. This process is often referred to as clipping. It is shown in Appendix A that such holograms can be just as easily reconstructed as those developed to a lower γ . The subsequent reduction in dynamic range or gray scale would require only one or two bits per resolution element to be transmitted. On the other hand, if the original transparency with a large dynamic range were transmitted, as many as 6 bits may be necessary.

The format size transmitted is another parameter which may be varied. In the case of a photographic transparency, the format size transmitted will determine the field of view; that is, in order to see the complete picture, the entire transparency must be transmitted. In the case of the hologram, it is known that a hologram can be sectioned and that each section reconstructs the image. Therefore, the format size does not affect the field of view. Transmitting a small format size, however, decreases the resolution in the image. To establish a physical basis for this result, it is convenient to compare a hologram to the entrance aperture of a simple optical system as shown in Figure 3-2. As the wavefront from an object approaches the x-y plane, it is either interfered with a reference wave and recorded to form a hologram, or it is imaged by the lens. If the constructed hologram were placed in front of the lens and illuminated with the appropriate reference wavefront, the wavefront originating at the object would be reconstructed and the lens would form an image of the object. The reconstructed wavefront extends over the area of the hologram plate. If that area exceeds the entrance aperture of the lens, the image formed by employing the hologram and that formed by the lens directly would be identical.* If, however, the area of the hologram is less than the entrance aperture of the lens, it becomes the limiting factor and the resolution in the hologram image would be less than that obtained in the direct image. Thus, the effect of varying the area of the hologram which is transmitted upon image resolution can be investigated by using the correspondence between hologram area and

* Assuming the hologram reconstructs the wavefront without degradation.

entrance aperture. For example, in the design of telescopes, it is known that obstructing the center portion of the aperture increases the two-point resolution of the image. This suggests that areas near the exterior of a hologram should be transmitted rather than those at the interior.

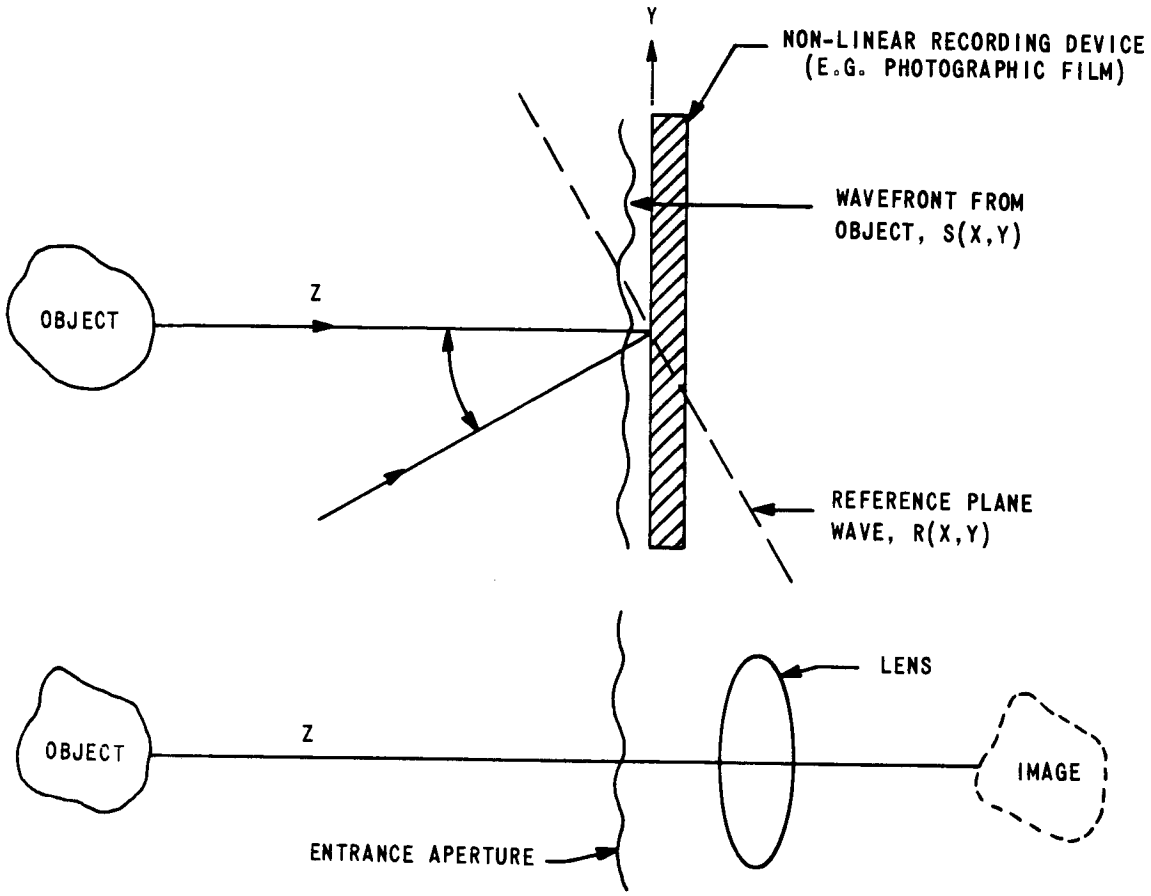

Figure 3-2 COMPARISON OF A HOLOGRAM TO THE ENTRANCE OF AN OPTICAL SYSTEM

The format area transmitted should be such that the resolution which one achieves in the reconstructed image is equivalent to that obtained when transmitting the original transparency.

One factor which tends to increase the bandwidth

required to transmit a hologram is the decreased size of a resolution element. As shown in Appendix A, the resolution element in one direction in the hologram must be less than half the size of the resolution element in the photographic transparency in order to avoid increasing the noise in the reconstructed image. This doubles the amount of information transmitted for a given length of scan. In cases where a higher carrier frequency is employed in making the hologram, the bandwidth requirement for transmission would increase further. The tradeoff is one of increasing the signal-to-noise ratio or contrast of the reconstructed image at the expense of increasing the bandwidth for transmission.

A very important consideration in assessing the feasibility of transmitting a hologram is the geometric fidelity required. The hologram can be viewed as a coherent superposition of a series of gratings of various fixed spacings. The spacing between the black and white structure of the holograms is critical since this is related to the original spacing of the gratings. Therefore the geometric fidelity required in transmitting a hologram must be given consideration with respect to its influence upon the reconstructed image.

The problems involved in transmitting a hologram discussed above have not received detailed attention and should be investigated further so that appropriate conclusions can be made.

3.6 Image Enhancement by Holographic Techniques

The final application for holographic techniques to be discussed is the possible enhancement of degraded photographic images which contain topographic data. The image can be degraded by operational degradations such as image motion, image vibration, and defocusing. These degradations will reduce the accuracy of the topographic data that can be obtained from the photographic image. The problem is to employ holographic techniques to restore some of the

"lost" data by compensating for the degrading mechanism or enhancing the image after it has been received from a spacecraft or remote station.

The property of a hologram which is useful to such enhancement or correction of degraded images is its ability to record and reconstruct a complex wavefront. Suppose that as indicated in Figure 3-3 the wavefront recorded by the hologram is that which results from the degraded image of a point, i.e., the degraded point spread or the Fourier transform of the transfer function of the degradation process. In the reconstruction of the hologram, the virtual image results from the reconstruction of the recorded complex wavefront, $S(x, y)$, whereas, the real image results from the reconstruction of its complex conjugate, $S^*(x, y)$. When the processed hologram is placed back into the plane in which it was formed and illuminated by the "degraded" wavefront, the wavefront emerging in the direction of the real image is $S(x, y) \cdot S^*(x, y)$ or a plane wavefront. If this wavefront is subsequently imaged by a high quality lens, the resulting image of the original degraded point spread is improved (i.e., narrowed). The reconstruction process is also shown in Figure 3-3. If a degraded photographic transparency whose transmission is $T(x, y)$ convolved with the degrading point spread now placed in the object plane, the resulting image will be corrected by the hologram because the point spread of the combined system is diffraction limited.

An experimental and analytical investigation of this technique should be undertaken to define its range of applicability. This should be done starting with the simplest form of degradation such as uniform image motion.

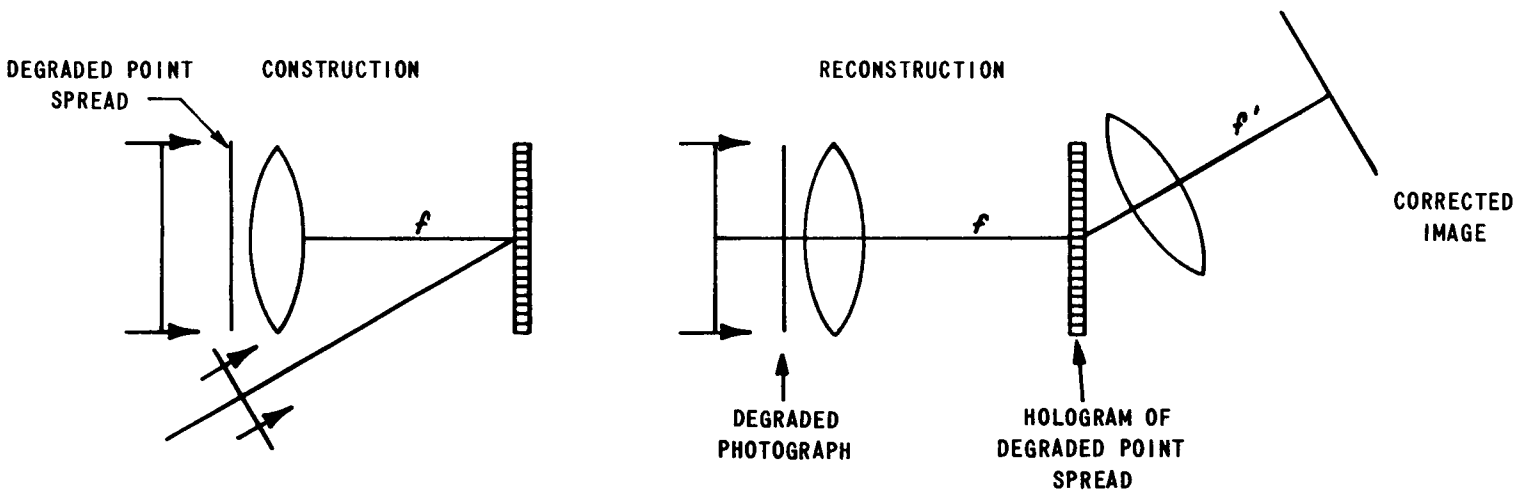

Figure 3-3 A POSSIBLE CONFIGURATION FOR IMAGE ENHANCEMENT USING HOLOGRAMS

3.7 Recommendations and Conclusions

It appears rather unfeasible to employ holographic techniques to acquire topographic data from spacecraft. Other applications such as ground based survey missions may be feasible. Any future study should be contingent upon the development of suitable coherent light sources. Such studies should include a feasibility analysis to define the various limitations of the techniques considered.

Investigations should be continued into the problems involved in employing holographic techniques for the transmission of data to define limitations and establish the areas that require further analysis.

In addition, an experimental and analytical investigation of image enhancement techniques using holograms should be performed to establish basic feasibility and to define limitations.

4. TRANSMISSION OF TOPOGRAPHIC INFORMATION

In this section some of the requirements and techniques for the transmission of topographic data from space are considered. In transmitting video information, the required bandwidth, channel capacity, carrier frequency and signal-to-noise ratio are all very important parameters to be determined. General considerations of these parameters are presented first.

For space applications where various mission functions and experiments compete for transmission time and/or frequency band, the techniques of bandwidth compression become increasingly important to video transmission. Such methods are described in the second part of this section.

The transmission of information in the optical band of the electromagnetic spectrum holds promise for the future with the advent of the laser. The philosophy and difficulties of this method of communication are discussed in the third major subsection.

The section terminates with some conclusions and recommendations concerning transmission.

4.1 General Considerations

There are many considerations that must be made when determining the requirements for the transmission of video information from space. The required frequency bandwidth[1] is one of the most important. It, in turn, determines the power and weight requirements for the mission. Other parameters such as the theoretical limit of the channel capacity, the carrier frequency and the required signal-to-noise ratio also influence these requirements. Calculations[2] indicate that even transmission for mapping purposes from the relatively nearby moon cannot be accomplished in a real time sequence due to the state of the art restrictions in these system parameters.

4.1.1 Bandwidth and Resolution

The bandwidth required to transmit an image in two dimensions is a function of the scanning rate, the resolution required and the size of the image. To show how these parameters are related let us take an example of a parallel raster scan system reading out an image of R_i line pairs per millimeter in a photoelectronic device. Such a scan samples an image discretely in one dimension and continuously in the other. To preserve the resolution in the image dimension normal to the raster lines, the number of sampling points required would ideally be equal to

$$N = 2 f_s^M(y)\, Y \tag{4-1}$$

where N is the number of raster lines (sampling points), $f_s^M(y)$ is the highest spatial frequency in the y dimension (equal to R_i), and Y is the magnitude of the y dimension of the image. The factor 2 appears in this equation because a minimum of two raster lines (or samples) are required in the y direction to reproduce one cycle (line pair) of the limiting spatial frequency.[3]

The highest spectral frequency component of the video signal generated by such a system (and therefore the bandwidth required) is determined by the continuous signal generated in the other dimension. The spectral frequency of the video signal is related to the spatial frequency being scanned by the velocity of scan. Thus we can write

$$B_S = f_V^M = f_s^M(x)\, v = f_s^M(x)\, \frac{X}{t} = f_s^M(x)\, \frac{X}{(\tau/N)} \tag{4-2}$$

where B_S is the signal bandwidth, f_V^M is the maximum video frequency, $f_s^M(x)$ is the maximum spatial frequency in the x dimension, v is the velocity of scan, X is the magnitude of the x dimension of the image, t is the time required to scan one line, and τ is the time required to scan N lines. The time required for one complete frame, τ_F, must include retrace or blanking time so that

$$\tau_F = \tau + \tau_R = \tau(1 + r) = b\tau \tag{4-3}$$

where τ_R is the total retrace time, r is the ratio of τ_R to τ, and b is the blanking factor. Substituting (4-1) and (4-3) into (4-2), one gets

$$B_S = \frac{2b f_s^M(y) f_s^M(x) XY}{\tau_F} . \tag{4-4}$$

In terms of the raster lines required, assuming equal resolution in both dimensions, (i.e., $f_s^M(x) = f_s^M(y) = N/2Y$), the signal bandwidth is

$$B_S = \frac{b}{2}\left(\frac{X}{Y}\right)\frac{N^2}{\tau_F} . \tag{4-5}$$

where (X/Y) is the aspect ratio.

If, however, the number of raster scan lines is less than that required, equation (4-1) is replaced by

$$N > L = 2 f_s(y) Y. \tag{4-6}$$

The resolution such a system can preserve is compromised by the fact that spatial frequencies exist in the image which cannot be adequately or unambiguously read out. For this system, a lower resolution of R line pairs per millimeter is designated as its capability where

$$R = k f_s(y) . \tag{4-7}$$

The factor k is often called the Kell factor and various methods of deriving and/or defining it have been suggested.[4] Values range from 0.34 to 1.00 depending upon the conditions or assumptions used to define it. The majority of authorities accept the value $\frac{1}{\sqrt{2}} \simeq 0.71$. From this we obtain

$$kL = 2RY \tag{4-8}$$

If we again require that the resolution in the x dimension be no better than that in the y dimension, equation (4-4) now becomes

$$B_L = \frac{bk}{2}\left(\frac{X}{Y}\right)\frac{L^2}{\tau_F} \tag{4-9}$$

where B_L is the scan-limited bandwidth of the signal. This would also be the bandwidth of the channel required if there were no noise. However, the noise internal to a transmission system such as resistor noise or tube noise from the amplifiers are noise sources which cannot be eliminated and must be overcome either by raising transmission power or using a

noise-cleaning method of transmission. The most effective (yet practically implementable) system at present is binary pulse code modulation.[5] Such a system can transmit a given number of quantized sample value levels with greater immunity to noise than other systems, but at a cost of greater bandwidth. By sampling, quantizing to ℓ levels and encoding in binary, the bandwidth requirement is increased by a factor n which is the number of bits per code group ($n = \log_2 \ell$). Bandwidth then becomes

$$B = \frac{bk}{2}\left(\frac{X}{Y}\right)\frac{L^2}{\tau_F}\log_2 \ell . \qquad (4\text{-}10)$$

Let us take, for example, the television system that was used in the Mariner 4 flyby of Mars. A 0.56 x 0.56 cm square ($\frac{X}{Y} = 1$) image was read out by a 200 line parallel raster scan to 64 grey levels. If the requirement of "real-time" had been placed on this system, the bandwidth required would have been 2.7 megacycles per second ($b \simeq 1.06$, $k \simeq 0.71$, $\tau_F = \frac{1}{30}$ sec.). However, to achieve this bandwidth would have also required a huge increase in power. (Approximately 650,000 times the actual power used.)

4.1.2 Channel Capacity

It is not only necessary that the bandwidth of the signal not exceed the bandwidth of the transmission system, but also that the required rate of transmission of information not exceed the channel capacity. The channel capacity is defined as

$$C = B\log_2\left(1 + S/N\right) \qquad (4\text{-}11)$$

where S is the total signal power received, B is the bandwidth, and N is the noise power received within that bandwidth. This equation applies for ideal encoding. The number of bits of information per second communicated without error cannot be greater than C, and in practice does not approach C. The encoding efficiency depends upon how well the output of the electro-optical transducer is encoded as an input to the transmission system, i.e., how good the match is.

If the encoder presents information to the channel at a rate equal to the channel capacity, maximum efficiency is achieved. If the rate is higher, information is lost. If the rate is lower, power is wasted. When compared with what could ideally be achieved, we find that actual encoders waste approximately 85% of the available signal power.[5]

Optimization requires not only that the number of information bits be made as low as possible without degrading the data excessively, but also that the encoding efficiency be made as high as possible. Requirements such as these have motivated many studies of bandwidth conservation and reduction. A discussion of these techniques will be presented in Section 4.2.

4.1.3 Carrier Frequency[2]

One of the first requirements for pictorial data transmission from a space vehicle is the selection of a carrier frequency. This frequency must be high enough to penetrate the ionosphere while affording good compromise with other noise sources and still lie within the state of the art. Figure 4-1 shows typical space noise densities and their sources in the microwave region of the electromagnetic spectrum. It may be concluded that the transmission range from 150 mc to 10 kmc offers the best choice. The present state of the art in transmitters and antennas coincides very well with this. A possible shift to the optical region of the electromagnetic spectrum for a choice of carrier has generated much enthusiasm. Laser transmission offers the advantages of greater available bandwidth and smaller possible beamwidth (see Section 4.3). However, space communications will most probably utilize a carrier in the microwave region cited above, at least until lasers prove themselves.

4.1.4 Signal-to-Noise Ratio

The errors incurred in a message when transmitted from space probes is a direct consequence of the received signal-to-noise

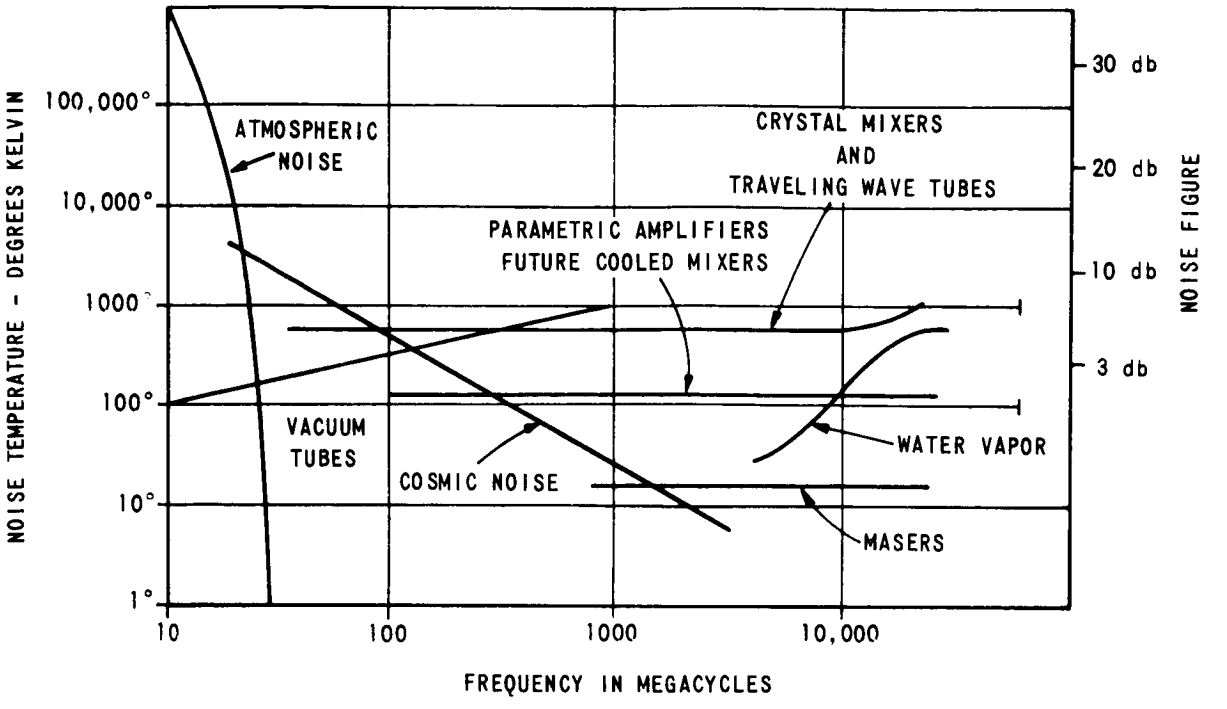

Figure 4-1 NOISE DENSITIES AND THEIR SOURCES (REFERENCE 2)

ratio. A number of special formulas have been derived to calculate this parameter, examples of which follow.[6]

The power received by a directional antenna of the receiver of a space communications system from a directional transmitting antenna of the space probe is given by

$$P_r = \frac{G_t G_r \lambda^2 P_t}{16\pi^2 R^2} \qquad (4\text{-}12)$$

where P_r is the received power, P_t is the transmitted power, λ is the carrier wavelength, R is the transmission distance, G_t is the gain of the transmitting antenna in the direction of the receiver (a dimensionless parameter reflecting the focusing capability of the antenna relative to an isotropic antenna), and G_r is the gain of the receiving antenna in the direction of the transmitter. The gain of the receiving antenna can be used

to define an effective area of the receiving antenna, which simplifies (4-12) to

$$P = \frac{G_t A_r P_t}{4\pi R^2} \tag{4-13}$$

where $A_r \equiv \frac{\lambda^2 G_r}{4\pi}$ is the effective receiver antenna area.

The noise power received from microwave transmission can be approximated by

$$P_n = k T_e B \tag{4-14}$$

where k is Boltzmann's constant, B is the bandwidth of the receiver, and T_e is the equivalent system noise temperature from all sources. The signal-to-noise ratio in db is given by

$$S/N = 10 \log_{10} \left(\frac{P_t G_t A_r}{4\pi R^2 k T_e B} \right) \tag{4-15}$$

For pulse code modulation and white noise, one needs a signal-to-noise ratio of approximately 20 to 1 (13 db).[5] From this we can obtain a range equation for acceptable transmissions.

$$R = \left[\frac{P_t G_t A_r}{80\pi k T_e B} \right]^{1/2} \tag{4-16}$$

State of the art considerations indicate that the edge of the solar system (7.1×10^9 km) is not outside our present reach.[7] However, transmission rates would be of the order of a few bits per minute at this range.

4.2 Bandwidth Compression

Bandwidth compression is the reduction in the bandwidth required to transmit information over a communication link. A given message (e.g., a number of frames of imagery) having an information content H (in bits) will have a duration T (in seconds) if it is transmitted at a rate R (in bits/sec.). When R is optimized, it is equivalent to the channel capacity given in Section 4.1.2. We then have

$$H = TB \log_2 \left(1 + S/N\right) \tag{4-17}$$

Information contained in a message can be classified into two basic classes: unique and redundant. Redundancy exists whenever data are repeated or the information content is wholly or partially reiterated. If a bit of information in a message is independent or totally uncorrelated with the rest of the message, it is said to be unique. Thus, the information in a message can be represented as the sum

$$H = H_U + H_R \tag{4-18}$$

Combining this with (4-17) and solving for B we have an expression for the bandwidth we desire to compress.*

$$B = \frac{H_U + H_R}{T \log_2 (1 + S/N)} \tag{4-19}$$

From this equation it becomes obvious that there are basically three general methods of bandwidth compression: signal-to-noise ratio increase, time expansion, and redundancy removal.

4.2.1 Signal-to-Noise Increase

Signal-to-noise ratio cannot be arbitrarily traded off against bandwidth.[8] Although it is not an impossibility, it is nevertheless impractical when the signal-to-noise ratio required is already high. For example, with pulse code modulation and white noise, one needs a signal-to-noise ratio on the channel of approximately twenty to one. If we compress the bandwidth required by a factor of two using a more complex encoding scheme, from equation (4-19) we see that to retain the same information transmission rate requires an eleven-fold increase in power

*It should be noted that for a channel affected by white noise, the noise power is proportional to the bandwidth. This has been taken into account in the subsequent discussion; however, to avoid a lengthy analysis here the explicit expression was not introduced.

output (remembering that noise power is proportional to bandwidth). The signal-to-noise ratio on the channel would now be 440:1. A five to one compression ratio (which is not unreasonable for some other methods) would require multiplying the original power by 40,841 and the encoder would even be more complex. The cost and weight quickly become prohibitive.

4.2.2 Time Expansion

By sacrificing a real time capability one can reduce the bandwidth required for transmission without losing information or increasing power. There are basically two such methods widely used in space communications for imagery. One uses a tape recording system to store the wideband signal from the sensor, and then transmits with a slower readout rate. The other utilizes the slow-scan technique described in an earlier section (Section 2.2.3.4). This technique stores an image formed during a short exposure time and reads it out in a longer time where the storage medium is the active element of a photo-electronic imaging device and the frame rate of the scanning beam is reduced to lengthen the readout time. A combination of these two methods is possible for deep space probes as in the Pioneer IV system[9] where a slow scan vidicon system having only 6 kcps bandwidth to start with is reduced to 2.5 cps transmitting bandwidth by using tape storage and reduced read out speed between the vidicon and the transmitter.

An important limitation of a tape recording system for such an application is its time base error, i.e., the time error in measuring two events. A time base error can lead to degradation of the geometric fidelity of the transmitted image (by shifting picture elements).* In comparison with high grade television systems which are capable of as little as 1% distortion (e.g., five elements in a five hundred element line), a recorder would need to hold its time base error to the order of a microsecond. Such

*Assuming that the recording occurs between signal generation and digital encoding.

recorders are presently within the state of the art. Current systems hold the time base error to 0.5 - 2.0 microseconds.[10]

4.2.3 Redundancy Removal

The third general method of bandwidth compression is redundancy removal. By eliminating or reducing the redundant information content of a message representing a picture, the saving accomplished can be taken in bandwidth. Many techniques have been devised to remove various aspects of this redundancy and are reported in the open literature. Two reviews of these methods are given by Massa[11] and Whelan[1]. However, most of these methods merely represent ingenious engineering inventions for limited applications and do not present a general method of redundancy removal.

The amount of redundancy which can be removed is a function of the data itself, and any attempt to remove redundancy must be tailored to fit the characteristics of the data, namely their statistics. Encoding systems have been proposed which rely on this redundancy to destroy information selectively with the intent that it be primarily redundant information. Such systems can offer compression up to a factor of two and are reasonably implementable for spacecraft. The selection is based on some a priori knowledge of the statistics of one or more aspects of the imagery. For example, if the imagery to be transmitted is that from a stellar camera, one can generally assume that the majority of the useful information content will be represented by the high frequency components of the signal. With a coarse quantization of the low frequencies and a fine quantization of the high frequencies, a bandwidth saving can be realized.

For obtaining topographic information for mapping purposes we cannot afford the luxury of information destruction. In this case, an information preserving method of redundancy removal should be used, namely, prediction. A section of the encoder is designed to predict what the next element will be based on a knowledge of element(s) preceding it.

Its prediction is then subtracted from the actual value and the difference is transmitted. At the receiver an identical predictor is used to reconstruct the data. The more nearly the predictor matches the statistics of the original signal, the more closely the difference signal will resemble noise centered around zero amplitude. This new signal can be sent over a channel with greatly reduced bandwidth requirements (exact prediction would require zero bandwidth).

There are many drawbacks to the use of prediction. First, information made less redundant by proper processing must be transmitted at lower error rate. Second, in order to handle the possibility of time varying statistics or statistics which may be stationary but are unknown a priori, it is necessary to make the prediction adaptive. This greatly increases the complexity of the implementing electronics. Most of the effort in this field has been theoretical up to the present but the approach holds promise for the future. Third, bandwidth compression by such techniques results in an uneven flow of signal from the encoder. Time buffering (memory and/or delay lines) would be necessary to maintain a constant transmission rate.*

4.2.4 Summary

There are basically three general methods of bandwidth compression: signal-to-noise ratio increase, time expansion and redundancy removal. A fourth might be added to include combinations of these three.

Signal-to-noise ratio increase by encoding for bandwidth compression although possible, is generally impractical when the signal-to-noise ratio is already high.

Time expansion is widely used at present with great success but it requires the sacrifice of real time viewing.

Redundancy removal offers the potential of real time bandwidth compression with the cost of greater complexity and weight. Some

*It is generally assumed that time buffering is a lesser complication than varying transmission rate.

simple techniques can be implemented at present for spacecraft; however, more powerful techniques hold promise for the future.

4.3 Transmission Using Lasers

The problem of transmitting information from a space vehicle to earth is to optimize the ratio of the received information to the weight of the transmission system. The major contributors to this weight are the power supply and the antenna. In this section, the capability of lasers to obtain this optimization will be discussed. Several reports[12-15] discuss the utility of the laser for this purpose and the problems involved in considerable detail. The objective here is to summarize these reports.

In order to maximize the channel capacity it is necessary to maximize the signal-to-noise ratio (see equation 4-11). The equation for the received power has been given by equation (4-13).

$$P_r = \frac{G_t A_r P_t}{4\pi R^2} \tag{4-13}$$

However, for transmission in the optical region, equation (4-14) does not apply. In this region the noise power is approximately

$$P_n = h\nu B \tag{4-20}$$

where h is Planck's constant, and ν is the frequency.

For a transmitting aperture A_t (lens), illuminated by a plane wave (laser output) of wavelength λ, the maximum gain is

$$G_t = \frac{4\pi A_t}{\lambda^2} \tag{4-21}$$

Such a beam is diffraction limited with a beamwidth

$$\theta_D = \frac{1.22\lambda}{D_t} \tag{4-22}$$

where D_t is the diameter of the aperture (assumed circular). We then have a signal-to-noise ratio for the diffraction limited case neglecting transmission and efficiency factors as

$$S/N = \frac{A_t A_r P_t}{h\nu\lambda^2 R^2 B} = \frac{\pi D_t^2 A_r P_t}{4hc\lambda R^2 B} \tag{4-23}$$

where c is the speed of light. Combining (4-22) and (4-23) gives

$$S/N = \frac{\pi(1.22)^2 A_r P_t \lambda}{4hcR^2 B \theta_D^2} . \tag{4-24}$$

For a non-diffraction limited beam, the gain is proportional to the inverse square of the beamwidth θ and the signal-to-noise ratio is reduced to

$$S/N = \frac{\pi(1.22)^2 A_r P_t \lambda}{4hcR^2 B \theta_D^2} \left(\frac{\theta_D^2}{\theta^2}\right) \tag{4-25}$$

In order to explain how to optimize the signal-to-noise ratio, let us assume temporarily that all the independent variables except wavelength are kept constant. In particular, the diameter of the transmitting aperture or antenna is kept constant. As the wavelength is decreased from a very large value, S/N increases according to equation (4-23). This occurs because in the diffraction limited case, the beam becomes narrower according to equation (4-22) and more power is intercepted by the receiver.

The above expressions have assumed that the transmitting and receiving apertures are pointed directly at each other. However, there is generally a certain error in pointing the beam. When the beamwidth is narrowed so that it becomes comparable to the pointing error, no further increase in signal-to-noise ratio can be achieved by reducing wavelength. However, if some means of widening the beam were resorted to, such as putting it out of focus or reducing the size of the transmitting aperture, beamwidth could be maintained greater than the pointing error and the signal-to-noise ratio would now increase as the wavelength increases according to equation (4-25).

Thus, there is an optimum wavelength for a fixed antenna size. This optimum wavelength is a function of the pointing error equivalent to the beamwidth as given by equation (4-22). The next problem in optimization is the determination of the pointing error.

An important factor in determining the pointing error is the necessary lead angle due to the finite velocity of light. The time required for light to travel the round trip between earth and a space vehicle separated by a distance, R , is

$$T = \frac{2R}{c} \tag{4-26}$$

where c is the velocity of light. During this time earth will have moved through an angle

$$\phi = \frac{V_n T}{R} \tag{4-27}$$

where V_n is the normal component of their relative velocity (as opposed to radial). Substitution for T gives

$$\phi = \frac{2V_n}{c} \tag{4-28}$$

Marsten et al[16] have calculated that for a Mars intercept the maximum normal velocity is 12.2 km /second. Thus, the maximum lead angle is 17 seconds of arc.

The disagreement among authorities with respect to the pointing accuracy which can be maintained is the main cause of disagreement in the calculated performance of laser communication systems. Some authorities assume that, at least for the first models, there will be no lead angle calculation and correction.[17] Thus, for the first Mars mission the beamwidth must be at least 20 seconds of arc. However, they concede that for other missions (such as vehicle to vehicle) or for missions which could afford the added complications of computing lead angle, pointing errors could be held to less than a second of arc. This, of course, is based on future progress in the solution of the attendant acquisition and tracking problems.[18]

If one were to compare laser transmission with microwave transmission, it is necessary to consider the effect of antenna size also. Let it be assumed that the optimum beam angle, as fixed by a previously determined pointing error is kept constant. Then equation (4-22) is a constraint equation with the fraction λ / D_t held constant. Now S/N is given by equation (4-24). The optimum wavelength is now as large as possible and D is as large as it is feasible to build.

The following table shows the required antenna diameter in meters for assumed values of θ .

TABLE 4-1

ANTENNA DIAMETER IN METERS AS A FUNCTION OF θ AND WAVELENGTH

Wavelength	20 Sec.	1 Sec.	1/20 Sec.
0.7 Micron	0.009	0.18	3.66
10 Microns	0.122	2.44	48.8
1 Centimeter	122	2,440	48,800
10 Centimeters	1220	24,400	488,000

It is necessary that the antenna shape stay within tolerances so that the beam is not excessively broadened. Optimization also requires that the weight of the antenna plus the weight of the power supply be at a minimum.

Equations (4-23) and (4-25) show that, if the wavelength or antenna diameter is not optimum, then S/N goes down inversely or directly (depending upon which side of the optimum λ is) with these variables. The table shows that, if some lead angle anticipation can be built into the transmission system, laser transmission could outperform microwave transmission on a weight limited basis by several orders of magnitude when efficiencies of components are comparable. (Present laser efficiencies for space application to communication are approximately two orders of magnitude lower in efficiency than microwave systems.)[17] Marsten et al[12]

state that, considering the complication of the earth's atmosphere, unless lead angle anticipation were present, laser transmission to earth would not perform as well as microwave transmission. However, for satellite to satellite communication, where no atmosphere would be present, lasers could outperform microwave transmitters.

Despite the fact that laser transmission has a tremendous inherent capability, the technology has not yet been developed to the point where it is practical for space use. There are many areas where further development is needed. They include improving the efficiency of lasers, designing pointing systems, making large reflecting mirrors for space use, modulating the laser, demodulation, removing atmospheric degradation due to turbulence, improving background discrimination and designing receiving stations. These problems and experiments to obtain basic data and to improve laser transmission are described in considerable detail by several investigators[14] and will not be repeated here. An important consideration is that the technology of using lasers is advancing very rapidly particularly in the area of modulation and demodulation so that one is optimistic.

4.4 Conclusions and Recommendations

The mission of the space probe (and its design to achieve that goal) will determine the resolution requirement for topographic information collection. This resolution requirement in turn determines the bandwidth requirement of the transmission system for real time display at the receiver or the delay in transmission required to communicate the same amount of information in a smaller band. The various methods available for accomplishing this task have various advantages and disadvantages in terms of power, signal-to-noise ratio, efficiency of bandwidth utilization, storage for detail transmission, complexity, and degree of information degradation.

There are basically three general methods of bandwidth compression: signal-to-noise ratio increase, time expansion and redundancy removal. A fourth might be added to include combinations of these three.

Signal-to-noise ratio increase by encoding for bandwidth compression, although possible, is generally impractical when the signal-to-noise ratio is already high.

Time expansion is widely used at present with great success but it requires the sacrifice of real time viewing.

Redundancy removal offers the potential of real time bandwidth compression with the cost of greater complexity and weight. Some simple techniques can be implemented at present for spacecraft; however, more powerful techniques hold promise for the future.

One can conclude the following about laser transmission:

(1) There is considerable uncertainty about the pointing accuracy which can be maintained. Until this can be determined there will be corresponding uncertainty with respect to the performance of laser data transmission.

(2) Despite this uncertainty, laser transmission has the capability of communication at a greater range than microwave transmission at the same bandwidth. Exactly how well the two compare cannot be calculated without an investigation of antenna weights and component performance.

(3) Before laser transmission is practical and competitive for transmission from a space vehicle, considerable development work is necessary; a practical system is several years away.

From our studies of these areas, it is recommended that:

The review of transmission techniques, to include the requirements for and applications to the problems peculiar to space missions, should be continued to maintain an awareness of new developments in such rapidly advancing fields as bandwidth compression and laser transmission.

Transmission of imagery should be reconsidered, not as an independent process, but as a subsystem of a total system of imagery collection considered from source to use.

Concerning laser transmission, work on solving the pointing problem should be given highest priority. Detailed recommendations are presented in Reference 14.

5. DISPLAYS

The following material reviews available methods of display which might be used either in a spacecraft or on the ground. The display methods are divided into two categories; those which provide a stereoscopic or three dimensional illusion and those which provide three dimensional information without the illusion of a three dimensional image. No consideration has been given to two dimensional displays from which three dimensional information cannot be derived. In each case, the display method is considered with respect to whether the information to be displayed must be stored or can be available in real time, whether the information may be supplied in color, and whether the display can be used by a group. Attention is also directed to whether the method is appropriate in cases where the user of the display must be able to view other instruments as well. In these cases, it may not be practical for the observer to wear goggles or position his head such that he could conveniently observe the other instruments.

Those displays which create a three dimensional illusion are considered first, followed by display methods which use three dimensional information without stereo illusion. A summary is then presented and those methods which are best for use in the spacecraft or on the ground are enumerated.

5.1 Stereoscopic Display Methods

Stereoscopic displays require that each eye be presented with a different image. The required separation of the images can be accomplished by a number of methods including the use of two separate optical systems (stereoscopes)[1], coding of the light by polarization[1, 2], lenticular prints and films[1, 3], coding of the light by color (anaglyphs)[1], and holograms. Each of these methods is discussed below. Because of the special nature of the holographic display, it is discussed in detail in Section 3.

Stereoscopes provide a separate image for each eye, with the images in proper registration, by using a separate optical system for each eye. Each optical system can provide magnification. Thus by using a stereoscope, any stored data could be stored in reduction, but a power reduction of approximately seven is the most that can be used with rapid viewing. A limitation of the stereoscope is that the eyes must be in registration with the optical system and, therefore, it is more difficult to shift attention to other objects.

For the purpose of real time display by this method, consideration should be given to the use of a kinescope with 1.59 cm diagonal and four power optical magnification. The optical system should be of the virtual image type to minimize light loss. The 1.59 cm size appears to be a practical minimum because electronic image tubes having smaller dimensions have poorer resolution in terms of the total number of resolvable elements and those with larger dimensions do not have much better resolution. Shielding must be provided to protect a viewer from the possibility of a kinescope implosion. Any optical components used can provide part of the shielding.

Two small kinescopes with magnification can be combined to provide a stereoscope. Such a device would be suitable for use by only one person. The registration problem would not be as severe as that encountered in the transmission of commercial color television, because the eyes can tolerate some misregistration. However, it is important that good geometrical fidelity be maintained because if a small area is displaced relative to the surrounding area differently in one image than in the other, a false stereo illusion results. For example, a flat area might look like a hill. Considerable magnetic shielding and perhaps electrostatic deflection and focusing would be required.

If a phosphor with adequately short persistence is used, it is possible to display both pictures of the stereo pair on the same kinescope sequentially. Each picture may then be sent to the proper eye by electro-optical or mechanical means. The switching can, for example, be done with motor driven rotating discs. However, all such systems have severe synchronization problems. Suitable electro-optical methods involve polarization and are discussed below.

The second class of methods of obtaining stereo display is to separate the two images by means of polarization. These methods may involve only polarization, or combinations of polarization and mechanical means. In the kinescope method described above, the mechanical switching from one image to the other image can be replaced by a combination of mechanical and polarization switching, thus reducing synchronization problems. Polarization separation can also be used with Polaroid's patented vectograph film or in projection systems which use two separate projectors and polarization to allow use of one screen. These methods are considered next.

Assuming a phosphor with a narrow wavelength band of radiation, a display for a single observer may be constructed using electro-optical switching. The principles of operation of such a device are: 1) use of a polarizer to obtain circularly polarized light, 2) use of a Pockels cell to convert this to two orthogonal polarizations, 3) use of a polarization sensitive beam-splitter to separate the two beams, and 4) use of additional polarizers, if necessary, to suppress leakage of the beam-splitter. One possible configuration is shown in Figure 5-1. The voltage applied to the Pockels cell would be reversed whenever the video image is to be switched to the other eye. Preliminary calculations indicate that the current consumption of the Pockels cell could be about 1/2 milliampere at high voltage, which might possibly be taken from the kinescope anode supply. Power consumption would be intolerably high for any system designed for more than one observer because in such a system the Pockels cell would be required to have a large linear and angular aperture, and the power consumption is approximately proportional to the product of the squares of the linear and angular apertures.

Another single observer display technique would use a disc with sectors of right and left circular polarizers driven in synchronism with the switching of the kinescope image (see Figure 5-2). These sectors would receive unpolarized light from the kinescope. By use of a linear polarizer and alternate positive and negative quarter wave plates, the light is made to be alternately right and left circularly polarized. The circularly

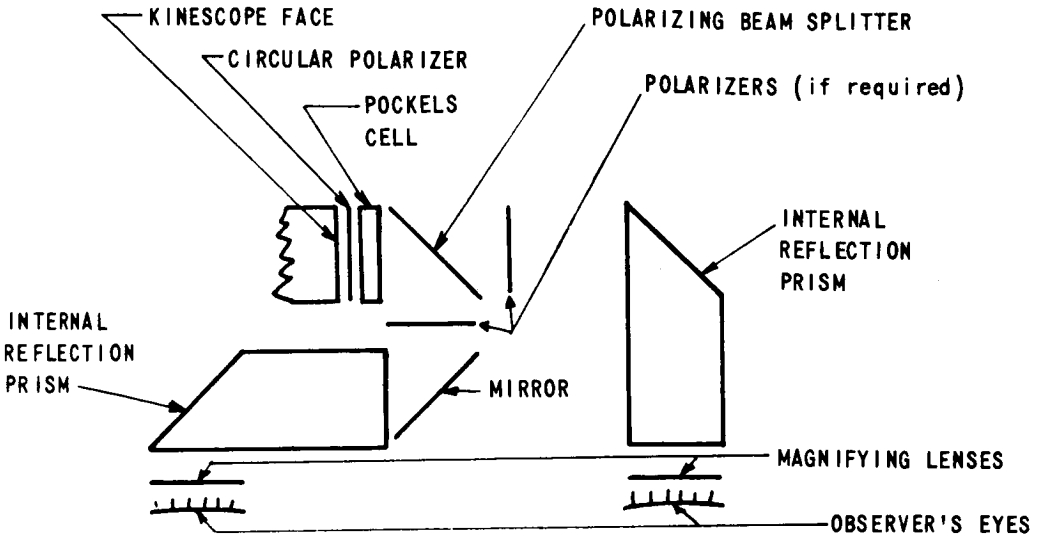

Figure 5-1 ELECTRO-OPTICAL SINGLE OBSERVER STEREO VIEWER (FULL SCALE)

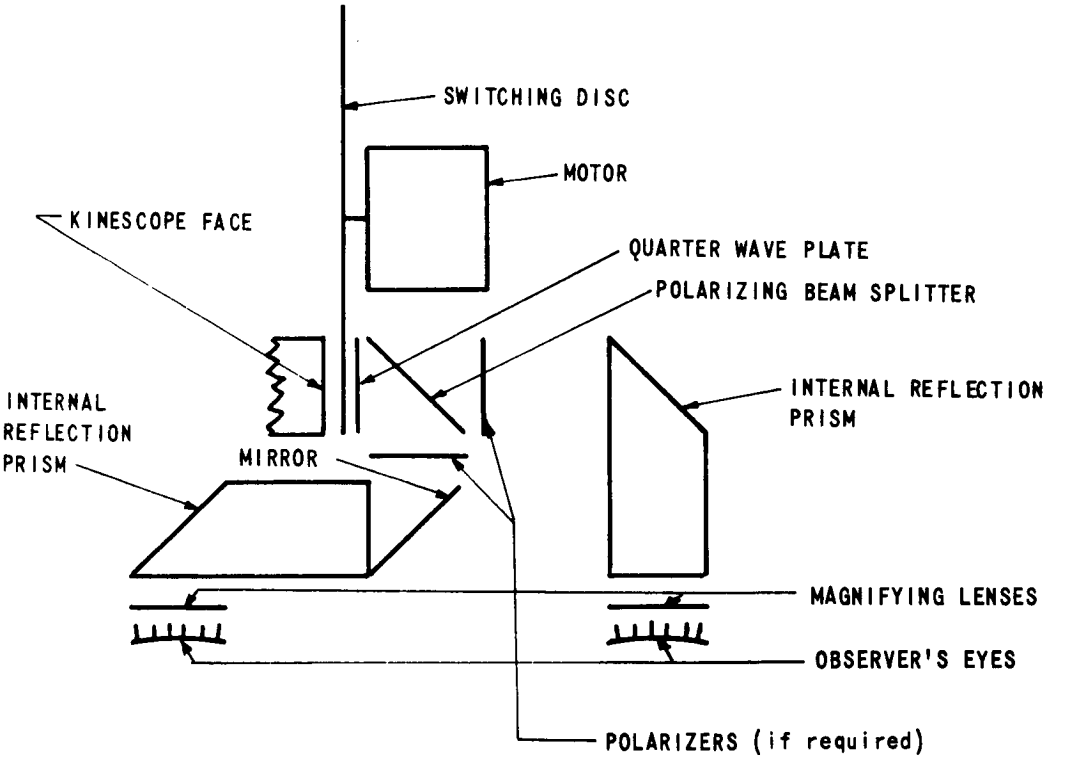

Figure 5-2 SINGLE OBSERVER STEREO VIEWER WITH MECHANICAL POLARIZATION SWITCHING (FULL SCALE)

polarized light may then be sent to the proper eye by the use of a quarter wave plate and polarization sensitive beam splitter, as discussed above.

If it is required to provide stereo information for several observers, this may be done by using the motor driven disc with circularly polarizing sectors, as discussed above, with viewing spectacles designed to separate right hand and left hand circularly polarized light. In this and the previous system, it is necessary to use circularly polarized light so that the polarization form will not change within a sector because of disc rotation.

Vectograph prints may be used to display stored information. These have a separate picture on each side of a transparent base. Each picture absorbs light of one of two perpendicular directions of linear polarization to create the desired shade of gray without disturbing the light of the other polarization. Vectograph films are illuminated with unpolarized light, and each eye is provided with an analyzer. This can be done by using viewing spectacles which will not interfere noticeably with normal vision. Reduction for the purpose of compactness is not worthwhile for vectograph prints because of the limited resolution of the dye transfer process used in printing them.

It is also possible to provide a group viewing capability as well as a real time capability by using two projectors and polarization separation, by projecting two images on the same screen and viewing the screen with polarized glasses. The two scenes of the stereo pair would be projected on the screen with the pictures being polarized in perpendicular directions. As in the case of the vectograph prints above, the polarized glasses still allow the operator to see other panels and controls.

For real time presentation, any of the methods which have been used to present TV to large audiences should be adequate. In particular, thermoplastic tape would be satisfactory. An electronic gun which is intensity or focus modulated, deposits lines of charge on a moving belt of plastic in an evacuated chamber. The plastic is heated and the electrostatic forces wrinkle the plastic. The image is viewed with a

Schlieren system and could be projected on a screen. The tape does not need to be moved out of the vacuum in order to be viewed.

If the number of lines per frame exceeds that which an electron gun can provide, and the data are received at a sufficiently low rate, then a mechanical-optical oscillograph may be used to expose photographic film. The development must be rapid and the film projected while wet. This would also preserve the geometrical fidelity.

Optical separation of the images by use of lenticular film or prints is the third method of stereo separation. Lenticular prints use a series of cylindrical lenses formed in a plastic coating which covers the print. The print itself is composed of alternating strips of the right eye picture and the left eye picture. On each of these strips, the width scale must be half of the length scale (or perhaps less) in order to have space to print all of the two pictures. The cylindrical lenses magnify each strip in only one dimension to restore the proper scale in the dimension which was compressed and, at the same time, permit each strip to be seen only by the proper eye. The lenses are made as small as practical to minimize the astigmatism inherent in the device.

The cylindrical lenses are usually formed in a plastic sheet which is bonded to the print. Because the plastic has many small grooves and is soft, it is difficult to clean without damaging it. Resolution is limited to approximately that which is comfortable to view with the unaided eye because of imperfections in the plastic lenses, misregistration, and astigmatism. The problems of imperfections and misregistration become more difficult when the lenses are made smaller, while the problem of astigmatism becomes worse when the lenses are made larger. Because of these difficulties, reduction and subsequent magnification does not appear promising with lenticular prints. If a lenticular print with a format size of the order of or greater than the eye spacing (65 ± 7 mm) is to function properly, the cycle spacing of the picture strips must be somewhat greater than the cycle spacing of the lenses because the directions from the print to the eyes depend on format position. The proper head position is near the center where the lenses are centered over the picture strips. Thus, lenticular

prints cannot be viewed at full effectiveness by more than one person at a time. (Commercial lenticular prints use equal cycle spacings and the head must be moved so as to permit viewing the desired section nearly normally.)

Lenticular film is made on a transparent base. The emulsion and the cylindrical lenses are on opposite sides of this support. Because the lenses are used in exposing the film (i. e., the film is exposed through the base), the registration problems are avoided. Also, because the lenses are formed prior to the coating of the emulsion, permitting the use of stronger material, and because they must be larger, cleaning is not as severe a problem as in the case of prints. However, the large separation between the lenses and the film introduces such a large amount of astigmatism that it must be compensated by the use of more cylindrical lenses, or in other words, a viewer must be used. Also, lenticular film must be viewed from the proper position, and hence is not suitable for viewing by more than one person at a time.

The fourth method of stereo display considered uses anaglyph prints in which the two stereo images are color coded. For example, one of the eyes may be covered with a cyan filter and the picture for that eye printed in red on a white background. Similarly, the other eye may be covered with a red filter and have a cyan print on the same support. Obviously, this system cannot be used to display colored pictures. Also, it is expected that the viewing spectacles would degrade the vision of the user if he left them on while performing other tasks.

The anaglyph technique can also be used for real time viewing systems by using a color kinescope tube and displaying one picture with, for example, the red gun* while the other picture is displayed with the green or blue gun. As in the case of the anaglyph prints, this method requires the use of colored glasses and, therefore, makes it difficult for the viewer to simultaneously examine other instruments on nearby panels. In addition to this difficulty, the kinescope display system will have geometric fidelity problems which create false impressions of terrain curvature.

* Red gun refers to the electron gun which excites the red phosphor on the kinescope face.

Holographic displays are discussed in detail in Section 3. It should be noted that to date it does not appear feasible to use holographic displays for real time viewing. However, in cases where real time viewing is not required, holograms offer several advantages. For example, color imaging is possible, although such systems are not yet common. In addition, the holographic display is the only three dimensional display system which provides the stereo illusion, while at the same time requiring no glasses or other aids which will interfere with the use of other instruments.

5.2 Non-Stereoscopic Display Methods

It is frequently useful to display three dimensional information without the use of the stereo illusion. Two methods for producing such displays are discussed below.

One method of presenting stored three dimensional information without the stereo illusion is by the use of contour lines. A limitation of this method for rapid use is that it is usually necessary to find two spot altitudes in order to determine the direction of increasing altitude. The only exception to this rule is when a body of water appears in the area of interest. This difficulty can be remedied by any of several methods. Among these are: 1) the use of short hachures extending in the downward (or upward) directions from contour lines, and 2) the use of arrows on contour lines such that if one were to proceed along the contour line in the direction of the arrow downhill would be to the right (or to the left). Certainly others exist.

Another method for rapid presentation of topographical information without the stereo illusion might use lines whose normal displacements are proportional to the altitude. The presentation would appear as if the scene were being viewed obliquely. For flat terrain, the display would consist of parallel straight lines. High areas would be denoted by deflections of the lines in one direction, low areas, by deflections in the opposite direction. This type of display can be as readily composed as any

real-time three dimensional display whose data are generated by a scanning profilometer.

A method was conceived on Project TECH TOP to generate these lines as moire fringes rather than store them directly. This could be done by superposing a Fresnel zone plate and a second piece of copy. This second piece of copy would be similar to a zone plate except that the bands would be deflected in proportion to the product of their widths and the altitudes which they are required to represent. This would permit variations in the number and general direction of the fringes.

For real time generation of such displays, almost any device which samples terrain altitude over a wide area may be arranged to give the parallel line presentation. The following paragraphs show how it is possible to derive coded contour lines or parallel lines with little computing from a scanning modulated C. W. rangefinder using techniques conceived on Project TECH TOP.

Modulated C. W. rangefinders measure range by transmitting a modulated carrier, and comparing the phase of the modulation on the signal which is reflected back to the phase of the transmitted modulating wave. Assume that a small angular field of view is being scanned by motion of the antenna or lens system. Then, if the wavelength of the modulating frequency is half the contour interval desired, wherever the phase of the return envelope is equal to some constant plus the phase of the modulating waveform, a point on a contour line should be displayed. Hence, a contour display may be generated by coupling the deflection circuit of a kinescope to the antenna, and unblanking the electron gun whenever the above phases agree.

A second method would be to make the modulating wavelength twice the contour interval, and detect certain phase differences, for example, 0^{o}, 90^{o}, 180^{o} and 270^{o}. By setting different thresholds for the separate phase matches, different line widths would result. This would create a code showing locally which contour was higher.

If a wider field of view is required, it becomes necessary to make a correction for the fact that the distances are measured as displacements from a sphere centered at the rangefinder, rather than as displacements from a distant plane. This requires additional phase shifts to be added as a function of antenna angles. These phase shifts could be added by the use of cam operated rotating winding transformers, or by superimposing a Fresnel zone plate over the kinescope face. In either case, the compensation would be aided if the contour interval were made proportional to the gross range so that the number of cycles to be added depended only on the antenna angle. If a variable modulation frequency is used, the use of at least two separate phase detectors is required in order to develop proper AGC. The contour line presentation may be changed to the parallel line type by a slight change of the spherical field compensation.

5.3 Summary of Characteristics of Three Dimensional Display Systems

The characteristics of the three dimensional displays described in the previous sub-sections are summarized in Table 5-1. The relative usefulness of the various display methods depends upon the particular application of the display and upon whether the display is to be used in the spacecraft or on the ground. Generally, the spacecraft display systems may be used by one or two persons while the ground display is primarily used by groups of persons. In either case, some of the persons using the display may, at nearly the same time, be required to read other instruments located nearby. Displays with the illusion of stereo are, generally, more useful in cases where measurements are not to be made but a general impression of the shape of topography is to be obtained rapidly. Geometrical distortions cause errors in measuring distances or in observing the shape of topography. Therefore, where the measurement or shape is critical, the geometrical errors must be reduced by avoiding methods which utilize cathode ray tubes.

TABLE 5-I
CHARACTERISTICS OF THREE DIMENSIONAL DISPLAYS

TYPE OF DISPLAY	REAL TIME VIEWING?	GROUP VIEWING?	GEOMETRIC FIDELITY PROBLEMS?	COLOR IMAGING?	USEFUL REDUCTION	DIFFICULTIES IN VIEWING OTHER DISPLAYS?
DISPLAYS WHICH CREATE STEREO ILLUSION						
STEREOSCOPE DISPLAYS						
FILM OR PRINT	NO	NO	NO	YES	7X	HEAD POSITION
2 KINESCOPES	YES	NO	YES	YES	4X	HEAD POSITION
1 KINESCOPE & ELECTRO-OPTICAL SWITCHING	YES	NO	YES	NO	4X	HEAD POSITION
1 SMALL KINESCOPE & MECHANICAL SWITCHING	YES	NO	YES	YES (1)	4X	HEAD POSITION
POLARIZATION DISPLAYS						
STEREOSCOPE WITH 1 SMALL KINESCOPE & MECHANICAL-POLARIZATION SWITCHING	YES	NO	YES	PARTIALLY (2)	4X	HEAD POSITION
VECTOGRAPH	NO	YES	NO	NOTE 3	NONE	NEGLIGIBLE
2 PROJECTORS & POLARIZATION SEPARATION	YES	YES	YES	YES	N/A	NEGLIGIBLE
LARGE KINESCOPE WITH MECHANICAL POLARIZATION SWITCHING	YES	YES	YES	PARTIALLY (2)	NONE	NEGLIGIBLE
LENTICULAR DISPLAYS						
PRINTS	NO	NO	YES	YES	NONE	HEAD POSITION
FILM	NO	NO	YES	YES	NOTE 4	HEAD POSITION
ANAGLYPH DISPLAYS						
FILM OR PRINT	NO	YES	NO	NO	NONE	LOSS OF COLOR
LARGE COLOR KINESCOPE	YES	YES	YES	NO	NONE	LOSS OF COLOR
HOLOGRAPHIC DISPLAY	NO	YES	NO	POSSIBLE	N/A	NONE
DISPLAYS WHICH DO NOT NOT CREATE STEREO ILLUSION						
CONTOURS OR PARALLEL CURVES FILM, PRINTS OR PAPER	NO	YES	NO	NOT APPLICABLE	NONE NOTE 5	NONE
CONTOURS OR PARALLEL CURVES ON KINESCOPE	YES	YES	NO	NOT APPLICABLE	NONE NOTE 6	NONE

NOTES:
1. COLOR RESOLUTION WILL BE LESS THAN B/W IF STANDARD.BROADCAST METHODS ARE USED.
2. PARTIAL LOSS OF STEREO FROM DISPERSION IN HALF WAVE PLATES.
3. THIS HAS BEEN DONE, BUT IS APPARENTLY VERY DIFFICULT, AS IT IS NOT DONE COMMERCIALLY.
4. NOT CLOSELY INVESTIGATED, WOULD BE LESS THAN 7X.
5. 7X POSSIBLE WITH SACRIFICE OF HEAD POSITION AND GROUP VIEWING.
6. 4X POSSIBLE WITH SACRIFICE OF HEAD POSITION AND GROUP VIEWING.

Examination of the data presented in Table 5.1 shows that lenticular film is generally unsatisfactory because of poor resolution and other problems. Similarly, anaglyph presentations rank low because they require colored glasses which make viewing other instruments difficult and because they provide no color image capability. The stereoscopic and polarization techniques appear to be the best of the display systems which create stereo illusion. The polarization techniques are preferred in cases where more than one person must use the display and, for this reason, are preferred for ground display systems.

When the illusion of stereo is not desirable or required, the contour method provides a convenient method of displaying three dimensional information. The information required to generate the contours can be derived from pairs of stereo photographs using standard stereo plotting techniques or from data obtained by a laser ranging/imaging system. The displaced line technique for presenting three dimensional information provides a method particularly suitable for real time presentations.

Holographic displays are currently at an early stage of development. Since it does not appear to be feasible to provide a real time capability with holograms at the present time, realization of the full potential of the holographic display must be reserved for the future.

6. STELLAR PARALLAX

In recent years the state of the art of trigonometric stellar parallax measurements has had few major developments. The failure to eliminate the degrading effects of the earth's atmosphere and the inability to increase the base line have limited the utility of distance measurements beyond 160 light years.

Realizing that the major limitations might be eliminated by the use of a space satellite, an exploratory study was conducted. The specific objectives were as follows:

(1) To determine the astronomical significance of improved stellar parallax measurements.

(2) To explore the feasibility of making stellar parallax measurements from a space vehicle.

(3) To determine where the basic engineering problems exist in performing such measurements.

(4) To recommend the areas of research which should be further investigated.

The general procedure used in arriving at the recommendations was initiated by an extensive literature survey and discussions with astronomers and astrophysicists concerning, in particular, the need for an improvement in accuracy. Calculations were made and estimates were determined for the accuracy of the different components of the entire measuring system.

The purpose of this section is to present the findings of this investigation. It will be presented in the following order:

First, sub-section 6.1 discusses the current method and technique for measuring stellar parallax;

Second, sub-section 6.2 gives a brief description of indirect measuring techniques and indicates the significance of improved stellar parallax measurements; then

Sub-section 6.3 describes engineering problems associated with stellar parallax measurements made from space vehicles; and

Finally, sub-section 6.4 reports the conclusions and recommendations.

In the appendix, direct references and a general bibliography are provided. The references indicated contain considerable information on indirect measuring techniques which are only briefly discussed in the text.

6.1 Current Methods and Technique for Stellar Parallax Measurement

This section defines trigonometric stellar parallax and describes briefly the current technique of performing earth-based stellar parallax measurements. The present limitations on accuracy are indicated and source references are given where trigonometric information can be obtained.

The trigonometric method involves determining the apparent displacement of a nearby star as seen from two different positions in space. In practice, the parallax star and a background of more distant reference stars are recorded on a series of photographic plates. If the same photographic plate could be exposed at equal intervals of time as the earth moves about the sun, the positions of the parallax star would describe an ellipse (assuming the star had zero proper motion). At approximately six-month intervals, the parallax star would appear at opposite ends of the semi-major axis of this parallactic ellipse and be most favorably displaced for photography. If, as is usual, the parallax star also exhibits a proper motion, corrections can normally be applied to reduce the apparent motion to the parallactic ellipse. Thus, the series of photographic plates can usually be taken at about six-month intervals when the apparent displacement is a maximum. By making linear measurements of the displacement on the plates, and using the focal length of the telescope employed, the angular displacement can be obtained. The star's annual parallax π, is defined as one-half this angular displacement, or ideally the maximum angle under which the radius of the earth's orbit would be seen from the star. This parallax is related to the star's distance d from the sun and the length a of the earth-sun base line by

$$\sin \pi = \frac{a}{d} \qquad (6\text{-}1)$$

Since the parallax of the nearest known binary system, Alpha Centauri, is only 0."760, π is small and the previous expression may be conveniently written

$$d = \frac{1.''0}{\pi} \qquad (6\text{-}2)$$

where the distance d is given in parsecs and π in seconds of arc.*

The above is a simplified presentation of trigonometric parallax determinations. In reality it is a process requiring extreme care and attention to detail in order to eliminate or reduce accidental and systematic errors.

In the past, trigonometric parallaxes have been derived from short series of 12 to 18 plates, whereas current practice at Sproul and Allegheny Observatories is to use a longer astrometric series of 50 to 100 plates to improve the statistical reliability of parallax measures for a single star. Lippincott's [1] investigation of the accuracy of parallaxes obtained for 53 stars using long series of plates indicates that further additions in the number of plates would not materially increase the accuracy because of latent sources of instrumental error. Van de Kamp[2] has noted that positional accuracy (probable error) on single plates taken with the Sproul 24-inch refractor is about $\pm$ 0."02; and "this accuracy for any one night may be regarded as the limit beyond which it is not easy to go". However, average probable errors of about $\pm$ 0."01 were found for short series of Sproul[2] parallaxes, and longer series gave values of about $\pm$ 0."005. It is not surprising, therefore, that systematic differences of the order of $\pm$ 0."005 between parallaxes determined at different observatories have been found by Lippincott[1] and Schilt[3].

* In this expression a = 1 astronomical unit (A. U.) and one parsec is defined as the distance at which a star has a parallax of 1". One parsec corresponds to a distance of 206265 A. U. or 3. 26 light years.

It should be pointed out, that with positional errors at their current values (i.e., $>\pm$ 0."005 sec), conventional trigonometric parallaxes less than 0.03" to 0.02", corresponding to distances greater than 33 to 50 parsecs respectively, are of limited reliability. For example, for distance measurements of 50 parsecs the error is on the order of 0.005/0.02 or 25%. Thus, 50 parsecs can be taken to be the upper significant limit for measuring distance by this technique. In order to achieve the angular accuracy that is indicated, the current state of the art of metrology is reached in making positional measurements on the photographic plates. Let us take, for example, a typical refractive telescope having a focal length of 600 cm. A probable error in angular displacement of 0."02 corresponds to a probable error in a linear displacement of approximately 0.5 microns in the image plane. Position measurements are usually made to the nearest micron. The smallest star images are seldom below 1 second of arc (apparent) diameter due to atmospheric effects. For the same focal length of 600 cm, this corresponds to a linear diameter of about 30 microns in the image plane. This implies that the position of the star image can be determined to a small fraction of its diameter. The positional data obtained from a series of plates is reduced through various mathematical formulations (see Smart[4], for example). Van de Kamp[2] has recently reviewed observational procedures and precautions and has discussed current reduction techniques based on Schlesinger's method of dependences[5]. Eichhorn and Jefferys[6] have employed a more elaborate reduction program.

The reduction of data by the techniques mentioned above yields the relative parallax of a star, i.e., relative to the set of background reference stars. To obtain the star's absolute parallax, and hence its true distance from the sun, the mean parallax of the reference stars must be added to this relative value. For earth-based measurements, the mean parallax of the comparison stars is small and usually amounts to only a few thousandths of a second of arc. It may be derived from statistical parallax using the average photo-visual magnitude and the spectra or colors of the reference stars. Data given by Binnendijk[7] and Vyssotsky and Williams[8] are often used for this purpose.

The primary catalogue of trigonometric stellar parallaxes is the one prepared by Jenkins[9] in 1952. It contains values for 5822 stars. Strand[10] has indicated some of the later work through 1960, and the most recent determinations include some 20 articles in the Astronomical Journal, Vols. 67-70.

6.1.1 Summary

Trigonometric parallax determinations require extreme care and attention to obtain a reliable distance measurement on the order of 50 parsecs.

6.2 Significance of Stellar Parallax Measurements

In order to arrive at an answer to two questions: (1) Would improved trigonometric stellar parallax measurements be helpful to the astronomical community?, (2) If so, how much improvement would be required?, it is necessary to describe briefly indirect techniques for distance measurement and location of certain objects that are of interest in our galaxy. It is the purpose of this section to answer the questions posed above.

There are essentially two groups of distance measuring methods* now in use: the geometrical ones which involve the solution of triangles using observational data, and the photometric and spectroscopic methods which involve the comparison of apparent stellar magnitudes and colors with a Hertsprung-Russell diagram of stars whose distances are already known, or comparison of the time variation of stellar magnitude with known period-luminosity relations.

* A more complete discussion of this topic appeared in the attachment to the Ninth Monthly Progress Report, March 1966.

The geometrical methods include principally the trigonometric, moving cluster, statistical and dynamic parallax approaches. The trigonometric approach is unique in that it yields the only direct determination of distances of single stars. The rest of the techniques involve more than one star and require additional information such as cluster convergent points, radial velocities and spectral classes of the stars, and orbital parameters of multiple systems.

The indirect techniques allow for expanding the distance scale which is fundamentally based upon the trigonometric measurements. Therefore, an improvement in trigonometric stellar parallax measurements would correspondingly improve the calibration techniques for indirect measurements. The question of improvement then is bounded by an upper limit. Obviously it would not be necessary to develop trigonometric techniques that could measure distant stellar objects if indirect techniques can provide this information accurately.

Current trigonometric parallaxes are not useful beyond about 50 parsecs and moving cluster techniques, which are also used for calibration, are of limited utility beyond a few hundred parsecs. Therefore, most of the objects used for calibration lie within a distance of about 500 parsecs of the sun. Objects of interest within 500 parsecs include several galactic clusters and associations, and representatives of essentially all the population I spectral types. A sampling of population II spectral types would be represented as well. In addition to establishing a firmer calibration of absolute stellar magnitudes over this 500 parsec distance, improved parallax measures would be of significance in determining the properties of interstellar absorption and investigating the uniformity of stellar chemical composition.

If distances up to 5000 parsecs could be measured by direct long base-line methods, a number of other objects of importance would be included. In particular, many of the population II, RR Lyrae variables would be within this range. Determination of the absolute stellar magnitudes of these type variables is of significance since they are used in

calibrating period-luminosity relations of the type II cepheids. In addition, stars within some 11 globular clusters, according to the list by Hoag[11], would be accessible for direct distance determination as well as a large number of other stars. Distance determinations over this scale would be of much utility in calibrating the extragalactic distance scales.

The astronomical significance of improving parallax measurements must be discussed in a qualified manner. In a gross sense, improved measurements would be significant, because they could be employed to fix more accurately distances of objects whose present distances must be determined by indirect means. It should be recognized that the parallax measures would be relatively insignificant if measures were made for only a few objects. A gain of a factor of roughly 10 over the 50 parsecs currently obtainable would be of the greatest significance, rather than a higher gain of say 100. A gain of a factor of 10 should provide sufficiently better calibrations of indirect parallax approaches that the understanding of stellar processes and galactic structure could be advanced considerably. Without this increased understanding it is likely that full utilization of the higher gain of 100 would not be realized.

The initial questions posed at the beginning of this section have been answered, but another question arises immediately: If the distance measurements would be increased by a factor of ten, would it be possible to find background stars which can be used as fixed references? It is necessary to examine what is currently known about our galaxy before we can answer this question. The galaxy is viewed as being a flattened disc-like structure with a central bulge of stars. Surrounding this disc-like structure is a nearly spherical halo of globular clusters. The distance from the sun to the center of this halo, and presumably the distance to the center of the galaxy is about 10, 000 parsecs in the direction of the constellation Sagittarius. Star counts indicate that the sun is very near the plane of the galactic disc. The distance from the sun to the farthest stars in the direction of the galactic anticenter, i. e., in the direction opposite to the center of our galaxy, is about 4600 parsecs. The total radius of our galaxy is thus about 14, 600 parsecs.

Blaauw's data[12] indicates that the bulk of the stellar systems in the vicinity of the sun lie within a few hundred parsecs of the galactic plane. Relatively few objects are found at distances normal to the galactic plane exceeding 500 parsecs. This situation is most unfavorable for making long base line parallax measures, because very few background stars in the directions far removed from the galactic plane will be suitable for use as reference stars. The presence of interstellar dust, which is relatively dense and opaque in certain regions, would require careful selection of objects for observation near the galactic plane to ensure the presence of a usable stellar background. Thus, while much greater freedom in the choice of objects to be observed would be possible away from the galactic plane, a reference system of galaxies would probably be required.

To summarize, an improvement in trigonometric stellar parallax measurements of a factor of ten would be helpful to the astronomical community. With such an improvement special consideration would have to be taken in determining background references. It is quite likely that extra-galactic objects would be necessary.

6.3 Stellar Parallax Measurement from Space Vehicles

This section describes the engineering problems associated with making stellar parallax measurements from a space vehicle. From this discussion a qualitative description of the current and near future feasibility of performing a successful mission is given. The areas in which improvements must be developed are mentioned and recommendations are made for areas which should be further explored.

Basically, two advantages are gained by making stellar parallax measurements from space vehicles: (1) the degrading atmosphere effects are removed, and (2) the base line can be extended. The first advantage can be realized by a satellite orbiting the earth. Both advantages can be realized by a deep space probe operating at large distances (perhaps 50 to 100 astronomical units) from the earth. The problem of parallax measurements from a fixed base on the moon is not considered in this study. The significance of an astronomical station on the moon is being examined within NASA.

A complete system analysis was not performed to determine all the interdependences of the various components. Because of time limitation, areas were investigated to observe the major dependence and estimates were made in regard to the needed accuracies. Only a complete and very extensive study could provide sufficient data to justify a series of trade offs that would be required in an actual mission. This section was written in this context and the material presented is reported by considering temperature, metrology, sensor, optical, transmission, and other related problem areas. In some cases it will be obvious where there is an interdependence of several factors that are discussed together.

We can look at some of the specific problems if a flight is considered where the base line is on the order of a 100 astronomical units. This could potentially increase the accuracy by approximately a factor of 50, or the required instrumental accuracy could be reduced by a factor of 5 over earth-based measurements in order to improve the overall measurements by a factor of 10.

At this great distance, the energy received from the sun at the spacecraft will be decreased by a factor of 10, 000 compared to that received at the earth. This, in turn, will result in the spacecraft being below 40° Kelvin. Assuming the instrumentation aboard the vehicle will be similar to that used for earth based measurements, a heat source would be required because the optical components and the mechanical measuring device are all extremely critical to temperature variations which cannot be tolerated in parallax measurements. Normally these variations with temperatures are non-linear and difficult to compensate during an experiment. It will, therefore, be necessary to maintain the entire system at a workable temperature, which must be held constant within a few degrees or less depending upon the component.

A power source would be required to supply energy to the telescope scanning device and, if present, to the plate development subsystem, in order to maintain proper development temperatures. Thus, a reactor or some large heat source would be necessary. The induced thermal gradients would be more difficult to compensate than uniform temperature

changes. If a reactor is used, shielding may become an important problem, especially if photographic plates or sensitive solid state detectors are used to record the stellar images. In order to obtain figures on how long temperature control would be required, a launch velocity of over 11.3 km/sec is assumed for the spacecraft. The trip would take over 10 years before the base line between earth and the spacecraft is separated by a 100 A. U. This figure assumes the spacecraft is fired in a direction opposite to the direction in which the solar system is traveling in space. (The solar system is moving with a velocity over 3 A. U. /year with respect to the constellation Hercules, where the Standard Apex of the Sun's Way is located.)

Basically, two methods can be considered for obtaining the image, recording and subsequent scanning, or real time measurement. In either case the scanning accuracy required to obtain the coordinates would be difficult to achieve in actual flight. The problem obviously could be alleviated by taking photographs in space and returning them to earth where scanning could be performed. For a baseline on the order of 100 A. U., approximately 30 years would be required to complete a round trip under the above conditions. A major disadvantage of such a mission is that the success would depend on whether or not the spacecraft is recovered. Because of the long duration of this flight, reliability would become extremely important; any failure in the system may render the entire trip worthless. For this reason, it appears some means should be provided onboard the spacecraft to determine the stellar coordinates and transmit them back to earth.

At the present state of the art the only recording sensor which has a high probability of being satisfactory is the photographic plate. As a recording medium it has a sensitivity and dynamic range which are not equaled by other methods which can record directly a large number of resolution elements with low distortion.

If photographic plates are used so that long time integrations are possible (so the very faint fixed stars can be detected), a microdensitometer will be necessary to scan them. However, this introduces a temperature control problem; the Mann Corporation[13], a manufacturer of precision microdensitometers, recommends for accuracies in measure-

ment on the order of one micron* that their instrument be maintained in an environment not varying by more than $1^{\circ}F$. The development of the photographic plates is sensitive to variations in temperature and the entire set of photographs should be processed at a constant temperature. After the plates are processed, they would have to be placed in the microdensitometer and properly aligned. This presents a difficult metrology problem, but the advantage of having a permanent record of the star field allowing several successive measurements make the problem worth investigating. Having the star field permanently recorded would allow corrections for a number of alignment errors.

In the survey conducted on sensors, as reported in Section 2, a discussion is given on electrophotography which has possibilities of being applicable for this type of mission. A selenium plate which has the advantages of being reusable, having high radiation resistance, and having an extremely high quantum efficiency may, with proper development, be useful for recording stellar images. Diazo film, which is developed by ammonia vapor, is a third possibility for a future sensor. Uncontrolled distortions are currently a problem. Although real time measurement, rather than recording and subsequent measurement, would be desirable because it would eliminate processing or alignment problems, it does not appear to be currently feasible. The major difficulty lies in achieving sufficient sensitivity and resolution, and a field of view large enough to permit a sufficient number of 16th or 17th magnitude celestial objects to be seen for reference purposes.

The metrology problem, as already mentioned in regard to temperature, must also be viewed from other aspects. The required accuracy of any measuring system will depend upon the focal length of the telescope. As the focal length is decreased or the angular resolution required is increased, the accuracy of the linear measurement at the imaging plane will have to be increased. The energy received at the image plane will increase directly as the area of the aperture of the collecting optics. Generally the largest aperture which is feasible should be used.

* (Current accuracy required in parallax measurements.)

In a diffraction limited system, as the aperture size is increased the size of the diffraction disc decreases, thus improving the accuracy to which the location of the star image can be determined.

Three different metrological techniques may eventually be used for determining the distance between star coordinates in a space vehicle before transmitting back to earth. These would employ systems based on a worm gear, grid network or an interferometer. A grid of fine lines appears to be the most feasible in that it offers considerable advantage over either of the other two techniques since mechanical scanning is not required and there would be few alignment problems. However, there may be difficulty in achieving the desired grid line accuracy. Currently a worm gear system is used in comparators to obtain linear measurements accurate to $1\,\mu$ over several inches. Interferometric techniques are being developed for measuring distances between stellar images. The Naval Observatory hopes to be able to measure to between $1/2 - 3/4\,\mu$ on a new instrument that is still in the developmental stage. Both interferometric and worm gear systems require temperature controls. All three techniques would need complex electronics on associated power sources to automate coordinate readings.

Considerations will also have to be given to minimizing the power required to transmit the stellar coordinates back to earth. A tracking system will be needed so the spacecraft antennae can be properly directed. At 100 A. U. from the earth, the angle subtended by the earth at the spacecraft is about 0. 18" of arc. The tracking is complicated by the fact that the illumination characteristics will vary depending upon the orbit of the spacecraft and the position of the earth in its orbit around the sun. The earth will be difficult to track because of the small and varying amounts of energy received at the detector. In the event the energy received from the earth is not sufficient for detection, the sun will have to be used. In this case, because there will be some uncertainity in the measured position of the earth, the signal energy must be transmitted in a larger solid angle. Hence, the power required for transmission will increase.

It will also be necessary to obtain an aberration constant for the space vehicle for very accurate antenna pointing. Assuming the normal velocity is 24 km/sec, the difference between the earth's true and apparent position would be about 17". If an accuracy of 0.18" of arc is required, lead angle calculation would be necessary to one part in two hundred.

Before obtaining a crude estimate of the required accuracies, several factors should be mentioned. If two different telescopes were used simultaneously, it would provide a means for eliminating the proper motion of the stars. This can be achieved provided that appropriate corrections can be made to account for the differences in the optical systems.

If the sensor-metrology system is precise for measuring stellar distances, it will be applicable to other measurements. For example, in the case of double stars where the intensity of one is too low to be detected, the movement of the bright star relative to the center of gravity of the pair can be determined. Some of the methods for the verification of gravitational and cosmological theories also involve measuring the angular deflection of stars (see Section 7).

In order to assess the needed accuracy for certain components of the system, let us assume we have a space satellite with a 36" telescope with an effective focal length of 300 feet. For the case where the satellite is revolving around the earth, calculation will be based on a factor of improvement of 10 (see previous section). The diameter of the Airy disc for a wavelength of 5300 Angstroms is 130 microns for this optical system. In order to obtain 0.0005 sec of arc, a factor of ten better than on earth, distance measurement in the image plane must be made to 0.2 micron. This is beyond the state of current technology, both in metrology and recording. There is an inherent error of 1/2 to 3/4 micron in photographic plates due to creeping of the image. Both of these problems could be overcome by increasing the focal length to several thousand feet and increasing the aperture. This again, is beyond the state of the art, but there is some thought that considerably larger telescopes can be built in space. Proposals have involved construction of liquid lenses. The elimination of

the weight and atmospheric problems in this type of a mission do offer future possibilities for telescopes having larger apertures and focal lengths. If we consider that the metrology, sensor and optical problems are solved for a satellite in orbit around the earth, the vehicle would have to be stabilized so that angular rotations over the exposure interval would not induce errors in the measurement of the locations of the star images greater than 0.0005 sec of arc. Also, the background reference star problem, as mentioned in the previous section, will require a large dynamic range for the sensor.

It is obvious that measuring parallax from a satellite in orbit about the earth requires considerable advancement in a number of areas. Therefore, the success of such a mission could not be achieved without major expenditure and development.

From the previous discussion it appears that long base line parallax measurements offer the best potential for improving the accuracy of current measurements by a factor of ten. However, considerable development will be required before such a mission is possible.

6.4 Conclusions and Recommendations

An improvement in the accuracy of stellar parallax measurements by a factor of 10 would permit the calibration of the indirect methods of measuring distance which can be used for our entire galaxy and possibly beyond. A factor of improvement, say of 100, while permitting direct measurements on more objects, would not provide a proportional gain in the accuracy of distance measurements determined by indirect techniques.

It does not appear practical to improve the accuracy of stellar parallax measurements by a factor ten by employing a space satellite in orbit about the earth. A deep space probe, which has the advantage of a long base line, would be preferred.

Various engineering problems exist in the areas of metrology, sensor sensitivity, stabilization of the space vehicle, temperature control, data transmission and reliability. The most severe problem appears to be in the sensor-metrology area.

It is recommended that if a space mission is planned a complete system analysis be made. This would afford the opportunity to examine, in detail, the above engineering problems and provide the required specifications for the individual parts of the system. A parametric study of the individual components of the entire system should be made to determine their interrelationships. Consideration should be given to reliability and cost of various alternative systems.

The development of telescopes with large focal lengths should be explored and studies of systems which would provide greater stabilization than is currently available should be investigated.

Specific research should be conducted to solve the sensor-metrology problems associated with accurate measurement of the angles between stars. The various metrology systems should be studied and the effects of temperature and lubricants should be examined.

Parallel methods of investigation on preserving the accuracy of photographic plates in the adverse environment and the non-destructive readout of selenium plates should also be made.

7. SOLAR TOPOGRAPHIC AND RELATIVISTIC MEASUREMENTS

This section describes the results of a limited literature survey of information on solar topography and discusses two relativistic experiments that could be performed in the neighborhood of the sun.

The objectives to which this preliminary investigation were directed are:

(1) The determination of the type of solar topographical information that would be scientifically significant.

(2) The determination of the different problem areas that would arise in acquiring topographical data for the sun.

(3) The determination of the types of measurements required to verify certain gravitational theories.

The procedure that was used, and is being continued, is to examine various solar models and determine areas where geometrical information about the shape of the sun is needed. In addition, several cosmological theories were examined which require more precise measurements of the oblateness of the sun and of the deflection of light at the solar limb for their verification.

This section is divided into four sub-sections:

I. Sub-section 7.1 describes very briefly several areas of solar research that require geometrical information.

II. Sub-section 7.2 discusses specific problem areas relating to acquisition of topographical data.

III. Sub-section 7.3 describes two solar experiments that would provide important information in regard to the nature of gravitational fields and would help determine which of the current cosmological theories is probably valid.

IV. Sub-section 7.4 presents conclusions and recommendations.

References and a bibliography are given in an appendix.

7.1 Dynamic Solar Topography

This section describes briefly the dynamical nature of solar topography and several areas of solar research which require geometrical information.

A large number of models have been developed to describe some of the various solar events. As a very general approximation, the sun is assumed to be in a state of radiative, hydrostatic and thermodynamic equilibrium with the geometric structure being basically spherical. It is known, from various transient phenomena such as flares, spicules and prominences that occur on the sun , that there are regions which deviate considerably from the above equilibrium condition. A large portion of solar physics is concerned specifically with describing these non-equilibrium conditions in detail.

Since the topography of the sun is continually varying, mapping in the usual sense has little significance. Longitudinal reference will be of little value in general because of the large differential rotation of the sun. However, recording of the latitude (and sometimes the longitude), the time and duration of the event, may be important in studying solar dynamics. Deviation from the spherical form is fundamental to certain proposed theories which attempt to describe the thermodynamics, hydrostatics, corpular emission, transient phenomena and velocity fields of the sun.

It has been pointed out by Athay[1] that one of the most pressing problems in solar physics is an accurate specification of the geometrical structure of the entire solar atmosphere. An example which typifies the need for more of this information is in the study of velocity fields. Observations by Leighton and Noyes[2, 3] have been used to determine vertical oscillatory motion in the photosphere and lower chromosphere. Their values, which are determined from the Doppler shift of lines in the solar spectrum, can be attributed either to a small vertical segment or to a large region of the atmosphere moving coherently. The choice between these two hypothesis has not been resolved.

Another area of study which requires dynamical topographical information is the large transport of matter in spicules. It is estimated that the transport is sufficient to replace the entire corona in a period of hours. There is a question whether the spicules are related to the granules of the photosphere or whether they are a result of the dynamic instability in the lower chromosphere.

Mustel[4] has discussed in detail the quasi-stationary emission of gases from the sun. Recurrent M-type geomagnetic disturbances, which are only made evident by their terrestrial effects, are regarded as emanating from an M-region which is a somewhat hypothetical feature (it has never been observed) on the sun's surface. The disturbances form 27 day sequencies which quite frequently repeat for 5 to 10 cycles before terminating. Considerable controversy has been generated over the localization on the sun of the source of particles which generate the terrestrial magnetic disturbances. Mustel[5] has indicated that active regions* themselves constitute the principal source of quasi-stationary corpuscular streams which are associated with the M-region. A second theory, called the cone of avoidance, has been developed which states that active regions are not sources of corpuscular emission but that they deflect the corpuscular emission from the sun, which in turn causes the terrestrial effects. Continuous photographic observations of the coronal streamers and the suspected location of the M-region correlated with corpuscular measurement should resolve which theory is correct.

The above discussion indicates that the surface of the sun is continuously varying and that an understanding of the physical phenomena will require dynamic topographical information. The above phenomena should be studied in more detail. In the second phase of the program, a more inclusive description of what is to be measured, what is the significance of the measurement, and what are the problem areas that will be encountered

*Active region - A region in which very complicated physical processes are found to occur, including the rise, development and subsequent disappearance of magnetic fields, faculae, sunspots, chromospheric flares, disturbed coronal regions and prominences.

will be examined. A description of some of the problem areas which must be investigated are presented in the next section.

7.2 Problem Areas in Acquiring Topographical Data

From our preliminary study there appear to be several problem areas in the acquisition of solar topographical information using optical sensors which will require more detailed consideration. The information reported here will give an indication of these areas.

One question to be answered is: At what distance from the sun can the maximum surface resolution be achieved? Several investigators[6, 8] have estimated on the basis of radiative heat transfer that the closest approach to the sun that would be feasible is about 0.05 astronomical unit. The consideration for feasibility has been based primarily on maintaining the electronics at a workable temperature. Little attention was given to the temperature gradient problem in optical systems. The closer the approach, the more important it will be to consider the possibility of thermal gradients in the optical system. Gradients will result in a degradation of the image. For certain topographical measurements, it may be better to use a telescope with a longer focal length, so that the spacecraft can remain at a greater distance from the sun.

Problems will also be encountered in obtaining a stereo pair for different depths within the sun's atmosphere. Since the opacity of the sun varies strongly with wavelength, we must consider at what depths we hope to examine the chromosphere or photosphere. For example, on a program conducted recently at the Lockheed Solar Observatory a one-half angstrom bandpass filter centered at the hydrogen alpha line was used to photograph the sun. In this case the region photographed was about 3000 km above the photosphere. When the filter was adjusted 1/2 A off the center of the Hydrogen Alpha line, the depth of penetration of the chromosphere was about 1000 km above the photosphere. In the event a three dimensional profile of some transient phenomenon which originates at the surface of the photosphere and passes through the chromosphere is desired, various filter-sensor combinations will be necessary.

One of the major problems will be to assess the limitations of a stereo pair of photographs of regions of the sun. There are many ambiguities involved in defining the surface of the sun. At different wavelengths the energy radiates from different depths. The depth from which energy is radiated and received at a detector depends on the angle of observation. It is doubtful whether current analytical stereophotogrammery can be applied without modification to a situation where a reflecting surface is replaced by a radiating volume. This problem requires more study and is currently being investigated.

In addition to defining the surface, consideration will have to be given to the fact that a stereo pair will have to be taken with two separate cameras operating simultaneously. This will involve two spacecraft so that a sufficient base line between camera stations can be obtained. Two problems then arise, the angular dependence of opacity in the solar atmosphere and the communication between spacecraft. The dependence of opacity on angle of observation would indicate that if the space vehicles are looking at different angles through the solar atmosphere, the regions observed could be at different elevations. The second problem presents itself in commanding the two space satellites. The high background noise in the region of the sun will result in the need for accurate antenna pointing and possibly large power transmission depending upon the goal of the space flight. Both of these problems must be examined further in order to obtain information on the feasibility of solar topography measurements.

7.3 Relativistic Measurements

This section discusses briefly the significance of performing experiments in the neighborhood of the sun which will provide valuable information in regard to the gravitational field. This study evolved as a result of investigating various solar models to assess what information would be topographically significant.

In 1938, Dirac[9] presented a cosmology based on the observation that a large number of dimensionless ratios computed from both atomic and astrophysical constants have a value on the order of 10^{39} or powers of -1, 1, or 2 of this value. One of these ratios includes Hubble's Age of the Universe. Dirac assumed that these equalities were significant and that if they are to hold for all times, other constants must vary directly as Hubble's Age of the Universe. Using this type of an argument, he concluded that the gravitational constant was decreasing as the age of the universe increased.

Jordan[10, 11] provided a theoretical basis for Dirac's Cosmology by requiring the existence of both a scalar and a tensor gravitational field. Later Brans and Dicke[12] developed a theory which has this same feature. As a result of these additional cosmologies, the validity of General Relativity, as formulated by Einstein, has been seriously questioned.

The above cosmologies show that if a scalar field existed on the order of 5 - 10% of the relativistic tensor field, the gravitational constant would decrease significantly with time. This in turn would have important consequences, such as:

(1) The apparent age of the older stars in the galaxy would be 2 to 3 times their current assumed age.

(2) Planetary periods would increase and there would be a gradual increase in the earth's rotation rate.

(3) The earth would gradually expand as the gravitational constant decreased.

(4) Due to changes in luminosity of the sun, the average temperature on earth would have been 20°C warmer a billion years ago. This would be important in the evolution of early life on earth.

The above factors are a few of the more important ones that are related to changes in the gravitational constant with time.

In a review paper, Dicke and Peebles[13] point out that the deflection of light grazing the sun's limb and the motion of the perihelion of Mercury are not adequately determined to substantiate Einstein's Theory.

The predicted deflection of light at the solar limb, 1".75 arc, has been poorly confirmed. Observed values taken since 1919 during solar eclipses vary from 1.18 to 2.81 seconds of arc. Part of this large deviation is caused by systematic errors from different stations which cannot be checked because of the infrequent occurrance of solar eclipses. The seeing condition during eclipses is poor due to the rapid change of temperature in the atmosphere. Also, the star plates used for comparison to determine deflection are taken six months later, when the earth is on the other side of the sun. Errors are introduced by parallax and proper motions, as well as seeing conditions which influence daytime and nighttime photographs differently.

For the other cosmologies, the expected light deflection is

$$(1-S)\ 1".75 \qquad (7-1)$$

where S is the fraction of the total gravitational field attributed to the scalar interaction and is zero for General Relativity. The relative strength of the scalar field manifests itself in S, which theory cannot predict. The value of S must be determined by experiment.

In the framework of the Dirac-Jordan or Brans-Dicke cosmologies, the expected excess rotation of the perihelion of Mercury is

$$\left(1 - \frac{4S}{3}\right) 43" \qquad (7-2)$$

seconds of arc per century rather than the 43 seconds of arc predicted by relativity. The difference, if it exists, could be attributed to solar oblateness. Dicke has shown that fractional difference between the solar equatorial and polar radii of 6×10^{-5} would result in an advance of 4".03 per century, such an effect would imply relativity does not describe the difference in the theoretical value obtained by Newtonian mechanics and the observed advance of the perihelion, which is 9 per cent of the relativistic effect. The oblateness could easily go undetected from earth-based measurements because of the poor daytime seeing conditions caused by atmospheric turbulence. The daytime spreading of the image is 3 sec. of arc where the difference in radii that would correspond to the above-mentioned scalar field would only be 0.06 sec of arc. From the above expression, it can be seen that the

scalar field can be determined if the proper excess rotation is known. The value should correspond with that obtained for the deflection of light.

In summary, there exist gravitational theories with different cosmological implications which are important. Present errors in measurement do not permit the determination of which of these theories is correct. The errors are due to atmospheric effects, the paucity of data caused by the infrequency of eclipses and the necessity of making comparison measurements six months later. Two experiments, (1) the measurement of the deflection of light on the solar limb and (2) the measurement of the oblateness of the sun, if performed to a sufficient accuracy, would prove which theory best describes the gravitational field.

By obtaining data from a space vehicle, it appears that these errors could be reduced sufficiently to provide this determination. Space vehicles operating about the sun would offer advantages over earth-based measurements. In measuring the deflection of light at the solar limb, two satellites might be used such that the star field on the back side of the sun could be photographed simultaneously with one satellite being optimized for observing the deflection on the near side of the sun. A larger amount of data could be taken and systematic errors could be estimated. The atmospheric turbulence problem would be eliminated. Since two satellites are used the corrections for proper motions and the six month time delay for measurements would not be necessary.

The metrology-sensor problem as described in the section on stellar parallax, while present, could be less severe. Some of these problems could be overcome by returning the space vehicle to earth, if feasible.

In measuring the oblateness of the sun, the removal of the effects of the earth's atmosphere would be a necessity. A single satellite in orbit about the earth could perform this measurement, if it possessed a sufficient angular resolution. The angle subtended by the solar surface can be increased by approaching the sun in a solar probe; an equivalent effect can be obtained by increasing the focal length of the optical system.

A number of problem areas would have to be investigated to assess the proper experimental technique for obtaining the data required to determine accurately the deflection of light at the solar limb and the solar oblateness. Questions which should be explored include the following:

1. Is it necessary to optimize the star field (stars of 4th magnitude or less are currently used for earth measurement) in the area of the solar limb?

2. Can one satellite perform the measurement accurately, by making measurements on successive days?

3. How will thermal gradients affect the optics?

4. Can an earth satellite or a moon base be used for both experiments?

5. What is the greatest angular resolution that can be obtained in the solar limb?

6. At what distance from the sun should the solar oblateness experiment be performed?

7.4 Conclusions and Recommendations

The measurement of topography, especially in areas which are under dynamic change would be scientifically significant. An accurate description of the solar atmosphere and the photosphere are necessary to the foundations of solar physics.

There will be problems relating to the acquisition of topographical data. Specifically, it will be necessary to optimize the resolution; the trade-offs between increased focal length and thermal degradation which result from a closer solar approach must be investigated. The choice of the proper spectral region will have to be made for obtaining a stereo pair at different depths in the solar atmosphere. The variations of opacity with the thickness of solar atmosphere to be penetrated will have to be considered when two spacecraft are photographing the same topographical features. The communication of satellites in the neighborhood of the sun will also present difficulties.

Only a preliminary effort has been expended on this initial study. It is recommended that the study be continued with two basic objectives in mind; the determination of what should be measured and the difficulties in acquiring this information.

It is also recommended that a study should be made to examine the feasibility of measuring, from a satellite, the deflection of light by the sun and the oblateness of the sun, and to select the best sensors and optics for performing these measurements. These experiments would provide the necessary information to determine which one of several proposed cosmologies most nearly represents the observed gravitational field.

APPENDIX A

A MODEL OF THE HOLOGRAM PROCESS

The effect of the non-linear nature of the recording device or medium used to construct a hologram is examined in this appendix. The analysis assumes two types of exposure amplitude transmittance characteristics are typical for most recording mediums: (1) an inverse γ th-law device, typical of photographic film, or (2) a "direct" γ th-law device. It will be seen that in either case the non-linearity produces harmonics of the complex amplitude as well as the complex amplitude to be reconstructed. If the resolution of the recording medium is not sufficient to allow an appropriate carrier frequency to be chosen, the harmonics can add noise to the reconstructed image and impair its quality.

In addition, it will be shown that the non-linearity causes the hologram process to be "self-degrading" by introducing multiplicative noise which depends upon the amplitude variations in the object wavefront. The effect is analogous to placing a mask of varying transmittance in front of a lens forming an image of a coherent object. This degrading effect is more pronounced the higher the modulation of the reference wavefront, that is, if the intensity of the object wavefront is near the intensity of the reference wavefront. To the extent that such degradations are important, small modulations may be required to maintain good quality in the image.

The analysis also indicates that exposures on the toe of the Hurter-Driffield response curve are desirable when constructing a hologram in order to increase the energy contained in the reconstructed image.

A.1 Hologram Construction

Assume that the wavefront to be recorded by the hologram is represented by the two dimensional function

$$S(x,y) = A_S(x,y)\, e^{i\phi_S(x,y)} \qquad \text{(A-1)}$$

and that the reference beam is described by

$$R(x,y) = A_R\, e^{-i2\pi \nu_c y}, \qquad \nu_c = \frac{\sin\alpha}{\lambda} \qquad \text{(A-2)}$$

As shown in Figure A-1, α is the angle between the normal to the reference wavefront and a line to an arbitrarily chosen point near the center of the object field. The spatial frequency ν_c corresponding to α is usually referred to as the carrier frequency of the hologram. The amplitude of the plane reference wave is assumed to be uniform across the hologram plane and, for convenience, the ratio of the amplitudes of the signal wavefront and the reference wavefront is set equal to $\rho(x,y)$ i.e.,

$$\rho(x,y) \equiv \frac{A_S(x,y)}{A_R}. \qquad \text{(A-3)}$$

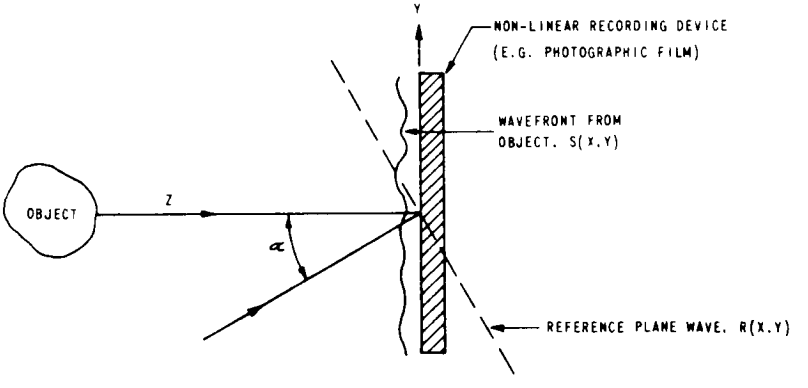

NOTE:
IN THIS STUDY THE OBJECT IS ASSUMED TO BE LOCATED ALONG THE NORMAL TO THE HOLOGRAM PLANE (i.e., ALONG THE Z-AXIS). IT IS POSSIBLE THAT THE ANGLE BETWEEN THE REFERENCE LINE TO THE OBJECT AND THE Z-AXIS MAY NOT BE ZERO IN WHICH CASE α IS MEASURED BETWEEN THE NORMAL TO THE REFERENCE PLANE WAVE AND THE Z-AXIS AND THE FORM OF S(X,Y) CHANGES TO INCLUDE THE EFFECT OF AN OFF-AXIS OBJECT.

Figure A-1 HOLOGRAM CONSTRUCTION

The intensity which produces the exposure on the non-linear recording device is given by

$$I(x,y) = \left| S(x,y) + R(x,y) \right|^2. \qquad \text{(A-4a)}$$

This may be written as

$$I(x,y) = I_R \left\{ 1 + \rho^2(x,y) + 2\rho(x,y) \cos\left[\phi_S(x,y) + 2\pi \nu_c y \right] \right\}. \qquad \text{(A-4b)}$$

Consider an inverse ν th-law device, whose amplitude transmittance is given by

$$T_A(x,y) = \left[\frac{I_o}{I(x,y)} \right]^{\nu}, \quad \nu = 0. \qquad \text{(A-5)}$$

where I_o is a normalizing constant and $0 \le T_A(x,y) \le 1$ When photographic film is used to record the hologram, as is customarily done, ν is the slope of the Hurter-Driffield response curve at the operating point divided by two. Combining expression (A-4b) and (A-5) one has

$$T_A(x,y) = \left(\frac{I_o}{I_R} \right)^{\nu} \left\{ 1 + \rho^2(x,y) + 2\rho(x,y) \cos\left[\phi_s(x,y) + 2\pi \nu_c y \right] \right\}^{-\nu}. \qquad \text{(A-6)}$$

Employing the binominal expression for negative exponent of the form

$$(a+x)^n = \frac{1}{a^{|n|}} \left\{ 1 - \frac{|n| x}{a} + \frac{|n|(|n|+1)}{2!} \frac{x^2}{a^2} - \cdots \right\}$$

and letting

$$a = 1 + \rho^2(x,y) \quad \text{and} \quad x = 2\rho(x,y) \cos\left[\phi_S(x,y) + 2\pi \nu_c y \right]$$

(A-6) becomes

$$T_A(x,y) = \left\{ \frac{I_o}{I_R\left[1 + \rho^2(x,y) \right]} \right\}^{\nu} \sum_{n=0}^{\infty} b_n \left(\frac{\rho(x,y)}{1+\rho^2(x,y)} \right)^n 2^n \cos^n\left[\phi_s(x,y) + 2\pi \nu_c y \right] \qquad \text{(A-7)}$$

where

$$b_0 = 1 \quad \text{and} \quad b_n = (-1)^n \frac{\nu(\nu+1)\cdots(\nu+n-1)}{n!} = \frac{(-1)^n \Gamma(\nu+n)}{n!\,\Gamma(\nu)}$$

This expansion converges for $x^2 < a^2$ or when $0 \le \rho(x,y) \le 1$.

Now expand the term $\cos^n\left[\phi_S(x,y) + 2\pi \nu_c y \right]$ using the binominal expansion for a positive exponent, viz.

$$\cos^n\left[\phi_s(x,y) + 2\pi\nu_c y\right] = \frac{1}{2^n}\sum_{i=0}^{n}\frac{n!}{(n-i)!\,i!}\, e^{i(n-2i)\left[\phi_s(x,y) + 2\pi\nu_c y\right]} \tag{A-8}$$

Combining (A-8) and (A-7) and setting $n = m + 2i$ the amplitude transmittance can be written as two double summations; one for $m \geq 0$ and another for $m < 0$. By adjusting the summation index in one of the double summations where $m < 0$, the two double summation terms may be combined into one double summation, and the amplitude transmittance written as

$$T_A(x,y) = \left\{\frac{I_0}{I_R\left[1+\rho^2(x,y)\right]}\right\}^{\nu}\sum_{m=-\infty}^{\infty} C_m(x,y)\,\rho^{|m|}(x,y)\, e^{im\left[\phi_s(x,y) + 2\pi\nu_c y\right]} \tag{A-9}$$

$$C_m(x,y) = \begin{cases} \left[\frac{-1}{1+\rho^2(x,y)}\right]^m \sum_{i=0}^{\infty}\left[\frac{\rho(x,y)}{1+\rho^2(x,y)}\right]^{2i}\frac{\Gamma(\nu+m+2i)}{\Gamma(\nu)\Gamma(m+i+1)\,\Gamma(i+1)}, & m \geq 0 \\ C_{|m|}(x,y), & m < 0 \end{cases}$$

The convergence of the summations involved in the coefficients $C_m(x,y)$ can be verified by examining the limit of the ratio of the term to the i term, viz.

$$\lim_{i\to\infty}\frac{(\nu+m+2i)(\nu+m+2i+1)}{(m+i+1)(i+1)}\left[\frac{\rho(x,y)}{1+\rho^2(x,y)}\right]^2 < 1$$

which is satisfied for

$$\rho(x,y) < 1$$

The convergence, of course, being more rapid for smaller values of $\rho(x,y)$.

It was assumed that $I(x,y) \geq I_0$ when expression (A-5) was written since the amplitude transmittance $T_A(x,y)$ cannot exceed one. Using this restriction and the minimum value of $I(x,y)$ determined from (A-4b) by setting $\cos\left[\phi_s(x,y) + 2\pi\nu_c y\right] = -1$, it is easily seen that the restriction on $\rho(x,y)$ is that

$$0 \leq \rho(x,y) \leq 1 - \sqrt{\frac{I_0}{I_R}} < 1 \tag{A-10}$$

which insures convergence. When photographic film is used to record the hologram, the analysis presented is valid when the intensity of the reference

beam is adjusted to lie in the region of the Hurter-Driffield response curve where a linear approximation over the range of exposures of interest can be made. That is, one desires linearity about the "operating point" determined by the intensity of the reference beam.

A.2 Reconstruction

The amplitude of the wavefront "reconstructed" by the hologram when it is illuminated by a plane reference wave is determined by multiplying the amplitude transmittance of the hologram, $T_A(x,y)$ by the complex amplitude of reconstructing plane wave. Except for a possible phase variation $\phi'(x,y)$, introduced by the hologram recording device itself (e.g., thickness variations of the photographic film), expression (A-9) represents the amplitude transmittance. Such a phase variation would degrade the reconstructed image to some extent.

To examine the reconstructed wavefront, it is convenient to examine the first few terms of the summation in expression (A-9).

For convenience, the x and y variations of $\rho(x,y)$ are assumed to be small so that $\rho(x,y)$ may be replaced, in the expression for the coefficients (A-9) by some appropriately chosen mean value denoted by $\bar{\rho}$. The effect of possible spatial variations of the coefficients, $C_m(x,y)$ is discussed later as a form of multiplicative noise in the reconstructed wavefront. Performing the operations described above, the amplitude transmittance becomes

$$T_A(x,y) = \left\{\frac{I_o}{I_R(1+\bar{\rho}^2)}\right\}^{\nu}\left\{C_o + C_1\rho(x,y)e^{i\phi(x,y)} + C_1\rho(x,y)\,e^{-i\phi(x,y)} + C_2\rho^2(x,y)\,e^{i2\phi(x,y)} + C_2\rho^2(x,y)e^{-i2\phi(x,y)} + \cdots\right\} \tag{A-11a}$$

where

$$C_m = \left(\frac{-1}{1+\bar{\rho}^2}\right)^m \sum_{i=0}^{\infty}\left(\frac{\bar{\rho}}{1+\bar{\rho}^2}\right)^{2i} \frac{\Gamma(\nu+2i+m)}{\Gamma(\nu)\,\Gamma(i+m+1)\,\Gamma(i+1)} \quad , \quad m = 0,1,2\cdots \tag{A-11b}$$

and

$$\phi(x,y) = \phi_s(x,y) + 2\pi \nu_c y \qquad \text{(A-11c)}$$

Assume that the normal to the plane wave used to reconstruct the hologram forms an incident angle i with the normal to the hologram plane in the y direction. This angle should be selected with care as discussed in Section A.3 of this appendix. Consider the first term of expression (A-11a) that is, $m = 0$ term. It simply corresponds to a portion of the reconstructing plane wave passing directly through the hologram as shown in Figure A-2 . The two terms involving c_1 produce the desired outputs. The first term corresponding to $m = +1$ reproduces a wavefront identical to the wavefront used to expose the hologram $S(x,y) \sim \rho(x,y)\, e^{i\phi_s(x,y)}$.*

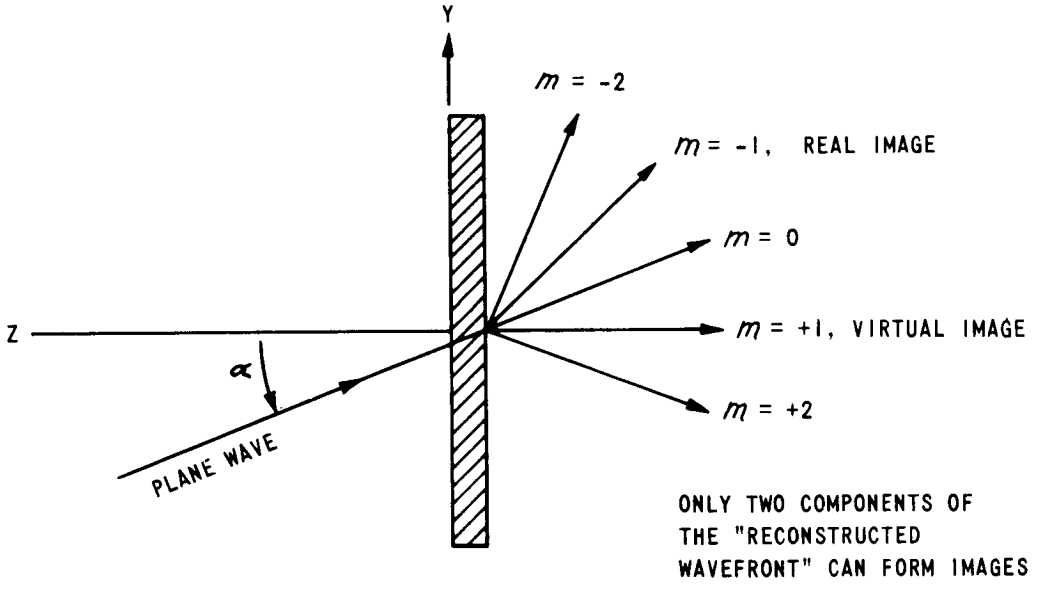

Figure A-2 HOLOGRAM RECONSTRUCTION FOR CONSTRUCTION CONFIGURATION OF FIGURE A-1 AND $i = \alpha$

* This is also dependent upon the reconstruction geometry as discussed in Section 3.3

If $i = \alpha$, this wavefront is diffracted at an angle $+\alpha$ from the normal to the reconstructing wavefront and when viewed by the eye, appears to originate at and "reconstruct" the original object. It is usually referred to as yielding "a virtual image" because an auxiliary lens (e.g., the eye) must be used to form an image. The other term involving c_1 corresponding to $m = -1$ produces a wavefront which is modulated by $\rho(x,y)\, e^{-i\phi_s(x,y)}$ and is diffracted in the opposite direction from the reconstructing wavefront compared to the "virtual" image wavefront. This wavefront is the complex conjugate of $S(x,y)$ and, therefore, is converging and will produce a real image of the object in space.

The remaining higher order terms, $|m| > 1$, in expression (A-11a) also produce reconstructed wavefronts. Each term corresponds to a component wavefront diffracted at different angles from the normal to the reconstructing wavefronts. The expression for the diffracting angles θ_m is derived later in Section A.3 and is given by $\theta_m = \sin^{-1}\left[m \sin\alpha - \sin i\right]$. However, values of m such that $|\theta_m| > 90^\circ$ do not have much significance*. Note that those harmonics which do have significance produce wavefronts modulated by the square, cube, etc. of the original wavefront and consequently the harmonic terms, in addition to being emitted at larger angles, diffract light over different angles than the terms corresponding to $m = \pm 1$. Thus if the geometry of the hologram construction process is not chosen carefully, the wavefront corresponding to a higher-order term or the $m = 0$ term may be superimposed upon the desired wavefront producing unnecessary noise in the reconstructed image.

The effects of any spatial dependence of the coefficients $c_m(x,y)$ due to the spatial variations of $\rho(x,y)$ are seen to be equivalent to multiplicative noise in the reconstructed image. That is, the reconstructed wavefronts would be of the form $c_1(x,y)\,\rho(x,y)\, e^{\pm i\phi_s(x,y)}$. If the spatial variations of $c_1(x,y)$ are of sufficient magnitude, the amplitude of the reconstructed wavefront will not be equal to that of the initial wavefront

* Thus, when $i = \alpha = 30^\circ$ the only significant orders are $m = -1, 0, +1, +2, +3$.

forming the hologram*. The effect is analogous to placing a mask of varying transmittance in front of a lens forming an image of a coherent object. Such a mask would degrade the image; the process being described by convolving the complex amplitude of the image without the mask by a degrading function given by the Fourier Transform of the amplitude transmittance of the mask. Practically, this means that the hologram process may be self-degrading and that the resolution in the reconstructed image will not approach the limit which has been investigated by Parrent and Reynolds.[1, 2] . The resolution in the reconstructed image is recognized to be dependent upon the size of the hologram, the resolution of the device used to record it, and the carrier frequency employed. In order to minimize the additional degrading factors discussed above, it is sufficient to make $\rho(x, y)$ small when constructing the hologram. In this case the summation in expression for the coefficients converges rapidly and neglecting the (x, y) dependence in writing (A-11b) is justified.

Experimentally, when photographic film is used to record a hologram, it is observed that the hologram may be developed to a high film gamma (large value of ν in the model). This technique, referred to as clipping, produces a "black and white" image. If a hologram is to be transmitted such a limited gray scale is desired to reduce the number of quantized levels necessary to describe its amplitude transmisson.

To investigate the effects of gray scale compression and to gain additional insight into the effects of the spatial dependence of the coefficients, it is convenient to examine the spectrum of the amplitude transmittance of the hologram which is equivalent to the Fourier Transform of equation (A-11a) viz. $\tau(\nu_x, \nu_y) = \iint T_A(x, y)\, e^{i2\pi(\nu_x x + \nu_y y)}\, dx dy$, see Figure A-3

For small values of spatial frequency $\nu_x, \nu_y << \lambda^{-1}$, the square of this spectrum is identical to the power spectrum of the light transmitted by the hologram when $i = 0$. Experimentally, it is formed by placing a lens directly behind the hologram and observing the light distribution in the focal plane.

---

* The distortion of the amplitude is a conclusion also reached by A. Kozma in his recent paper (Ref. 3).

The area of the square of the peaks represents the relative energy contained in each order and is proportional to c_m^2 . The spectrum components labeled $m = 1$ and $m = -1$ are those of the desired reconstructing wavefronts and, therefore, it is desirable to have c_1^2 as large as possible to obtain a high energy content.

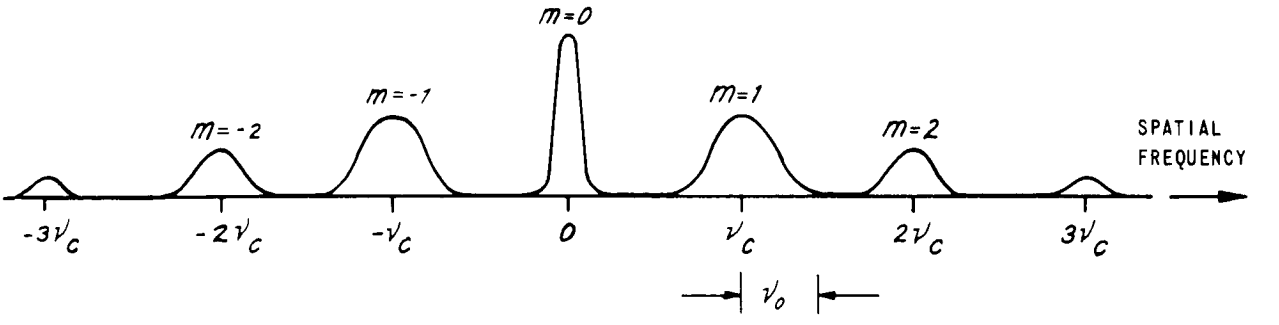

Figure A-3 SPECTRUM OF THE AMPLITUDE TRANSMITTANCE OF A HOLOGRAM

The width of the spectrum component corresponding to $m = 0$ depends upon the spatial variation of the coefficient $c_0(x,y)$ and hence upon $\rho(x,y)$. The more detailed the variations of $\rho(x,y)$ and the larger their magnitude, the more significant the spatial variations of $c_0(x,y)$ and consequently the larger the width of this spectrum component. If $c_0(x,y)$ were a constant, the width would be "diffraction limited" depending only on the size of the illuminated area in the hologram. An important practical consequence of this effect is the separation of the spectrum components corresponding to $m = +1, -1$ from $m = 0$. For a narrow zeroth order spectrum component the carrier frequency ν_c may be decreased and consequently the resolution requirement of the recording device is decreased. For example, if ν_o is a frequency corresponding to the "resolution limit" desired in the reconstructed image, then the resolution limit of the recording device must exceed the frequency $\nu_c + \nu_o$. In order to separate the zeroth and first order components, ν_c must be greater than ν_o (depending on the width of the zeroth order component) and consequently the

resolution limit of the hologram recording device must exceed twice the desired resolution in the reconstructed image. If the spectrum components are not separated, then the $m = 0$ component will represent a source of high frequency noise in the reconstructed image since the components at $m = 1$ and $m = -1$ correspond to the spectrum of the reconstructed images.

We note that if the coefficient $c_1(x, y)$ is not constant, the spectrum of the reconstructed images will be distorted and will not correspond to the spectrum of the original object. This is equivalent to the multiplicative noise effect suggested earlier. Because of these degrading effects, it is desirable to limit the spatial variations of $\rho(x, y)$ which, as previously mentioned, is easily accomplished by making the intensity of the reference wavefront larger than the signal intensity.

To evaluate the effect of gray scale compression upon the hologram transmittance, the coefficients c_m were evaluated for various values of ν and $\bar{\rho}$. Larger values of ν representing a "black-white" hologram structure. The coefficients were numerically evaluated on the IBM 7044. Some of the results are presented in Table A-1. Attention was confined to small values of $\bar{\rho}$ *. For very small values of $\bar{\rho}$ (e.g., $\bar{\rho} = 0.01$) most of the energy transmitted by the hologram occurs in the zeroth order spectrum component which is undesirable. As $\bar{\rho}$ is increased, the ratio of c_1^2/c_0^2 increases so that the relative energy contained in the first-order spectrum components increases. In general, the effect of increasing ν or compressing the gray scale increases the ratio of c_1^2/c_0^2 . This can be seen by examining the values in the table. The energy content of the spectrum components relative to the zeroth-order component therefore are increased. This result is expected and can be predicted by a simple physical argument. If the amplitude transmission of a photograph were a pure sine-wave, the effect of clipping or compressing the gray scale would be to form a square-wave and consequently introduce higher order harmonics.

* The reader is reminded that $\bar{\rho}$ is the ratio of amplitude of the signal wavefront to the amplitude of the reference wavefront and, therefore, $\bar{\rho}^2$ is the ratio of their respective intensities.

Table A-1

COEFFICIENTS C_m^2 , EQUATION A-11b

ν	$\bar{\rho} = 0.01$				
	C_0^2	C_1^2	C_2^2	C_3^2	C_4^2
0.25	1.00	6.25×10^{-6}	2.44×10^{-10}	1.37×10^{-14}	9.06×10^{-19}
0.50	1.00	2.50×10^{-5}	1.40×10^{-9}	9.76×10^{-14}	7.47×10^{-18}
0.75	1.00	5.62×10^{-5}	4.31×10^{-9}	3.62×10^{-13}	3.18×10^{-17}
1.0	1.00	1.00×10^{-4}	1.00×10^{-8}	1.00×10^{-12}	1.00×10^{-16}
2.0	1.00	4.01×10^{-4}	9.02×10^{-8}	1.60×10^{-11}	2.50×10^{-15}
5.0	1.01	2.51×10^{-3}	2.26×10^{-6}	1.23×10^{-9}	4.91×10^{-13}
10.0	1.02	1.01×10^{-2}	3.05×10^{-5}	4.87×10^{-8}	5.15×10^{-11}
ν	$\bar{\rho} = 0.05$				
	C_0^2	C_1^2	C_2^2	C_3^2	C_4^2
0.25	1.00	1.56×10^{-4}	1.53×10^{-7}	2.15×10^{-10}	3.55×10^{-13}
0.50	1.00	6.28×10^{-4}	8.83×10^{-7}	1.53×10^{-9}	2.93×10^{-12}
0.75	1.02	1.41×10^{-3}	2.71×10^{-6}	5.69×10^{-9}	1.25×10^{-11}
1.0	1.02	2.52×10^{-3}	6.31×10^{-6}	1.58×10^{-8}	3.94×10^{-11}
2.0	1.03	1.02×10^{-2}	5.75×10^{-5}	2.55×10^{-7}	9.98×10^{-10}
5.0	1.16	6.90×10^{-2}	1.53×10^{-3}	2.06×10^{-5}	2.05×10^{-7}
10.0	1.69	3.45×10^{-1}	2.42×10^{-2}	9.35×10^{-4}	2.41×10^{-5}
ν	$\bar{\rho} = 0.1$				
	C_0^2	C_1^2	C_2^2	C_3^2	C_4^2
1.25	1.01	6.30×10^{-4}	2.46×10^{-6}	1.39×10^{-8}	9.15×10^{-11}
0.50	1.02	2.66×10^{-3}	1.50×10^{-5}	1.04×10^{-7}	7.96×10^{-10}
0.75	1.03	5.78×10^{-3}	4.43×10^{-5}	3.72×10^{-7}	3.27×10^{-9}
1.00	1.04	1.04×10^{-2}	1.04×10^{-4}	1.04×10^{-6}	1.04×10^{-8}
2.0	1.13	4.42×10^{-2}	9.88×10^{-4}	1.75×10^{-5}	2.73×10^{-7}
5.0	1.79	3.72×10^{-1}	3.14×10^{-2}	1.65×10^{-3}	6.49×10^{-5}
10.0	6.77	3.47	8.09×10^{-1}	1.12×10^{-1}	1.09×10^{-2}

It should be mentioned that although the relative energy in each of the spectrum components is observed to increase with increasing ν and $\bar{\rho}$ this does not mean the resulting reconstructed image intensity is higher. In order to obtain the maximum energy in the reconstructed image, the maximum exposure

$$I_{max} = I_R (1+\rho)^2 \qquad \text{(A-12)}$$

should be made as small as possible to maximize the minimum transmittance of the hologram.* This can be achieved by choosing the "intensity" of the reference wavefront to be close to I_o From expression (A-10) we require that

$$I_R \geq \frac{I_o}{(1-\rho)^2} \tag{A-13}$$

and therefore, when photographic film is used as the hologram recording device, the hologram exposure should be adjusted so that it falls as near to the toe of the Hurter-Driffield response curve as possible without sacrificing the linearity between the density and log exposure. Some research personnel actively producing holograms have observed that such apparent underexposures produce better holograms[3,4]. For small values of $\rho (\bar{\rho} \leq 0.1)$ the maximum intensity transmittance that can be obtained with $\gamma = 2.0$ is less than 45%. Currently, the most common type of hologram recording device is the Kodak Type 649-F Spectroscopic plate. This plate has a very high resolution capability allowing large carrier frequencies to be employed in recording the hologram. It also has a very high film gamma (corresponding to γ = 2 or 3) which automatically provides a "black and white" hologram transparency.

Some hologram recording techniques may be γ th-law devices, e.g. vidicon tubes rather than "inverse" γ th-law devices. Such devices would have an amplitude transmittance or characteristic function given by

$$T_A(x,y) = K\left[I(x,y)\right]^{\gamma}, \qquad \gamma \geq 0 \tag{A-14}$$

Employing the same procedure used previously, expression (A-11) may be written as:

$$T_A(x,y) = K\left[I_R(1+\bar{\rho}^2)\right]^{\gamma} \sum_{m=-\infty}^{\infty} C_m \rho^{|m|}(x,y)\, e^{im\{\phi_s(x,y)+2\pi\nu_c y\}} \tag{A-15a}$$

* This also causes the average transmittance at the hologram to be high.

with

$$c_m = \left(\frac{1}{1+\bar{\rho}^2}\right)^m \sum_{i=0}^{\infty} \left(\frac{\bar{\rho}}{1+\bar{\rho}^2}\right)^{2i} \frac{\nu(\nu-1)\cdots(\nu-2i-m+1)}{\Gamma(i+m+1)\Gamma(i+1)}, \quad m > 0$$

$$c_m = c_{|m|}, \quad m < 0 \tag{A-15b}$$

and

$$c_o = 1 + \sum_{i=1}^{\infty} \left(\frac{\bar{\rho}}{1+\bar{\rho}^2}\right)^{2i} \frac{\nu(\nu-1)\cdots(\nu-2i+1)}{\Gamma^2(i+1)} \tag{A-15c}$$

corresponding to expressions (A-11a) and (A-11b) for the inverse ν th-law device. The summations in (A-15b) and (A-15c) converge more rapidly than (A-11b) for corresponding values of m. The values of the coefficients were not evaluated in this case; however, it can be seen that they are smaller than the corresponding coefficients for the inverse ν th-law device. Many of the conclusions reached for the inverse ν th-law device hold in this case, especially those relating to the degrading effect of the spatial variation of $\rho(x,y)$. (In the expressions for the coefficients the spatial dependence has been eliminated by assuming that $\rho(x,y)$ is small.) Also, the effect of gray scale compression (increasing ν) will be to increase the first order and high spectrum components relative to the zeroth-order spectrum component as discussed previously.

As a result of the analysis, it is seen that the gray scale needed to produce a hologram may be limited by the hologram recording device without distorting the spectra of the reconstructed images which are obtained in the resulting hologram. Although this conclusion is reached by examining a continuous gray scale compression process, it is reasonable to assume such results would hold for the discrete quantization of amplitude transmittance levels. In transmitting photographs or aerial images over digital data links, it is common to employ 64 levels (6 binary bits). Four gray levels (two binary bits) may be sufficient to transmit a hologram over such a digital transmission link.

It is also concluded that modulation of the reference wavefront by small signal wavefronts (i.e., small values of $\rho(x,y)$) are desirable when constructing a hologram in order to minimize possible contributions to the degradation of the reconstructed image. In this respect, if the amplitude

of the wavefront to be recorded, $A_s(x, y)$ is a slowly varying function so that most of the information is contained in the phase, then $\rho(x, y)$ can be assumed to be constant. An experiment to measure the variation of $A_s(x, y)$ for typical objects would be useful.

A. 3 Diffraction Effects

Another question which warranted further study is the influence of the non-linearity between spatial frequency and diffracting angle upon the reconstructed image. It appears that the use of high spatial frequencies as carrier frequencies may distort the spectra of the reconstructed images if the reconstruction geometry is not appropriately chosen.

The diffraction of light by an aperture is a common optical phenomenon. A hologram is essentially a diffracting object which reconstructs wavefronts which carry information needed to form an image of an object. These wavefronts are capable of providing an image of the object because they represent the correct spatial distribution of energy. It is necessary that the amplitude transmittance of the hologram diffract the energy of the reconstructing plane wave into the same spatial distribution represented by an initial wavefront originating at the object or its complex conjugate. Consider a photographic transparency or a hologram having an amplitude transmittance $T_A(x)$. It will diffract the energy of an incident plane wave in accordance with the equation

$$\sin i + \sin \theta = \nu \lambda \qquad \text{(A-16)}$$

which is a form of the more familiar grating equation. The variable i represents the incident angle of the plane wave illuminating the transparency, ν represents spatial frequency and θ the diffracting angle corresponding to this spatial frequency. Prior to the popularization of holograms, most transparencies consisted of spatial frequencies $\nu << \lambda^{-1}$ and in applications were illuminated with coherent plane waves such that $i = 0$. In this case $\sin \theta$ is small and may be replaced by θ in expression (A-16) viz.

$$\theta = \nu\lambda \qquad \text{(A-17)}$$

This is fortunate since the angle of diffraction is directly proportional to spatial frequency and recording the amplitude transmittance upon a carrier frequency, if the carrier frequency is small, simply means that the resulting wavefront is diffracted through an additional angle corresponding to the carrier frequency and the diffracted energy distribution remains undistorted. If, however, the carrier frequency is large, then the spatial frequencies corresponding to the amplitude transmittance of the transparency are large and (A-17) no longer applies. This is often the case with holograms as for example, when the reference beam and object are separated by an angle $\alpha = 30$ degrees corresponding to a carrier spatial frequency of about 1000 lines/mm. Illuminating a hologram formed in the manner shown in Figure 3-1 of the main text, with a reconstructing plane wave having $i = 0$, as shown in the figure below, would result in reconstructed wavefronts which are distorted since the diffracting angle is no longer directly proportional to the spatial frequency but is determined by expression (A-16).

To say it in other words, although the shape of the spectrum of the amplitude transmittance is identical to the shape of the spectrum of the complex amplitude of the desired wavefront, the wavefront will not be reconstructed because the shift in the center frequency of the spectrum has caused the diffracted energy distribution to be distorted so that it does not represent the desired wavefront (see Figure 3-3 in the main text). This effect is ignored by many authors when discussing and illustrating the hologram reconstruction process.[5, 8] In practice, the hologram is usually reconstructed with the same plane wave that was used in forming the hologram (see part (b) of the figure). In this case $i = \alpha$ and expression (A-16) becomes

$$\sin\theta = \lambda\left(\nu - \frac{\sin\alpha}{\lambda}\right) = \lambda\,(\nu - \nu_c) \qquad \text{(A-18)}$$

where ν_c is the carrier spatial frequency as defined in the main text. This condition insures that the term in the amplitude transmittance of the hologram representing the virtual image, viz.

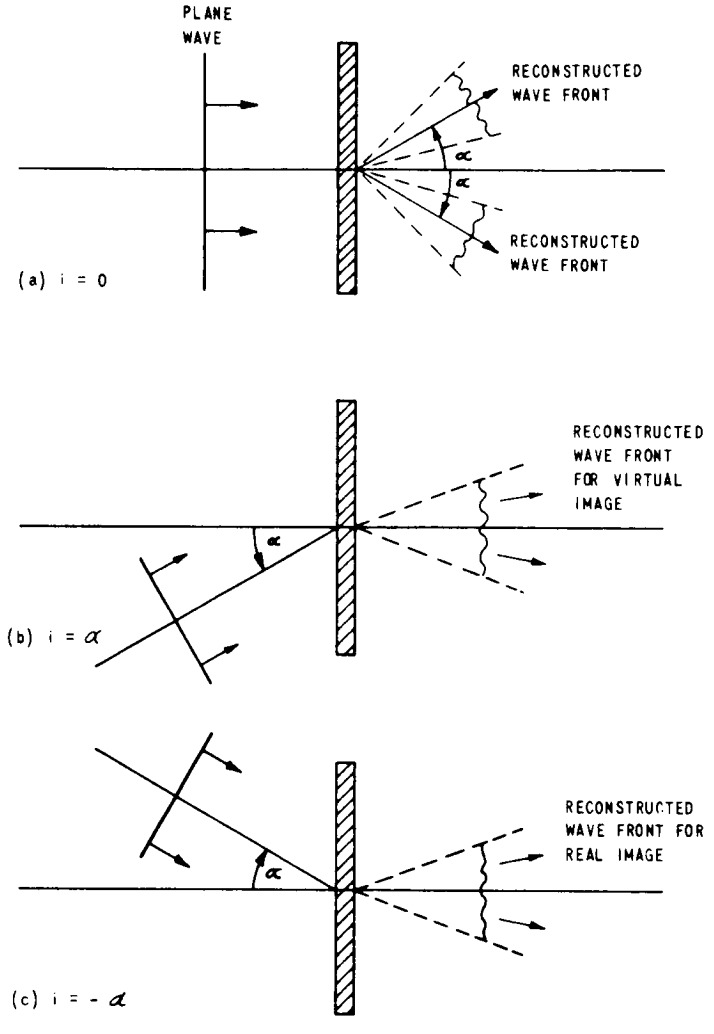

Figure A-4 HOLOGRAM RECONSTRUCTION CONFIGURATION

$$c_1(x,y)\, e^{i[\phi_s(x,y) + 2\pi \nu_c y]}$$

correctly reconstructs the wavefront corresponding to the object. However, the amplitude transmittance of the real image, $m = -1$, is modulated on a carrier frequency of $2\nu_c$ so that the diffracting angles are distorted and do not diffract the energy to form a wavefront which will reconstruct the object faithfully, if at all. To reconstruct the real image one must employ a reconstructing plane wave with $i = \alpha$ (see part (c) of the figure) so that

$$\sin\theta = \lambda(\nu + \nu_c). \tag{A-19}$$

Expression (A-16) may also be used to determine the angle at which the various orders are diffracted from the hologram by setting $\nu = m\nu_c$ viz.

$$\begin{aligned}\theta_m &= \sin^{-1}[m\lambda\nu_c - \sin i] \\ &= \sin^{-1}[m\sin\alpha - \sin i]\end{aligned} \tag{A-20}$$

where α is defined in Figure 3-1 of Section 3-1, as the angle between the hologram plane and the reference wavefront.

If $i = \alpha$, as is customary, then and indeed the $m = 1$ term reconstructs the virtual wavefront in the normal direction as shown in part (b) of the figure above.

REFERENCES

ACQUISITION OF TOPOGRAPHIC INFORMATION

(Section 2)

1. Rindfleisch, T., "Photometric Method for Lunar Topography," Photogrammetric Engineering 27, No. 2, March 1966, pp. 262-276.

2. Levine, Daniel, "Radargrammetry," McGraw-Hill Book Co., Inc., New York, 1960.

3. Thompson, Morris, M., Ed., "Manual of Photogrammetry," Vol. I and II, 3rd Ed., American Society of Photogrammetry, Falls Church, Va., 1966.

4. Whelan, J. W., "Digital TV Bandwidth Reduction Techniques as Applied to Spacecraft TV," AIAA Unmanned Spacecraft Meeting, L. A., Calif., Publication CP-12, 1 -4 March 1965.

5. Ives, G. M., "Television Broadcasting from Satellites," National IAS-ARS Meeting, L. A., Calif., 13-16 June 1961.

6. Anon: "Manual of Physical Properties of Kodak Aerial and Special Sensitized Materials," Eastman Kodak Company, Department GS, Rochester, New York.

7. Mesner, M. N. and Staniszewski, J. R., "Television Cameras for Space Exploration," Astronautics, May 1960.

8. Rose, A., "Advances in Electronics," Vol. 1, Academic Press, 1948, pp. 131-166.

9. Zworykin, V. K. and Morton, G. A., "Television," John Wiley & Sons, New York, Second Edition, 1954.

10. Wiemer, P. K., "Advances in Electronics and Electron Physics," Vol. XIII, Academic Press, 1960, pp. 387-437.

11. Bedford, L. H., "Problems of TV Cameras and Camera Tubes," J. Brit. IRE, Vol. 14, 1954, pp. 464-474.

12. Cope, A. D. and Borkan, H., "Isocon Scan, a Low Noise, Wide Dynamic Range Camera Tube Scanning Technique," Applied Optics, Vol. 2, March 1963, pp. 253-261.

13. DeWitt, J. H., "A Report on the Image Orthicon Using Slow Readout", Adv. in Elect. Phys., Vol. 16, Academic Press, New York, 1962, pp. 419-430.

14. Heil, H., "On Image Defects Arising from the Electron Velocity Distribution in the Reading Beam of Image Orthicons", Image Intensifier Symp., Army Engr., Research & Dev. Labs., No. AD-220160, 6-7 Oct. 1958, pp. 201-214.

15. Livingston, W. C., "Resolution Capability of the Image-Orthicon Camera Tube under Standard Scan Conditions", J. or SMPTE, Vol. 72, Oct. 1963, pp. 771-786.

16. Day, H. R., Hanna, H. J., and Wargo, P., "An Image Orthicon with a New Target", Image Intensifier Symp., Army, Engr. Res. & Dev. Labs., No. AD-220160, 6-7 Oct. 1958, pp. 163-170.

17. Burns, J., "Strong Field Focusing for Signal Generating Image Tubes", NASA TN-D-2698, March 1965.

18. Cope, A. D., Luedicke, E. and Flory, L. E., "The Capabilities and Prospects of TV Camera Tubes in Applications for Astronomy", J. of SMPTE, Vol. 74, Sept. 1965, pp. 765-769.

19. Fink, D. G., "TV Engineering Handbook", McGraw-Hill, 1957.

20. Southworth, G., "Narrow Band Video Communication Systems", Fourth Meeting, Society for Information Display, October 1964, pp. 41-59.

21. Anon: "Vidicon Applications for Space-Borne TV Cameras", J. of SPIE, Vol. 3, Feb.-Mar. 1965, pp. 90-94.

22. Nathanson, F. E., "Survey of Vidicon Tubes for Missile Guidance Systems", APL/JHO/CF-2776.

23. Mesner, M. H., "Televisions Toughest Challenge", Electronics, 17 May 1965, pp. 80-90.

24. Shade, O. H., Vine, B. H., et al, "Applied Research on High Resolution Camera Tubes", AF, Avionics Lab., Tech. Doc. Report No. 64-171, (AD-602425), 8 July 1964.

25. Shigemoto, F. H., Bishman, B. H., "Image Dissector Aperture Geometrics and Scan Patterns for use in Star Tracker Systems", NASA, Ames Res., Tech. Note D-2990, September 1965.

26. Misso, C. E. F., "1-1/2 Inch Electrostatic Image Dissector", CBS Labs, 27 August 1964.

27. Papp, G. A., "On A Novel Application of the Image Dissector", J. of SMPTE, Vol. 74, Sept. 1965, pp. 782-783.

28. Kohlmeyer, R. B., "Some Evaluations of S/N Ratio and Bandwidth Restriction Effects on Television Picture Quality", Space Technology Labs., Inc., Report No. 8949-005-NU-000, 19 April 1961.

29. Shelton, C. T. and Stewart, H. W., "Pickup Tube Performance with Slow Scanning Speeds", J. of SMPTE, Vol. 67, July 1958.

30. Hall, J. A., "Camera, Display and St orage Tubes" presented at National Electronics Conference, Chicago, Ill., 1965.

31. Rose, A., "A Unified Approach to the Performance of Photographic Film, TV Pickup Tubes and the Human Eye", J. of SMPTE, Vol. 47, Oct. 1947, pp. 273-294.

32. Nitka, H. F., "Sensitivity and Detail Rendition in the Recording of Light Images and Electron Beams", PSE 1, May-June 1963, pp. 188-195.

33. Morton, G. A., "Image Intensifiers and the Scotscope", Applied Optics, Vol. 3, June 1964, pp. 651-673.

34. Dessauer, J. H. and Clark, H. E., "Xerography and Related Processes", Focal Press, 1965.

35. Schaffert, R. M., "Electrophotography", Focal Press, 1965.

36. Ibid, p. 58.

37. Powers, W. T., "Nondestructive Readout with a Field-Mesh Image Orthicon," Applied Optics, Vol. 3, June 1964, pp. 673-675.

38. Novotny, G. V., "Fiber Optics for Electronics Engineers," Electronics, 1 June 1962, pp. 37-40.

39. McClure, G. W. and Dute, J. C., "Probability Characteristics of Sensor Output Data," Institute of Science and Technology, University of Michigan, Report No. 2900-329-R, September 1963.

40. Condon, E. V. and Odishaw, H., "Handbook of Physics," McGraw-Hill, 1958.

REFERENCES

HOLOGRAPHIC TECHNIQUES

(SECTION 3)

1. E. Lieth and J. Upatnieks, "Holograms: Their Properties and Uses," SPIE JOURNAL, 4, 3 (1965).

2. R. Powell and K. Stetson, "Interferometric Vibration Analysis by Wavefront Reconstruction," J. Opt. Soc. Am., 55, 1953 (1965).

3. E. Lieth and J. Upatnieks, "Wavefront Reconstruction with Diffused Illumination and Three-Dimensional Objects," J. Opt. Soc. Am., 54, 1295 (1964).

4. A. Hardy and F. Perrin, The Principles of Optics, (McGraw-Hill, 1932).

5. E. Lieth and J. Upatnieks, "Reconstructed Wavefronts and Communication Theory," J. Opt. Soc. Am., 52, 1123 (1962).

6. E. Lieth and J. Upatnieks, "Wavefront Reconstruction with Continuous Tone Objects," J. Opt. Soc. Am., 53, 1377 (1963).

7. E. Lieth, J. Upatnieks and K. Haines, "Microscopy by Wavefront Reconstruction," J. Opt. Soc. Am., 55, 981 (1965).

8. A. Kozma, "Photographic Recording of Spatially Modulated Coherent Light," J. Opt. Soc. Am., 56, 428 (1966).

9. G. Parrent and G. Reynolds, "Resolution Limitations of Lensless Photography," SPIE JOURNAL 3, 219 (1965).

10. G. Parrent, "Resolution Considerations in the Hologram Process," Paper presented at Annual Meeting of Optical Society of America, 5 - 8 October 1965.

11. M. Lehman, "Lasography--Photographic Techniques with Coherent Monochromatic Light," Paper presented at 10th Technical Symposium, SPIE, 16 - 20 August 1965.

12. K. Haines and P. Hildebrand, "Contour Generation by Wavefront Reconstruction," Paper presented at 50th Anniversary Meeting of the Optical Society of America, 15 - 18 March 1966.

REFERENCES

TRANSMISSION OF TOPOGRAPHIC INFORMATION

(Section 4)

1. Whelan, J. W., "Digital TV Bandwidth Reduction Techniques as Applied to Spacecraft TV," AIAA Unmanned Spacecraft Meeting, Los Angeles, Calif., 1-4 March 1965, Publication CP-12.

2. Baumonk, J. F. and Roth, S. H., "Pictorial Data Transmission from a Space Vehicle," Jour. of the SMPTE, Jan. 1960, pp. 27-31.

3. Schade, O. H., Sr., "A 60-Megacycle Video Chain for High-Definition Television Systems," RCA Review, Vol. 26, June 1965, pp. 178-199.

4. Lewis, N. W., "TV Bandwidth and the Kell Factor," Electronic Technology, Vol. 39, Feb. 1962, pp. 44-47.

5. Mayer, H. F., "Principles of Pulse Code Modulation," Advances in Electronics, Vol. III, Academic Press, New York, 1951, pp. 221-260.

6. Viterbi, A. J., "Design Techniques for Space TV," California Institute of Technology, Jet Propulsion Lab., Publication No. 623, 16 July 1959.

7. Corliss, W., "Space Probes and Planetary Exploration," D. Van Nostrand, Princeton, 1965, p. 92.

8. Oliver, B. M., "Efficient Coding," Bell System Technical Journal, July 1952, pp. 724-750.

9. Scule, J. R., "A System for Lunar Photography and Data Transmission," California Institute of Technology, Jet Propulsion Laboratories, Tech. Report 34-142, 28 May 1960.

10. Lindsey, R., "Recorders Slash Time Base Error," Missiles and Rockets, Vol. 17, 4 Oct. 1965, pp. 40-41.

11. Massa, R. J., "Visual Data Transmission," Air Force, Cambridge Research Laboratories, Report 64-323, April 1964, p. 65.

12. Marsten, R. B., Silverman, D., and Gubin, S., "Communication Requirements Between Manned Spacecraft on Interplanetary Voyages," (RCA) American Institute of Aeronautics and Astronautics, Paper No. 65-324.

13. Moss, E. B., "Some Aspects of the Pointing Problem for Optical Communication in Space," (Douglas Aircraft) American Institute of Aeronautics and Astronautics, Paper No. 64-420.

14. Wishnia, F. H., Hemstreet, H. S., and Atwood, J. G., "Determination of Optical Technology Experiments for a Satellite," (Perkin Elmer) NASA CR-252, July 1965.

15. Anon: "Optical Communications System Study," Final Report Volume 1, Office of Advanced Research and Technology, HQ, NASA, 3 March 1964.

16. Marsten, R. B., Silverman, D., and Gubin, S., "Performance of Communication Systems Between Manned Spacecraft on Interplanetary Voyages," Journal of Spacecraft and Rockets, Vol. 3, No. 6, June 1966, pp. 828-833.

17. Gubin, S., Marsten, R. B. and Silverman, D., "Lasers vs. Microwaves in Space Communications," Journal of Spacecraft and Rockets, Vol. 3, No. 6., June 1966, pp. 818-827.

18. Moss, E. B., "Aids to Acquisition in Optical Communications," Journal of Spacecraft and Rockets, Vol. 3, No. 6, June 1966, pp. 834-838.

REFERENCES

DISPLAYS

(Section 5)

1. Nowicki, A., "Stereoscopy", Manual of Photogrammetry, American Society of Photogrammetry, Falls Church, Virginia, 1966, pp. 521-522.

2. Shorcliff, W., Polarized Light, Harvard University Press, Cambridge, Massachusetts, 1962, pp. 138-142.

3. Neblette, C., Photography, Van Nostrand, New York, New York, New York, 1952, pp. 445-447.

REFERENCES

STELLAR PARALLAX

(Section 6)

1. Lippincott, S. L., "Accuracy of Positions and Parallaxes Determined with the Proul 24 Refractor", Astronomical Journal 62, 55 (1957), pp. 55-69.

2. Van de Kamp, P., "Astrometry with Long-Focus Telescopes", Astronomical Techniques, ed. W. A. Hiltner, University of Chicago Press, Chicago, Illinois, 1962.

3. Schilt, J., "Parallax Problems Old and New", Astronomical Journal 59, 55 (1954), pp. 55-58.

4. Smart, W. M., Spherical Astronomy, 4th Edition, Cambridge University Press, Cambridge, 1949.

5. Schlesinger, F., "Photographic Determination of Stellar Parallax made with Yerkes Refractor", Astrophysical Journal 33, 161, (1911).

6. Eichhorn, H., and Jefferys, W. H., "Algorithm for the Rigorous Determination of Differential Astrometric Data", Astronomical Journal 68, 71 (1963).

7. Binnendijk, L., Bulletin Astronomique deas Netherland 10, 91 (1943).

8. Vyssotsky, A. N. and Williams, E. T. R., Pub. McCormick Obs. 10, 33 (1948).

9. Jenkins, L. F., General Catalogue of Trigonometric Stellar Parallaxes, Yale University Press, New Haven, 1952.

10. Strand, K. A. A., "Trigonometric Stellar Parallaxes", Basic Astronomical Data, ed. K. A. A. Strand, University of Chicago Press, Chicago, 1963.

11. Hoag, H. S., "Star Clusters" in Hanback der Physik, Bond 53, Berlin: Springer-Verlag 1959, pp. 129-207.

12. Blaauw, A., "Galactic Structure," ed. A. Blaauw and M. Schmidt, University of Chicago Press, Chicago, Chapter 7, 1964.

13. Mann Corporation, Personal Communication.

Photoelectric Studies I - "Color-Luminosity Array for Members of the Hyades Cluster" pp. 65-80.
Photoelectric Studies II - "Color-Luminosity Array for Members of the Plerades Cluster" pp. 81-98.
Photoelectric Studies III - "Color-Luminosity Arrays for the Coma Berenices and Ursa Major Clusters" pp. 414-425.

REFERENCES

SOLAR TOPOGRAPHIC AND RELATIVISTIC MEASUREMENTS
(Section 7)

1. Athay, G. R., "Astronautical Investigations of the Sun", Advances in Space Science and Technology, Academic Press, Vol. 5, 1963, pp. 1-18.

2. Leighton, R. B., "Observations of Solar Magnetic Fields in Plague Regions", Astrophysical Journal, Vol. 130, No. 2, Sept. 1959, pp. 366-380.

3. Noyes, R. W. and Leighton, R. B., "Velocity Fields in the Solar Atmosphere", Astrophysical Journal, Vol. 138, No. 3, 1 Oct. 1963, pp. 631-647.

4. Mustel, E., "Quasi-Stationary Emission of Gases From the Sun", Space Science Reviews, Vol. 3, 1964, pp. 139-231.

5. Mustel, E. R., "The Role of Active Regions in the Formation of Quasi-Stationary Corpuscular Streams From the Sun", Soviet Astronomy, Vol. 9, No. 3, November-December, 1965.

6. Dugan, D. W., "A Preliminary Study of a Solar Probe Mission", NASA Technical Note D-783, Ames Research Center, April, 1961.

7. Hall, C. F., Nothwong, G. J., and Hornby, H., "A Feasibility Study of Solar Probes", Institute of the Aerospace Science Paper No. 62-21.

8. Dickstein, D. H., "A Solar Probe", IAS Paper 61-179-1873.

9. Dirac, P.A.M., "A New Basis for Cosmology", Proceeding Royal Society London, A-165, pp. 199-208.

10. Jordan, P., "Schwerkraft and Weltall", Vieweg, Braunschweig, 1955.

11. Jordan, P., Z. Phys., Vol. 157, 1959, pp. 112.

12. Brans, C. and Dicke, R.H., "Mach's Principle and Relativistic Theory of Gravitation", Physical Review, Vol. 124, 1961, pp. 925-935.

13. Dicke, R.H. and Peebles, P.J., "Gravitation and Space Science", Space Science Reviews, Vol. 4, 1965, pp. 419-460.

REFERENCES

APPENDIX A

1. G. Parrent and G. Reynolds, "Resolution Limitations of Lensless Photography", SPIE Journal, 3, 219 (1965).

2. G. Parrent, "Resolution Considerations in the Hologram Process", Paper presented at Annual Meeting of Optical Society of America, 5 - 8 October 1965.

3. A. Kozma, "Photographic Recording of Spatially Modulated Coherent Light", J. Opt. Soc. Am., 56, 428 (1966).

4. M. Lehman, "Lasography - Photographic Techniques with Coherent Monochromatic Light", Paper presented at 10th Technical Symposium, SPIE, 16 - 20 August 1965.

5. E. Lieth and J. Upatnieks, "Holograms: Their Properties and Uses", SPIE Journal 4, 3 (1965).

6. R. Powell and K. Stetson, "Interferometric Vibration Analysis by Wavefront Reconstruction", J. Opt. Soc. Am. 55, 1593 (1965).

7. E. Lieth and J. Upatnieks, "Wavefront Reconstruction with Diffused Illumination and Three-Dimensional Objects", J. Opt. Soc. Am. 54, 1295 (1964).

8. J. P. Dudley, Applied Optics and Optical Engineering, Vol. II, Chapter 2 (Academic Press, 1965).

BIBLIOGRAPHY

ACQUISITION OF TOPOGRAPHIC INFORMATION

(Section 2)

Allen, J. Denton, "A Mars Spacecraft Photographic System", J. SMPTE 74, No. 6, June 1965, p. 497.

Atkinson, J. H., Calvert, J. D., Cook, G. E. and Parham, J. F., "Environmental Effects of Photosensitive Materials", Wright Patterson AFB, (AFAL-TR-64-274), Oct. 1964. (From STA Rept. 3, No. 3, 8 Feb. 1965, p. 498, Abstract N65-13024).

Bogatov, G. B., "How a Picture of the Other Side of the Moon was Obtained", Joint Publications Res. Service, Washington, D.C., 19 February 1962.

Brinkman, J. R., and Eggleston, J. M., "Photographic Requirements for Manned Space Missions", (NASA), J. SPIE, Vol. 3, No. 3, Feb. - Mar. 1965, pp. 83-89.

Brown, Earle B., "Environmental Considerations of Aerospace Optical Systems", SPIE Newsletter, Feb.-Mar. 1962, pp. 12-16.

Campbell, C. E., "The Optimization of Photographic Systems", Photogrammetric Engineering 38, No. 3, July 1962, pp. 446-455.

Davies, M. E., "Lunar Exploration by Photography from a Space Vehicle", The Rand Corp., Paper P-1671, 5 March 1959.

Eriksen, Col. J. G., "Lunar Charting", Air University Review 16, No. 4, May-June 1965, pp. 76-90.

Evans, Dallas E., Pitts, David E., et al, "Venus and Mars Nominal Natural Environment for Advanced Manned Planetary Mission Programs", NASA Special Publications No. 3016, 1965.

Fry, Glenn A., "The Detection of Light and Infrared Radiation", Applied Optics and Optical Engineering, Academic Press, Vol. 2, (1965), pp. 22-26, 55-60.

Graham, Clarence H., "Vision and Visual Perception", John Wiley, 1965.

Hardy, Arthur C., "The Lunar Albedo", J. SMPTE 74, Nov. 1965, p. 1028.

Johnson, Evert W., "Limit of Parallax Perception", Photogrammetric Engineering 23, No. 5, December 1957, pp. 933-934.

Julesz, B., "Binocular Depth Perception of Computer Generated Patterns", Bell System Technical Journal 39, No. 5, Sept. 1960.

Julesz, Bela, "Stereopsis and Binocular Rivalry of Contours", J. Opt. Soc. Am. 53, August 1963, pp. 994-999.

Katz, Amrom, "Observation Satellites: Problems and Prospects", Astronautics 5, May-Sept. 1960.

Kosofsky, Leon J., "Topography from Lunar Orbiter Photos", Photogrammetric Engineering 27, No. 2, Mar. 1966, pp. 277-285.

Kinzly, R. E., Roetling, P. G. and Holladay, T. M., "A Study of Lunar Orbiter Photographic Evaluation", Cornell Aeronautical Laboratory, prepared under Contract No. NAS 1-5800 for Langley Research Center (to be published).

Lewis, Jack C. and Watts, Harold V., "Effects of Nuclear Radiation on the Sensitometric Properties of Reconnaissance Films", Air Force Avionics Lab., AFAL-TR-65-113, April 1965.

Manfred, Elmer, "Photography of the Moon from Space Probes", Jet Propulsion Lab., NASA N63-14677.

Michael, W. H., Tolson, R. H. and Gapcynski, J. P., "Feasibility of a Circumlunar Photographic Experiment", NASA, TN-D-1226, May 1962.

Palmer, D. A., "Stereoscopy and Photogrammetry", Photogrammetric Record 4, No. 23, (APSEL 2414/64), April 1964, pp. 391-394.

Rindfleisch, T., "A Photometric Method for Deriving Lunar Topographic Information", Jet Propulsion Lab. Tech. Rept. 32-786, 15 Spetember 1965.

Rostron, Joseph P., "Equipment and Techniques for the Utilization of Convergent Photography in Mapping", Army Eng. Res. & Dev. Labs., Ft. Belvoir, Report No. 1583-TR, (AD-226689), 28 August 1959.

Stevens, S. S., "Handbook of Experimental Psychology", Wiley, (1963), pp. 885-895.

Taback, Israel, "Lunar Orbiter: Its Mission and Capability", 10th Annual Meeting of the American Astronautical Society, Preprint 64-7, 4-7 May 1964.

Anon: "Space Handbook: Astronautics and Its Applications - Observation Satellites", Staff Report of the Select Committee on Astronautics & Space Exploration, U.S. Congress, U.S. Gov't. Print Office, pp. 171-191, 1959.

Anon: "Airborne Photographic Equipment", Data Corporation, (AD-452117), 1964.

Anon: "Space Materials Handbook", Second Ed., Lockheed Aircraft Corp., ML-TDR-64-40, January 1965.

Anon: "Space Programs Summary", Vol. VI, Jet Propulsion Lab. Rept. 37-33, Mar. 1-Apr. 30, 1965.

Anon: "Natural Environmental and Physical Standards fortthe Apollo Program", NASA Manned Spacecraft Center, NASA M-DE 8020.008B, April 1965.

Anon: "Manual of Photogrammetry", 3rd Ed., Am. Soc. of Photogrammetry, Falls Church, Va., 1966.

Anon: "Unmanned Lunar Reconnaissance" Part 2 of Lunar Flight Programs, Vol. 18 of Advances in Astronautical Sciences, Pergamon Press.

Anon: "Manual of Physical Properties of Kodak Aerial and Special Sensitized Materials", Eastman Kodak Company, Department GS, Rochester, New York.

BIBLIOGRAPHY

(Section 2. 2. 3)

Allen, J. D. and Malling, L., "Mariner-Mars - TV System", Wescon 1965, Space Electronics, Section 4. 9, Part 5.

Beall, W. H., "Statistical Analysis of Degradation in Scanned Image Systems", J. Opt. Soc. A. 54, Aug. 1964, (Abstracts PSEL 504/64), pp. 992-997.

Becker, R. A., "Design and Test Performance of Mariner IV TV Optical System", Calif. Inst. of Tech., Jet Propulsion Lab., Tech. Rept. 32-773, 1 July 1965.

Brinkman, J. R. and Eggleston, J. M., "Photographic Requirements for Manned Space Missions", (NASA), J. SPIE, Vol. 3, No. 3, Feb. -Mar. 1965, pp. 83-89.

Canvel, H., "A Slow Scan TV Film Recorder", J. SMPTE, Vol. 74, Sept. 1965, pp. 770-773.

Flory, L. E., Gray, G. W., Morgan, J. M. and Pike, W. S., "Television System for Stratoscope I", Electronics, 17 June 1960, pp. 45-53.

Fried, D. L. Shaffer, J. J. and Turner, R. G., "A Theoretical Analysis of Image Orthicon Performance", Applied Optics 4, July 1965, pp. 785-792.

Frost, W. T. and Singer, B. H., "Increased Areal Density in Magnetic Tape", Inst. Elec. Eng. 1964, (APSEL 1855/65), pp. 44-47.

Green, P. S., "Vidicon Deflection System", APL/JHU, CF-2783, BNM-RMM-067, 20 January 1959.

Hacking, K., "An Analysis of Film Granularity in Television Pre-production", J. SMPTE 73, No. 12, Part 1, Dec. 1964, p. 1015.

Hagedorn, G. E., "Image Peak Detector", APL/JHU, CF-2756, 28 August 1958.

Kindt, Donald A. and Staniszewski, Joseph R., "Design of the Ranger Television System to Obtain High-Resolution Photographs of the Lunar Surface", Jet Prop. Lab. TR-32-717, 1 March 1965.

Larson, C.C. and Gardner, B.C., "The Image Dissector", Electronics, Oct. 1939, pp. 24-27, 50.

Malling, L.R., "Space Age Astronomy and the Slow-Scan Vidicon", J. SMPTE 72, Nov. 1963, pp. 872-875.

Mason, J.F., "Ranger's Vidicon TV", Electronics, Vol. 35, No. 8, 23 February 1962, pp. 26-27.

Mesner, M.H. and Staniszewski, J.R., "Television Cameras for Space Exploration", Astronautics, May 1960.

Mesner, M.H., "Vidicon Applications for Space-Borne TV Cameras", J. SPIE 3, No. 3, Feb.-Mar. 1965, (PA-2400-65), pp. 90-99.

Mesner, M.H. and Gravel, A.J., "The TV-Camera System for Ranger", IEEE Transactions, Broadcasting BC-11, No. 1, July 1965, pp. 1-5.

Montgomery, W.D., "Reconstruction of Pictures from Scanned Records", IEEE Transactions on Information Theory IT-11, No. 2, (APSEL-65-2892), April 1965, pp. 204.

Montgomery, D.R. and Willingham, D.E., "A Study of the Photometric Conditions and IRIS Requirements for a Lunar Approach Television Camera", Jet Propulsion Lab., Technical Memorandum 33-151, 15 September 1963.

Moseley, R.D., Jr., Holm, T. and Low, I.H., "Performance Evaluation of Image Intensifier Television Systems", Am. J. Roentgehology 92, No. 2, (APSEL 1860/65), Aug. 1964, pp. 418-42

Powers, W.T., "Non-Destructive Readout with a Field Mesh Image Orthicon", Applied Optics, Vol. 3, June 1964, pp. 673-677.

Quinn, S.F. and Dickson, J. Bowie, "New CBC Vidicon-Telecine Operating Standards with Particular Reference to Gray-Scale Characteristics", J. SMPTE 73, No. 12, Part 1, December 1964, pp. 1009.

Raisbeck, G. and Goldhammer, J., "Transmission of Photographic Data by Electrical Transmission", IRE Transactions on Information Theory IT-6, No. 4, Sept. 1960, pp. 503-504.

Sandefur, K.L., "Space Reconnaissance", Aerospace Engineering, Vol. 19, November 1960, pp. 28-31.

Smith, F., "Technical Details of Camera and Photographic Recording Equipment of Ranger-B on Moon Photo Flight", PSE 8, No. 6, Nov.-Dec. 1964, pp. 361-362.

Southworth, G. R., "A Video-Modulation Test System for Space TV", J. SMPTE, Vol. 74, Part 1, April 1965, pp. 307-313.

Spaulding, S. W., "Television and Lunar Exploration", J. SMPTE, Vol. 69, Jan. 1960, pp. 39-43.

Spitzah, A. W., "Spacecraft Film System for Planetary Photography", J. SPIE, Vol. 3, No. 3, Feb.-Mar. 1965, pp. 100-101.

Stark, M. C. and Cahn, L., "Study, MTS, Stereo Input", NAVTRADEVCEN-1-59-1, Order NA 61339-1-59, January 1964, From STA Report 3, No. 13, 8 July 1965, (AD-430702, APSEL 65-3422), p. 2191.

Zenel, Joseph A., "Narrow-Bandth Video Tape Recorder Used in the Tiros Satellite", J. SMPTE 69, No. 11, Nov. 1960, pp. 818-820.

Anon: "Scientific Experiments for RANGER 3, 4 and 5", California Inst. of Tech., Jet Propulsion Lab. Tech. Rept. 32-199, 5 December 1961.

Anon: "Ranger's Vidicon TV" Electronics 35, No. 8, 23 February 1962.

Anon: "New TV Camera Designed for Rough Usage", Missiles and Space 8, March 1962, p. 24.

Anon: "A Study of the Image Orthicon in Ruggedness in Simulated Missile Environments", Naval Ordnance Test Station, China Lake, Calif., Sept. 1962. (Confidential).

Anon: "Performance Evaluation of TRAP Image Orthicon System", General Electric Co., Space Sciences Lab Rept. No. R635D1042, Dec. 1963.

Anon: "The Lunar Camera", Phot. Soc. Am. 30, Feb. 1964, (APSEL 2159/64), pp. 37-38. (See also Ind. Phot. 13, Feb. 1964, pp. 55-57).

Anon: "Mission Description and Performance, Ranger VII", Part 1, Calif. Inst. of Tech., Jet Prop. Lab. Tech. Rept. 32-700, 15 December 1964.

Anon: "No Smear", Electronics 38, No. 9, May 1965, pp. 32-33.

Anon: "CRT, Storage Tubes, Camera Tubes, Image Converters", Electronic Design News, Vol. VII, Jan. 1966, pp. 150-157.

Anon: "Wescon Technical Papers", Part 5, Space Electronics: Systems, Spacecraft, Communications, Western Periodicals Co., North Hollywood, California, 1965.

BIBLIOGRAPHY

(Section 2.2.4)

Aftergut, S., Bartfai, J.J. and Gaynor, J., "Photoplastic Recording for Electro-Optical Photography", Photographic Science and Engineering 9, No. 2, Mar.-Apr. 1965, pp. 80-81.

Behringer, A., Moore, R. and Smith, M., "Final Report on Camera Speed Xerographic Plate", Xerox Corp., (AD-430004L), Oct. 1962 - Sept. 1963.

Bickmore, J.T. and Claus, C.J., "Charge Transfer Frost Xerography", Photographic Science and Engineering 9, No. 5, Sept.-Oct. 1965, pp. 283-293.

Glenn, W.E., "Thermoplastic Recording: A Progress Report", J. of SMPTE 74, August 1965, pp. 663-665. (Also Kirk, Norman, "Thermoplastic Recording Tape Systems", same, pp. 666-668.)

Lorant, M., "Photoplastic Recording", Brit. J. Phot. 111, 18 Sept. 1964, (APSEL 254/65), pp. 752-753, 766.

Mott, George R., "Electrostatic Electrophotography 1964, Tonal Reproduction by Cascade Development", Society of Photographic Scientists and Engineers, Unconventional Photographic Systems, Symposium, Washington, D.C., 29-31 Oct. 1964, pp. 80-81.

Neugebauer, Hans E.J., "A Describing Function for the Modulation Transfer of Xerography", Applied Optics 4, April 1965, pp. 453-459.

Novotny, G. V., "Fiber Optics for Electronics Engineers", Electronics, 1 June 1962, pp. 37-40.

Ohbuchi, K., "On the Digital-Indicating Electrostatic Sensitometer for Electrophotography", Scientific Publications of the Fuji Photo Film Co., Ltd. 11, 1963, pp. 48-52. (Also Denshi Shashin 4, No. 2, 1963, p. 1). (APSEL 65-2615).

Olson, O. H. and Pontarelli, D. A., "Study of Facsimile Scanning and Recording Techniques Employing Fiber Optics", ITT Res. Inst., Rept. No. A-1203-28, 3 September 1964.

Potter, R. J. and Hopkins, R.E., "Fiber Optics and its Application to Image Intensifier Systems", Image Intensifier Symp., No. AD-220160, 6-7 Oct. 1958, pp. 91-109.

BIBLIOGRAPHY

(Section 2. 3)

Baker, Robert A., "Astronomy", 8th Ed., D. Van Nostrand, 1964.

Duncan, Robert C., "Dynamics of Atmospheric Entry", McGraw-Hill, 1962.

Thompson, Morris M., "Manual of Photogrammetry", Vol. II, America Society of Photogrammetry, Falls Church, Va., 3rd Ed., 1966.

BIBLIOGRAPHY

HOLOGRAPHIC TECHNIQUES

(Section 3)

An extensive bibliography exists in the following:

Chambers, R.P. and Courtney-Pratt, J.S., "Bibliography on Holograms", Jour. of the SMPTE, Vol. 75, No. 4, p. 373, April 1966.

BIBLIOGRAPHY

TRANSMISSION OF TOPOGRAPHIC INFORMATION

(Section 4)

Baldwin, M. W., Jr., "Demonstration of Some Visual Effects Using Frame Storage in TV Transmission," IRE Convention Record, Part IV, 1958.

Budrikis, Z. L., "An Estimate of Channel Requirements for Run Length Coded TV Picture Signals," Comm. of Australia, PGM, Dept. Research Lab, Report No. 5057, 1959.

Buhl, David and Spinazze, Larry, "A Practical Infrared TV System", Electronic Industries 25, January 1966, pp. 48-52.

Chatterton, E. J., "Semiconductor Laser Communications through Multiple-Scatter Paths", Proceedings of the IEEE 13, December 1965, pp. 2114-2115.

Cherry, C., Kubba, M. H., Pearson, D. E. and Barton, M. P., "An Experimental Study of the Possible Bandwidth Compression of Visual Image Signals", Proc. IEEE (Special Interim Issue) 51, (APSEL 1249/64), November 1963, pp. 1507-1518.

Cherry, E. C., et al, "An Experimental Study of Possible Bandwidth Compression of Visual Image Signals," Proc. of the IEEE, Vol. 51, 1963, pp. 1507-1517.

Cherry, E. C. and Gouriet, G. G., "Some Possibilities for the Compression of Television Signals by Recording," Proc. Inst. of Elec. Eng., Vol. 100, 1953, pp. 9-18.

Cohen, J. J., "Military Serives' Satellites Will Ring the Earth," Electronics, Vol. 39, No. 9, 2 May 1966, pp. 96-99.

Davis, J. I., "Consideration of Atmospheric Turbulence in Laser Systems Design", Applied Optics 5, January 1965, pp. 139-146.

DeMaria, A. J., "Ultrasonic Laser Modulation Techniques", Third Quarterly Progress Report, Jan. 1 - Mar. 31, 1965, United Aircraft Corp., Res. Labs, Report D 920259-9, (AD-465667), 6 July 1965.

Deutsch, S., "Narrow-band TV Uses Pseudo-Random Scan," Electronics, April 1962.

Filipowsky, Richard F. and Bickford, Louise C., "Modulation and Channels", Space Communications: Theory and Applications, A Bibliography; Vol. 1, NASA Report SP-7022(01), June 1965.

Gabor, D., Proc. Inst. of Elec. Eng., Vol. 108, 1961, pp. 303-315.

Goldstein, I., Miles, P. A. and Chabot, A., "Heterodyne Measurements of Light Propagation through Atmospheric Turbulence", Proc. of IEEE 53, September 1965, pp. 1172-1180.

Gouriet, G.G., "Bandwidth Reduction in Relation to Television," Brit. Comm. and Elec., Vol. 3, 1956, pp. 424-429.

Graham, R.E., "Communication Theory Applied to TV Coding," Acta Electronica, Vol. 2, 1957, pp. 333-343.

Harrison, C.W., "Experiments with Linear Prediction in Television," Bell System Technical Journal, Vol. 31, 1952, pp. 764-783.

Huang, Thomas,S., "PCM Picture Transmission," IEEE Spectrum 2, December 1965, pp. 57-63.

Ives, G.M., "Television Broadcasting from Satellites," National LAS-ARS Meeting, 13-16 June 1961, L.A. Calif.

Jesty, L.C., "Television as a Communication Problem," Proc. Inst. of Elec. Eng., Vol. 99, 1952, pp. 761-770.

Julesz, B., "A Method of Coding Television Signals Based on Edge Detection," Bell System Technical Journal, Vol. 38, July 1959.

Kelly, D.H., "Spatial Frequency, Bandwidth and Resolution", Applied Optics 4, April 1965, pp. 435-437.

Kinoshita, K., "Image Transmission Carrier and Image Spectrum in Generalized Photographic System", (APSEL 731/64).

Kretzmer, E.R., "The Statistics of Television Signals," Bell System Technical Journal, Vol. 31, Feb. 1952, pp. 751-763.

LaFond, Charles D., "Laser Communication Qualified Success," Missiles and Rockets 17, No. 2, 12 July 1965, pp. 20-21.

Maschhoff, R. H., "Delta Modulation," Electro-Technology, Jan. 1964.

Massey, G. A., "Photomixing with Diffusely Reflected Light," Applied Optics 4, July 1965, (APSEL 65-2553), pp. 781-784.

McClure, George W. and Dute, J. C., "Probability Characteristics of Sensor Output Data," Univ. of Michigan, Institute of Science and Technology, Report 2900-329-R, Sept. 1963, p. 31.

Michel, W. S., "Statistical Coding for Text and Picture Communication," Bell Telephone Laboratories Monograph 3035, 1957.

Miller, Barry, "Gemini Laser May Speed Future Use," Aviation Week and Space Technology, 13 December 1965.

Morton, G. A., "Image Intensifiers and the Scotoscope," Applied Optics, Vol. 3, June 1964, pp. 651-673.

Nishikawa, S., Massa, R. J., and Mott-Smith, J. C., "Area Properties of Television Pictures," Air Force, Cambridge Research Laboratories, Physical Sciences Research Paper 23, June 1964.

Noble, P. J. W., "A Low Temperature Laser Demodulator for High Frequency Operation", J. Sci. Instrum. 42, October 1965, pp. 757-758.

Oliver, B. M., "Applications of Laser to Space Communications", Proc. IRE 50, 135, 1962.

Ordway, Edward F. I. III, "Interplanetary Communications Advances in Space Science", Volume I, Academic Press, 1959.

Renn, R. L., and Schaphorst, R. A., "An Image Coding System which Reduces Redundancy in Two Dimensions," Proc. of the NAECON, Dayton, 1962.

Roberts, L., "Picture Coding Using Pseudo-Random Noise," IRE Trans. PGIT, IT-8, 1962-pp. 145-154.

Schiel, E. J., Bullwinkel, E. C. and Weimer, R. B., "Pulse Code Modulation Multiplex Transmission Over an Injection Laser Transmission System," Proc. of the IEEE 13, December 1965, pp. 2140-2141.

Schreiber, W. F., "The Effect of Scanning Speed on the Signal to Noise Ratio of Camera Tubes," Proc. of the IEEE, Feb. 1964, p. 217.

Schreiber, W.F., Knapp, C.F. and Kay, N.D., "Synthetic Highs - An Experimental TV Bandwidth Reduction System," Jour. of the SMPTE, Vol. 68, 1959, pp. 525-537.

Scott, R.M., "Electro-optics in Space Operation and Research", IEEE Spectrum 3, 1966, pp. 85-88.

Scull, John R., "A System for Lunar Photography and Data Transmission" Calif. Inst. of Tech., Jet Propulsion Lab., Tech. Release 34-142, 28 May 1960.

Seyler, A.J., "Frame-run Coding of Television Signals, A New Method for Bandwidth Reduction," Comm. of Australia, PGM Dept. Research Report No. 5064, Sept. 1959.

Seyler, A.J., "Real-time Recording of Television Frame Difference Areas," Proc. IEEE, Vol. 51, 1963, pp. 478-480.

Seyler, A.J., "Channel Capacity Utilization of TV Relay Links," Fortschritte des Hochfrequenztechnik, Vol. 5, 1960, pp. 263-306.

Southworth, Glen R., "A Video Modulation Test System for Space Television", Jour. SMPTE 74, April 1965, pp. 307-313.

Steele, E.L. and Davis, W.C., "Optical Laser Amplifiers", North American Aviation, Autonetics, 29 July 1964.

Targ, R., "Optical Stereodyning System of Sylvania", Proc. IEEE 52, 1964, p. 303.

Toulon, P.M., "Le Balayage Cavalier," L'Onde Elec., Vol. 28, 1948, pp. 412-416.

Wholey, Joseph S., "The Coding of Pictorial Data", IRE Transactions on Information Theory 7, April 1961, pp. 99-104.

Wischnia, Herbert F., Hemstreet, Harold S., et al, "Determination of Optical Technology Experiments for a Satellite", Perkin-Elmer, NASA Contractor Report 252, July 1965, Report No. 7846, Phase I, Contract No. NAS 8-11408.

Young Blood, W.A., "Picture Processing," RLE QPR, Jan. 1958, pp. 95-100.

Zenel, J.A., "Narrow Bandwidth Video Tape Recorder Used in the Tiros Satellite," Jour. of the SMPTE, Vol. 69, Nov. 1960, pp. 818-820.

Anon: "Ultrasonic Laser Modulation Techniques", United Aircraft Corp., First Quarterly Report No. C-920259-3, (AD-454484), 11 January 1965.

Anon: "Rings for the Laser", Electronics 38, No. 9, 3 May 1965, pp. 29-30.

Anon: "Laser Communication is Partial Success", Missiles and Rockets 17, No. 2, July 1965, pp. 18.

Anon: "NASA's Gemini 7 Laser Voice Communication Project", Laser Focus, 1 August 1965, p. 6-9.

Anon: "Conference on Atmospheric Limitations to Optical Propagation, Proceedings of the Conference on Atmospheric Limitations to Optical Propagation", Central Radio Propagation Lab., and National Center for Atmospheric Research, Boulder, Colorado, 1965.

Anon: "Laser TV System", Jour. SPIE 4, No. 2, December 1965 - January 1966, p. 82.

Anon: "Sun Powered Laser Transmits TV", Laser Focus 2, No. 1, 1 January 1966, p. 8.

Anon: "Laser TV System Demonstrated", Laser Focus 2, No. 1, 1 January 1966, pp. 9-12.

Anon: "Noise in Lasers and Laser Detectors", Spectra Physics Laser Technical Bulletin, No. 4.

Anon: "Optical Transmitter Techniques", Electro-Optical Systems, Inc., Interim Report, (AD-62-1630), 15 July - 15 October 1964.

Anon: "Space Programs Summary, Volume I: The Lunar Program (Sept. 1 - Oct. 31, 1965), " California Institute of Technology, Jet Propulsion Laboratory, Report 37-36, Vol. I, (30 Nov. 1965), p. 105.

BIBLIOGRAPHY

DISPLAYS

(Section 5)

Bartleson, C. J., "Interrelations Among Screen Luminance, Camera Exposure and Quality of Projected Color Transparencies", Phot. Sci. & Eng., Vol. 9, No. 3, May-June 1965, pp. 174-178.

Fugita, T., "Evaluation of Errors in the Graphical Rectification of Satellite Photographs", Satellite and Mesometeorology Res. Proj., Re Paper, (AD-603547), July 1964.

Harshbarger, John H., "Evaluation Technique", Test and Evaluation of Electronic Image Generation and Projection Devices, Vol. 1, AF, Aerospace Med. Div. Tech. Report. 65-116, Aug. 1965.

Hitt, W. D. and Schutz, H. G., "Development of Design Criteria for Intelligence Display Formats", AF, Rome Air Dev. Ctr., Report TR-60-201, (AD-245138), 26 Spetember 1960.

Sachtlehen, L. T., "High Resolution Display Media", RCA Defense Electronic Products, Camden, New Jersey, 7 May 1962.

Sanford, L. C., Harvey, D. I. and Kohler, R. J., "The Application of Photographic Photometry to Electronic Display Systems", Phot. Sci. & Eng., Vol. 8, No. 1, Jan.-Feb. 1964, pp. 2-6.

Anon: "Rectifier, Electronic Printing, Photogrammetric", Final Study Report EN-28, Fairchild Graphic Equipment, AF, RADC-TR-57-167, (AD 131323), 13 Sept. 1957.

Anon: "Investigation of Solid-State Displays", Quart. Prog. Report 4, Kaiser Aircraft & Electronics, (AD-254439), Dec. 15, 1960 - Mar. 14, 1961.

Anon: "A Human Factors Bibliography on Display Communication, Controller Workload, Aircrew Activity and Man-Machine Relationships", Courtney & Co., Report 59, (AD-459032L), 31 January 1962.

Anon: "Photography and Photometry of Cathode Ray-Tube Displays", Phot. Sci. & Eng., Vol. 1, No. 5, Sept. - Oct. 1963, pp. 289-313.

Anon: "4th National Symposium on Information Display", Society for Information Display, October 1964.

Anon: "Surveyor Mission Operations System", NASA Technical Memo No. 33-264, Jet Propulsion Laboratory, 4 April 1966.

BIBLIOGRAPHY

STELLAR PARALLAX

(Section 6)

Aller, L. H., Astrophysics. The Atmospheres of the Sun and Stars, Vol. 1, New York: Ronald Press, 1953, pp. 171-321.

Arp, H. C., "Cepheids in Galactic Clusters. III, EV SCT in NGC 6664", Astrophys. J. 128, 166 (1958).

Arp, H. C., Sandage, A. and Stephens, C., "Cepheids in Galactic Clusters. IV, DL CAS in NGC 129", Astrophys. J. 130, 80 (1959).

Baum, W. A., Hiltner, W. A., Johnson, H. L. and Sandage, A. R., "The Main Sequence of the Globular Cluster M13", Astrophys. J. 130, 749 (1959).

Belton, M. J. S. and Woolf, N. J., "The Problem of Beta Lyrae. I. Six-Color Photometry", Astrophys. J. 141, 145 (1965).

Bertiak, F. C., "Absolute Magnitudes of Stars in the Scorpio-Centaurus Association", Astrophys. J. 128, 533 (1958).

Blaauw, A., "On the Luminosities, Motions and Space Distribution of the Nearer Northern O-B5 Stars", Astrophys. J. 123, (1956), pp. 408-439.

Blaauw, A., "The Calibration of Luminosity Criteria", Basic Astronomical Data, Ed. K. A. A. Strand, Chicago: Univ. of Chicago Press, 1963. (Chap. 20).

Bloomer, J. H., "Liquid Space Optics", S. P. I. E. Journal, Vol. 4, No. 2, December 1965 - January 1966, pp. 65-70.

Conti, P. S., Wallerston, G., and Wing, R. F., "The Composition of Main-Sequence Stars of Types A-K in the Hyades Cluster", Astrophys. J. 142, (1965), p. 999.

Cuikay, R. and Callahan, T., "Orbiting Observatory to Measure Stars Dim Light", Electronics, 28 February 1964, pp. 28-31.

Eggin, O. J., Astrophys. J. 111 (1950).
Photoelectric Studies I - "Color-Luminosity Array for Members of the Hyades Cluster", pp. 65-80.
Photoelectric Studies II - "Color-Luminosity Array for Members of the Pleiades Cluster", pp. 81-98.
Photoelectric Studies III - "Color-Luminosity Arrays for the Coma Berenices and Ursa Major Clusters", pp. 414-425.

Eggin, O. J., "Photoelectric Studies IV" "Color-Luminosity Array for Stars in the Region of the Sun", Astrophys. J. 112, (1950), pp. 141-177.

Eggin, O. J., Astron. J. 60 (1955).
"Magnitudes and Colors for 833 Northern & Southern Stars", pp. 65-92.
"The Color-Luminosity Array for Stars Near the Sun", pp. 401-407.
"The Color-Luminosity Array for Same Galactic Clusters", pp. 407-414.

Eggin, O. J., "Distribution of the Nearer Bright Stars in the Color-Luminosity Array", Astron. J. 62 (1957), pp. 45-55.

Eggin, O. J., "Color, Luminosity and Evolution of the Stars", Vistas in Astronomy, Vol. 3, ed. A. Beer, New York: Pergamon Press, (1960), pp. 259-288.

Eggin, O. J., Monthly Notices of Royal Astronomical Society 118 (1958), pp. 65-154.

Eggin, O. J., "Colors, Luminosities, and Motions of the Nearer G-Type Stars", Astron. J. 69 (1964), pp. 570-609.

Eggin, O. J., "Masses, Luminosities, Colors & Space Motions of 228 Visual Binaries", Astron. J. 70 (1965), pp. 19-93.

Eichhorn, H., "The Relationship between Standard Coordinates of Stars and the Measured Coordinates of Their Images", Applied Optics, Vol. 2, No. 1, January 1963, pp. 17-21.

Glasstone, S. Sourcebook on the Space Sciences, Princeton: Van Nostrand Company, (1965).

Hardie, R. H., "An Improved Method for Measuring Extinction", Astrophys. J. 130 (1959), p. 663.

Harris, D. L. III, Strand, K. A. A., and Worley, C. E., "Empirical Data on Stellar Masses, Luminosities and Radii", Basic Astronomical Data, Ed. K. A. A. Strand, Chicago: University of Chicago Press, 1963, Chapter 15.

Hiltner, W. A., Morgan, W. W. and Neff, J. S., "Studies in Spectral Classification II. The HR Diagram of NGC 6530", Astrophys. J. 141 (1965), p. 183.

Irwin, J. B., "South Cepheid Photometry", Astrophys. J. Suppl., No. 58, (1961).

Johnson, H. L. and Morgan, W. W., "Fundamental Stellar Photometry for Standards of Spectral Type on the Revised System of the Yerkes Spectral Atlas", Astrophys. J. 117, (1953), p. 313.

Johnson, H. L., Astrophys. J. 126, (1957).
"Three-Color Photometry of Nearby Stars", pp. 113-120.
"Photometric Distances of Galactic Clusters", pp. 121-133.
"The Color-Magnitude Diagram for 1 Orionis", pp. 134-137.

Johnson, H. L., "Infrared Stellar Photometry", Astrophys. J. 135, (1962), p. 69.

Johnson, H. L., Bull. Tonantzintla and Tacubaya Obs. 3, (1964), p. 305.

Johnson, H. L., "Interstellar Extinction in the Galaxy", Astrophys. J. 141, (1965), p. 923.

Keenan, P. C., "Classification of Stellar Spectra", Basic Astronomical Data, Ed. K. A. A. Strand, Chicago: Univ. of Chicago Press, (1963), Chapter 8.

Kraft, R. P., "Cepheids in Galactic Clusters II. Radial Velocities and Spectral Types in NGC 129, NGC 6664 and NGC 7790", Astrophys. J. 128, (1958), p. 161.

Kraft, R. P., "Color Excesses for Supergiants and Classical Cepheids V. The Period-Color and Period-Luminosity Relations: A Revision", Astrophys. J. 134, (1961), p. 616.

Kraft, R. P., "The Absolute Magnitudes of Classical Cepheids", Basic Astronomical Data, Ed. K. A. A. Strand, Chicago: Univ. of Chicago Press, (1963), Chapter 21.

Kron, G. E., White, H. S. and Gascoigne, S. C., "Red and Infrared Magnitudes for 282 Stars with Known Trigonometric Parallaxes", Astron. J. 62, (1957), pp. 205-220.

Kron, G. E., "Multiple Color Photometry", Vistas in Astronomy, Vol. 3, Ed. A. Beer, New York: Pergamon Press, (1960), pp. 171-183.

Kron, G. E. and Mayall, N. U., "Photoelectric Photometry of Galactic and Extragalactic Star Clusters", Astron. J. 65, (1960), p. 581.

Lassen, H. A., and Park, R. A., "Deep Space Probes: Sensors and Systems", Symposium on Unmanned Exploration of the Solar System, Reprint 65-22, 8-10 February 1965, Denver, Colorado.

Loewen, E. G., "Answer to Precise Positioning", Control Engineering, 12 September 1965, pp. 118-124.

Low, F. J. and Johnson, H. L., "Stellar Photometry at 10 ", Astrophys. J. 139, (1964), p. 1130.

Mendoza, E. E. V. and Johnson, H. L., "Multicolor Photometry of Carbon Stars", Astrophys. J. 141, (1965), p. 161.

Morgan, W. W., Keenan, P. C., and Kellman, E. An Atlas of Stellar Spectra, Chicago: Univ. of Chicago Press, 1943.

Morgan, W. W., Harris, D. L. and Johnson, H. L., "Some Characteristics of Color Systems", Astrophys. J. 118, (1953), pp. 92-105.

Morgan, W. W. and Hiltner, W. A., "Studies in Spectral Classification I. The HR Diagram of the Hyades", Astrophys. J. 141, (1965), p. 177.

Morgan, W. W., Hiltner, W. A., Neff, J. S. and Garrison, R., "Studies in Spectral Classification III. The HR Diagrams of NGC 2244 and NGC 2264", Astrophys. J. 142, (1965), p. 974.

Mumford, G. S., "Distance Modulus", Sky and Telescope 29, (1965), p. 274.

Oke, J. B. and Conti, P. S., "Absolute Photoelectric Spectrophotometry of Stars in the Hyades", Astrophys. J. 143, (1966), p. 134.

Pay, R., "300-in-dia. Liquid 'Orbiting Eye' Proposed", Missiles and Rockets, 14 June 1965, p. 43.

Sandage, A., "Cepheids in Galactic Clusters I. CF CAS in NGC 7790", Astrophys. J. 128, (1958), p. 150.

Sandage, A. R., and Eggin, O. J., Monthly Notices of Royal Astronomical Society 119, (1959), p. 278.

Saunders, J., "The Globular Cluster Omega Centauri", Sky and Telescope 26, (1963), p. 133.

Scott, R. M., "Electrooptics in Space Operation and Research", IEEE Spectrum, January 1966.

Stebbins, J. and Whitford, A. E., "Six-Color Photometry of Stars I. The Law of Space Reddening from the Color of O and B Stars", Astrophys. J. 98, (1943), p. 20.

Strand, K. A., "The 60-in (152 cm) Astrometric Reflector of the U. S. Naval Observatory", Applied Optics, Vo. 2, No. 1, January 1963, pp. 1-8.

Strand, K. A., "Determination of Stellar Distances", Science, Vol. 144, No. 3624, 12 June 1964, pp. 1299-1309.

Stromgren, B., "Quantitative Classification Methods", Basic Astronomical Data, Ed. K. A. A. Strand, Chicago: Univ. of Chicago Press, 1963, Chapter 9.

Struve, O., "The Distance Scale of the Universe I", Sky and Telescope 12, (1953), p. 203.

Struve, O., "The Distance Scale of the Universe II", Sky and Telescope 12, (1953), p. 238.

Struve, O., Stellar Evolution, Princeton: Princeton Univ. Press, 1950.

Tifft, William G., Gill, J., and Roberts, L., "The Overall Spectrum of Astronomical Research Pssibilities utilizing Manned Earth Orbital Spacecraft", Symposium AAS, 18-19 March 1965.

Van de Kamp, P., "Masses of Visual Binaries", Astron, J. 59, (1954), pp. 447-454.

Van de Kamp, P., "Stars Nearer Than Five Parsecs", Sky and Telescope 14, (1955), p. 498.

Van de Kamp, P., "Problems of Long Focus Photographic Astronomy", Applied Optics, Vol. 2, No. 1, Jan. 1963, pp. 9-17.

Vasilevskis, S., "Some Aspects of the Lick Proper Motion Program", Astron. J. 59, (1954), pp. 40-43.

Vasilevskis, S., "The Use of Galaxies and Astrographs for Absolute Proper Motions", Astron. J. 62, (1957), pp. 126-128.

Vasilevskis, S., "TheReference System of Bright, Intermediate, and Faint Stars and of Galaxies", Basic Astronomical Data, Ed. K. A. A. Strand, Chicago: University of Chicago Press, 1963, Chapter 3.

Weaver, H. F., "Development of Astronomical Photometry", Popular Astronomy 54, (1946), pp. 211-301, 287-99, 339-351, 389-404, 451-464, 504-526.

Weaver, H. L., "The Galactocentric Circular Velocity and Corrections to the Precession Constant and the Motion of the Equinox", Astron. J. 61, (1956), pp. 268-271.

Woolley, R. V. D. R., Monthly Notices of Royal Astronomical Society 118, (1958), p. 45.

Anon.: "Orbiting Ultraviolet System Will Map Stars and Sky's Radiant Intensity", Electronics, 23 Feb. 1963, pp. 22-23.

Anon.: "First Series of Lick Survey Completed", Sky and Telescope 13, (1954), p. 335.

Anon.: Trans. -International Astronomical Union 1, (1922), p. 79.

BIBLIOGRAPHY

SOLAR TOPOGRAPHIC AND RELATIVISTIC MEASUREMENTS

(Section 7)

Allen, C. W., "M-Regions", Planetary and Space Science, Vol. 12, 1964, pp. 487-494.

Athay, R. G., "The Challenge of Chromospheric Physics", Science, Vol. 143, 13 March 1964, pp. 1129-1138.

Billings, D. E., "Velocity Fields in a Coronal Region with a Possible Hydromagnetic Interpretation", Astrophysical Journal, July 1959, pp. 215-220.

Bryant, D. A., Cline, T. L., Desai, U. D., and McDonald, I. B., "New Evidence for Long-Lived Solar Streams in Interplanetary Space", Physical Review Letters, Vol. 11, No. 4, 15 August 1963, pp. 144-146.

DeMoraes, C. A., "Mission Objectives and Design Considerations for A Scientific Solar Probe", AIAA Unmanned Spacecraft Meeting, 1 - 4 March 1965, pp. 413-443.

DeWitt, B. S., "Gravity", Advance in Space Science and Technology, Academic Press, Vol. 6, 1964, pp. 1-36.

Dicke, R. H., "Long Range Scalar Interaction", Physical Review, Vol. 126, No. 5, pp. 1875-1877.

Dicke, R. H., "Gravitation - An Enigma", American Scientist, Vol. 47, March 1959, pp. 25-40.

Dicke, R. H., "Implications for Cosmology of Stellar and Galactic Evolution Rates", Reviews of Modern Physics, Vol. 34, No. 1, January 1962, pp. 110-122.

Eddington, A., "Space, Time and Gravitation", 1920, Harper & Row, Reprint 1959.

Evans, J. W. and Michard, R., "Observational Study of Microscopic Inhomogeneities in the Solar Atmosphere", Astrophysical Journal, Vol. 135, No. 3, May 1962, pp. 812-821.

Foschetti, J. A., "Vehicle Technology Considerations for a Solar Probe", NASA Technical Note D-7147, Goddard Space Flight Center, Greenbelt, Md., April 1963.

Goldberg, L., "Solar Experiments", Astronomical Journal, Vol. 65, No. 5, June 1960, pp. 274-277.

Jordan, P., "Geophysical Consequences of Dirac's Hypothesis", Reviews of Modern Physics, Vol. 34, No. 4, Oct. 1962.

Kononovich, E. V., "Possible Models of Chromospheric Spicules", Soviet Astronomy, Vol. 9, No. 2, September-October 1965, pp. 183-190.

Kopal, Z., "Tasks for the Manned Orbital Telescope", Astronautics and Aeronautics, December 1965, pp. 16-21.

Larmore, Lewis, "The Influence of Solar Flares on the Space Environment", Space Exploration, McGraw-Hill, 1964, pp. 97-115.

Lindsay, J. C., "Scientific Results of OSO-1", A/AA/CAS/RAeS 9th Anglo-American Conference, 63-470, 16-18 October 1963.

Newkirk, G., Jr., "Solar Optics", Applied Optics, Vol. 3, No. 12, December 1964, pp. 1319-1320.

Roberts, L., "Designing the Manned Orbital Telescope", Astronautics and Aeronautics, December 1965, pp. 22-26.

Schlesinger, E. R., "Aiming a Three Ton Telescope Hanging from a Balloon", Electronics, Vol. 36, No. 6, 8 February 1963, pp. 47-51.

Singh, Jagjit, "Great Ideas and Theories of Modern Cosmology", Dover, 1961.

Wood, R. M., and Wood, K. D., "Solar Motion and Sunspot Comparison", Nature, 9 October 1965, pp. 129-131.

BIBLIOGRAPHY

GENERAL
(All Sections)

Boni, Albert, "Photographic Literature", Morgan and Morgan (1962).

Kopal, Z., "Essentials for Mapping the Moon", American Scientist, Vol. 47, No. 4, Dec. 1959, pp. 505-508.

Kosofsky, L. J. and Broome, G. C., "Lunar Orbiter: A Photographic Satellite", J. SMPTE, Vol. 74, Sept. 1965, pp. 773-778.

Pennington, John T., "Study of Stereophotogrammetric Systems for Topographic Mapping with very High Altitude Photography", Engineer Research & Development Labs., Ft. Belvoir, Va., Rept. No. 1352, (AD-46126), 14 June 1954.

Anon: "Image Intensifier Symposium, October 6-7, 1958", U.S. Army Engineer Research & Development Labs., J. Opt. Soc. A., 50, January 1960, p. 90.

Anon: "Television, Photogrammetry, Photometry and Radiometry Adaptable to Space Reconnaissance", Literature Search No. 490, Jet Propulsion Lab., November 1963.

Anon: "Space Program Summary", Space Exploration Programs and Space Sciences, Vol. VI, May 1-June 30, 1965.

Anon: "The Lunar Program", Vol. 1, (Sept. 1-Oct. 31, 1965) Calif. Inst. of Tech., Jet Propulsion Lab., Rept. No. 37-36, Vol. 1, 30 November 1965, Space Programs Summary.

Anon: "Abstracts of Photographic Science and Engineering Literature", Engineering Index, Inc., 345 East 47th St., New York.